

UNIVERSITÉ DU QUÉBEC À MONTRÉAL

COMBINAISON DE MATÉRIAUX PLASMONIQUES ET DE CATALYSEURS ORGANOMÉTALLIQUES
POUR LA RÉDUCTION DU CO₂

MÉMOIRE
PRÉSENTÉE
COMME EXIGENCE PARTIELLE
DE LA MAÎTRISE EN CHIMIE

PAR
MINA ASGHARZADEH

AVRIL 2025

UNIVERSITÉ DU QUÉBEC À MONTRÉAL

COMBINATION OF PLASMONIC MATERIALS AND ORGANOMETALLIC CATALYSTS FOR CO₂
REDUCTION

THESIS
PRESENTED
AS A PARTIAL REQUIREMENT
FOR THE MASTER'S DEGREE IN CHEMISTRY

BY
MINA ASGHARZADEH

APRIL 2025

UNIVERSITÉ DU QUÉBEC À MONTRÉAL
Service des bibliothèques

Avertissement

La diffusion de ce mémoire se fait dans le respect des droits de son auteur, qui a signé le formulaire *Autorisation de reproduire et de diffuser un travail de recherche de cycles supérieurs* (SDU-522 – Rév.12-2023). Cette autorisation stipule que «conformément à l'article 11 du Règlement no 8 des études de cycles supérieurs, [l'auteur] concède à l'Université du Québec à Montréal une licence non exclusive d'utilisation et de publication de la totalité ou d'une partie importante de [son] travail de recherche pour des fins pédagogiques et non commerciales. Plus précisément, [l'auteur] autorise l'Université du Québec à Montréal à reproduire, diffuser, prêter, distribuer ou vendre des copies de [son] travail de recherche à des fins non commerciales sur quelque support que ce soit, y compris l'Internet. Cette licence et cette autorisation n'entraînent pas une renonciation de [la] part [de l'auteur] à [ses] droits moraux ni à [ses] droits de propriété intellectuelle. Sauf entente contraire, [l'auteur] conserve la liberté de diffuser et de commercialiser ou non ce travail dont [il] possède un exemplaire.»

Acknowledgments

I want to express my deepest gratitude to my supervisor, Professor Guillaume Goubert, for his invaluable guidance, support, and encouragement over the past two years. His expertise and insights have been instrumental in completing this project.

I am also deeply grateful to the members of our research group, whose collaboration and assistance have been essential to this work. Your camaraderie and contributions have made this journey both productive and enjoyable.

I would like to thank the University of Montreal for providing access to the gas chromatography machine, which was crucial for our experiments. I would also like to thank the Polytechnic Montreal University for their assistance with TEM techniques, which significantly contributed to the analysis and understanding of our results.

I am profoundly thankful to the University of Quebec in Montreal (UQAM) and the NanoQAM department for their outstanding facilities and equipment, without which this research would not have been possible. Your support has been pivotal in enabling this study.

Thank you all for your invaluable support and contributions to this project.

Dedication

This thesis is dedicated to my beloved family, whose unwavering support and encouragement have guided me throughout my academic journey. Your love and belief in me have given me the strength to achieve my goals.

I also want to express my heartfelt gratitude to my esteemed supervisor, Dr. Guillaume Goubert. Your invaluable guidance, insightful feedback, and constant support have been instrumental in completing this work. Thank you for believing in my potential and for helping me navigate the complexities of this research.

Preface

This thesis investigates integrating plasmonic materials with organometallic catalysts for CO₂ reduction, a subject of critical importance in electrochemistry. The growing urgency to address climate change and the demand for sustainable energy solutions has driven my decision to delve into this research.

From the outset, my interest has been centred on the potential of combining advanced nanomaterials with catalytic processes to achieve more effective CO₂ reduction. This work seeks to explore novel approaches that could lead to developing more efficient and sustainable catalytic systems in the long term.

Throughout this journey, I have been motivated by the idea that scientific research can offer tangible solutions to some of the most pressing challenges of our time. By contributing new insights and methodologies to the field, I hope this thesis will serve as a stepping stone for further advancements in sustainable catalysis.

Table of Contents

Acknowledgments.....	iii
Dedication	iv
Preface.....	v
List of Figures.....	viii
List of Abbreviations, Acronyms, and Symbols	xi
List of Symbols and Units	xiii
RÉSUMÉ.....	xv
ABSTRACT	xvi
CHAPITRE 1 Introduction.....	1
1.1 Introduction	1
1.2 Background of the study	3
1.3 Research Objectives.....	4
1.3.1 Synthesis of Gold Nanoparticles with Different Methods	5
1.3.2 Investigating the Plasmonic Effect of Gold Nanoparticles in the Photocatalytic CO ₂ Reduction ..	8
1.3.3 Combining Gold Nanoparticles with FeTPP to Increase Effectiveness in CO ₂ Reduction	9
1.4 Methodology.....	10
1.4.1 Characterization of Gold Nanoparticles:.....	10
1.5 Structure of the Thesis	16
CHAPITRE 2 Literature Review	18
2.1 Introduction	18
2.2 Overview of Plasmonic Materials.....	19
2.2.1 Hot electron and Plasmonic Effects in Catalysis	20
2.2.2 Influence of Size and Shape on Gold Nanoparticles (AuNPs) in Plasmonic Catalysis:	22
2.3 Organometallic Catalyst.....	24
2.3.1 Fundamental Properties of Organometallic Catalysts.....	24
2.3.2 Iron Tetraphenyl Porphyrin (FeTPP) as a Catalyst for CO ₂ Reduction	24
2.4 CO ₂ Reduction Techniques.....	28
2.4.1 Chemical Absorption and Adsorption.....	28
2.4.2 Biological Fixation	29

2.4.3	Chemical and Electrochemical Reduction.....	30
2.4.4	Photocatalytic Reduction.....	31
2.4.5	Hybrid Catalytic Systems.....	32
2.5	Synergy between Plasmonic Materials and Organometallic Catalysts.....	35
2.5.1	Mechanisms of Synergy.....	35
2.5.2	Applications and Future Development.....	36
2.6	Deposition Techniques.....	38
2.6.1	Drop casting.....	38
2.6.2	Electrodeposition.....	39
2.6.3	Sol-Gel Method.....	39
2.6.4	Dip Coating.....	40
CHAPITRE 3 Synthesis and Characterization of AuNP.....		42
3.1	Introduction.....	42
3.2	Synthesis of gold nanoparticles with seed growth method.....	42
3.3	Synthesis of Gold Nanoparticles by Citrate Reduction Method.....	45
3.4	Electrodeposition of gold nanoparticles on FTO.....	48
3.5	Result and Discussion.....	49
3.6	Electrodeposition gold nanoparticles.....	59
CHAPITRE 4 Photocatalysis experiments.....		66
4.1	Introduction.....	66
4.2	Deposition Optimization.....	67
4.2.1	Experimental Setup.....	67
4.2.2	Optimization Results.....	70
4.2.3	Effect of Deposition Parameters.....	71
4.3	Catalysis tests.....	72
4.3.1	Ru as a photosensitizer and Gold as a catalyst in the solution.....	72
4.3.2	FeTPP as a catalyst and Gold as a Photosensitizer in the solution.....	74
4.3.3	Gas phase CO ₂ Reduction.....	78
4.3.4	Photocathode gold nanoparticle and FeTPP.....	81
Conclusion.....		84
References and Bibliography.....		86

List of Figures

Figure 1.1. Synthesis of gold nanoparticles (AuNPs) via the Turkevich method, where sodium citrate reduces Au ³⁺ ions from HAuCl ₄ and stabilizes the formed nanoparticles by capping their surface. (Facchi <i>et al</i> 2023) reproduced with permission	5
Figure 1.2. Synthesis of gold nanoparticles using seed-mediated growth. (a) Formation of seeds using HAuCl ₄ and NaBH ₄ . (b-e) Growth of various shapes (spheres, bipyramids, triangles, and stars) by adjusting the capping agents, reducing agents, and pH in subsequent steps. (Mehere et Chaure, 2020) reproduced with permission	7
Figure 1.3. Schematic of the fabrication procedure of AuNSs on FTO. (Siampour <i>et al.</i> , 2020) reproduced with permission	8
Figure 1.4. Schematic representation of a UV-Vis spectroscopy setup.	11
Figure 1.5. Schematic representation of the SEM technique. (Zhou <i>et al.</i> , 2007) reproduced with permission	12
Figure 1.6. Schematic representation of an AFM technique. (Tsenova-Ilieva et Karova, 2020) reproduced with permission	13
Figure 1.7. Schematic representation of a DLS technique. (Brookhaven Instruments).....	14
Figure 1.8. Schematic representation of a TEM technology. (NanoScience).....	15
Figure 1.9. Schematic representation of a (GC) Gas Chromatography. (Bitesize Bio)	16
Figure 2.2. Schematics of plasmon-induced hot electron generation on AuNP and mechanistic representation of H ₂ dissociation on the AuNP surface. (Mukherjee <i>et al.</i> , 2013) reproduced with permission	21
Figure 2.3. Iron tetraphenyl porphyrin structure.....	25
Figure 2.10. Dip coating method. (Yin-Fen <i>et al.</i> , 2023) reproduced with permission.....	41
Figure 3.1. The color changes after adding the first reducing agent (a), and again after 90 minutes at 80 degrees (b).....	43
Figure 3.3. Stages of gold nanoparticle synthesis via citrate reduction: (a) Au(III) ions in yellow solution, (b) nucleation with darkening color, (c) formation of colloidal gold with deep red color.	46
Figure 3.4. Electrodeposition of Au on FTO with 4,8,12 cycles.....	48
Figure 3.6. The UV-Vis spectrum of 0.3 ml of Gold Seeds added to growth solution.....	51
Figure 3.7. The UV-Vis spectrum of 3 ml of Gold Seeds was added to the growth solution.	51

Figure 3.9. The UV-Vis spectrum of 12 mL of gold seeds, which was added to the growth solution.....	53
Figure 3.10. DLS for Au seeds.....	54
Figure 3.11. DLS for 0.3 ml seed in growth solution. The average size of nano bipyramids is 100nm.....	54
Figure 3.13. DLS for 7 ml seed in growth solution. The average size of nano bipyramids is 60nm, 3nm...	55
Figure 3.15. TEM images of gold nanoparticles synthesized with 0.3 mL seed solution, showing bipyramidal and smaller aggregated particles. Scale bars: 100 nm (left), 200 nm (center and right).	56
Figure 3.16. TEM images of gold nanoparticles synthesized with 3 mL seed solution, showing clusters of bipyramidal nanoparticles. Scale bars: 200 nm (left), 100 nm (right).	57
Figure 3.20. UV-VIS for Gold Nanoparticles Synthesized by Citrate Reduction Method	59
Figure 3.22. Cyclic Voltammetry (CV) results for 8 cycles of electrodeposition of gold on FTO substrate with Ag/AgCl reference electrode and potassium phosphate buffer solution as a supporting electrolyte.	62
Figure 4.3. Structure of tris (bipyridine) ruthenium (II) chloride.	73
Figure 4.4. (Left) Sun simulator used for photocatalytic experiments. (Right) Blue light illumination setup with a sampling line leading from the reactor to the GC (not visible).	81

List of Tables

Table 1. Experimental conditions and detected products for CO ₂ reduction using Ru as a photosensitizer and gold as a catalyst in solution.....	74
Table 2. Experimental conditions and detected products for CO ₂ reduction using FeTPP as a catalyst and Gold as a Photosensitizer in the solution.	77
Table 3. Experimental conditions and detected products for Gas-phase CO ₂ Reduction.....	80
Table 4. Experimental conditions and detected products for CO ₂ reduction using photocathode gold nanoparticles and FeTPP.	83

List of Abbreviations, Acronyms, and Symbols

AFM: Atomic Force Microscopy

AuNP: Gold Nanoparticles

BIH: 1,3-Dimethyl-2-phenyl-2,3-dihydro-1H-benzo[d]imidazole

CTAB: Cetyltrimethylammonium Bromide

CTAC: Cetyltrimethylammonium Chloride

CV: Cyclic Voltammetry

DMF: Dimethylformamide

DLS: Dynamic Light Scattering

FTO: Fluorine-doped Tin Oxide

GC: Gas Chromatography

ITO: Indium Tin Oxide

LSPR: Localized Surface Plasmon Resonance

M: Molar Concentration

SEM: Scanning Electron Microscopy

SPR: Surface Plasmon Resonance

TEM: Transmission Electron Microscopy

TEOA: Triethanolamine

UV-Vis: Ultraviolet-Visible Spectroscopy

Au NPs: Gold Nanoparticles

Au NRs: Gold Nanorods

Au NBPs: Gold Nanobipyramids

PZT: stands for Lead Zirconate Titanate, which is a piezoelectric material

List of Symbols and Units

λ : Wavelength (nm)

ν : Frequency (Hz)

c : Speed of Light (m/s)

E : Energy (Joules)

T : Temperature (K)

P : Pressure (Pa)

V : Volume (L)

m : Mass (g)

M : Molarity (mol/L)

e^- : Electron

A : Absorbance (unitless)

I : Intensity (a.u.)

k : Rate Constant (s^{-1})

d : Diameter (nm, μm)

r : Radius (nm, μm)

t : Time (s, min, h)

pH: Acidity (unitless)

η : Efficiency (unitless or %)

σ : Conductivity (S/m)

μ : Micron or Micro- (10^{-6})

Q: Charge (Coulombs)

A: Area (cm^2 , m^2)

RÉSUMÉ

La recherche présentée dans ce mémoire se concentre sur l'application des nanoparticules d'or plasmoniques (AuNP) pour améliorer la réduction catalytique du dioxyde de carbone (CO_2) en molécules de valeur, telles que le monoxyde de carbone (CO). L'objectif est de développer un processus respectueux de l'environnement pour la conversion du CO_2 , contribuant ainsi à une économie de carbone durable sans dépendance aux combustibles fossiles.

Nous explorons la synthèse et l'optimisation des catalyseurs à base d'AuNP, en tirant parti de leurs propriétés plasmoniques pour augmenter l'efficacité et la sélectivité de la réduction du CO_2 . Bien que le couplage des nanoparticules d'or avec la tétraphénylporphyrine de fer (FeTPP) pour former un catalyseur hybride n'ait pas été entièrement réalisé, les résultats partiels indiquent que les AuNP accélèrent le processus de réduction du CO_2 sous irradiation lumineuse. Cette approche utilise l'énergie solaire pour les transformations chimiques, offrant une alternative prometteuse aux méthodes basées sur les combustibles fossiles.

Pour optimiser la performance, nous avons étudié divers paramètres, y compris la taille, la forme et la chimie de surface des nanoparticules. Un éventail de techniques expérimentales — spectroscopie UV-Vis, chromatographie en phase gazeuse, microscopie électronique à balayage, microscopie à force atomique et diffusion dynamique de la lumière — a été utilisé pour caractériser les nanoparticules synthétisées et évaluer leur efficacité dans la conversion du CO_2 .

Dans cette étude, différentes méthodes de synthèse ont été employées pour fabriquer des nanoparticules d'or, notamment la méthode de croissance assistée par des graines et la réduction au citrate. Ces nanoparticules ont ensuite été combinées avec la tétraphénylporphyrine de fer (FeTPP) pour former des structures hybrides, qui ont été minutieusement analysées afin de déterminer leurs propriétés catalytiques et plasmoniques. Diverses techniques de caractérisation et d'évaluation des performances ont été utilisées pour examiner les interactions entre les hybrides AuNP-FeTPP synthétisés et leur efficacité dans les applications catalytiques.

Les résultats démontrent le potentiel des AuNP plasmoniques en photocatalyse et réduction du CO_2 , fournissant une voie pour réduire les émissions de gaz à effet de serre et produire des produits chimiques de valeur.

Mots clés : Nanoparticules d'or plasmoniques (AuNP), réduction du CO_2 , efficacité catalytique, Fe tétraphényl porphyrine, catalyseur hybride, spectroscopie UV-Vis, chromatographie en phase gazeuse, MEB, AFM, diffusion dynamique de la lumière, propriétés plasmoniques, photocatalyse, énergie renouvelable, émissions de gaz à effet de serre, économie circulaire du carbone.

ABSTRACT

The research presented in this thesis focuses on the application of plasmonic gold nanoparticles (AuNP) to enhance the catalytic reduction of carbon dioxide (CO₂) into valuable molecules like carbon monoxide (CO). The goal is to develop an environmentally friendly process for CO₂ conversion, contributing to a sustainable carbon economy without reliance on fossil fuels.

We explore the synthesis and optimization of AuNP catalysts, leveraging their plasmonic properties to increase the efficiency and selectivity of CO₂ reduction. Although the coupling of gold nanoparticles with iron tetraphenylporphyrin (FeTPP) to form a hybrid catalyst was not fully realized, the partial results indicate that AuNP accelerates the CO₂ reduction process under light irradiation. This approach harnesses solar energy for chemical transformations, offering a promising alternative to fossil fuel-based methods.

We studied various parameters to optimize performance, including the nanoparticles' size, shape, and surface chemistry. A range of experimental techniques—UV-Vis spectroscopy, gas chromatography, scanning electron microscopy, atomic force microscopy, and dynamic light scattering—were used to characterize the synthesized nanoparticles and assess their efficiency in CO₂ conversion.

In this study, different synthesis methods were employed to fabricate gold nanoparticles, including the seed-mediated growth method and citrate reduction. These nanoparticles were subsequently combined with iron tetraphenylporphyrin (FeTPP) to form hybrid structures, which were thoroughly analyzed to determine their catalytic and plasmonic properties. Various characterization and performance evaluation techniques were used to investigate the interactions between the synthesized AuNP-FeTPP hybrids and their efficiency in catalytic applications.

The results demonstrate the potential of plasmonic AuNP in photocatalysis and CO₂ reduction, providing a pathway for reducing greenhouse gas emissions and creating valuable chemical products.

Keywords: Plasmonic gold nanoparticles (AuNP), CO₂ reduction, catalytic efficiency, iron tetraphenyl porphyrin, hybrid catalyst, UV-Vis spectroscopy, gas chromatography, SEM, AFM, dynamic light scattering, plasmonic properties, photocatalysis, renewable energy, greenhouse gas emissions, circular carbon economy.

CHAPITRE 1

Introduction

1.1 Introduction

Our work focuses on the chemical reduction of carbon dioxide (CO₂), transforming it into more valuable molecules through catalytic processes. This approach offers a sustainable and innovative solution by converting CO₂ into useful compounds, such as carbon monoxide (CO), which can be utilized in various industrial applications. This approach promotes the transformation of CO₂ into valuable products, making it a key element in sustainable chemical processes.

The goal of this thesis is to explore an innovative approach that combines the unique properties of plasmonic gold nanoparticles (AuNP) with an organometallic catalyst, iron tetraphenyl porphyrin (FeTPP), to enhance the efficiency and selectivity of CO₂ conversion processes. The use of AuNPs in catalysis aims to leverage their plasmonic properties, which allow them to absorb and concentrate light at specific wavelengths, significantly enhancing photocatalytic reactions. This plasmonic effect is intended to be harnessed to drive CO₂ reduction processes, offering a promising pathway to utilize solar energy for chemical transformations.

Plasmonic gold nanoparticles exhibit exceptional optical properties due to their ability to support surface plasmon resonances. These resonances result in strong absorption and scattering of light, leading to localized surface plasmon resonances (LSPRs) that generate intense electromagnetic fields at the nanoparticle surface. When exposed to sunlight, these LSPRs can excite electrons to higher energy states, so-called "hot electrons", enabling electron transfer to catalytic sites crucial for catalytic reactions (Wang *et al.*, 2017). Integrating AuNPs with an organometallic catalyst like FeTPP can develop a hybrid catalytic system that exploits the synergistic effects of both components (Zhang *et al.*, 2022).

The primary objective of this research is to synthesize and optimize gold nanoparticles for use in hybrid catalytic systems for CO₂ reduction. Several parameters, including the nanoparticles' size, shape, and surface chemistry, are systematically varied to identify conditions that maximize their plasmonic effect and catalytic activity. The synthesis process involves the controlled reduction of gold precursors to form nanoparticles with desired morphologies, followed by functionalization with FeTPP to create the hybrid catalyst.

A comprehensive suite of experimental techniques is employed to characterize and assess the synthesized nanoparticles' performance. UV-Vis spectroscopy monitors the optical properties and plasmonic behaviour of the nanoparticles. At the same time, gas chromatography provides quantitative analysis of the reaction products, allowing for the evaluation of catalytic efficiency and selectivity. Scanning electron microscopy (SEM) and atomic force microscopy (AFM) offer detailed insights into the morphology and surface characteristics of the nanoparticles. Dynamic light scattering (DLS) determines nanoparticle suspensions' size distribution and stability. Transmission electron microscopy (TEM) is also included to confirm the shape and size of the nanoparticles, rather than to provide high-resolution images or analyze their internal structure and composition.

The integration of AuNPs with FeTPP in the hybrid catalyst is expected to create a system where the gold nanoparticles' plasmonic excitation enhances the organometallic component's catalytic activity. Under light irradiation, the excited electrons generated by the plasmonic effect can be transferred to the FeTPP molecules, facilitating the reduction of CO₂ at the catalytic sites. This light-driven enhancement of catalytic activity represents a novel approach to utilizing solar energy for CO₂ reduction, potentially reducing reliance on fossil fuels and contributing to a circular carbon economy.

The significance of this research lies in its potential to advance the field of photocatalysis and CO₂ reduction. By fine-tuning the properties of plasmonic gold nanoparticles and integrating them with organometallic catalysts, this study aims to develop a catalytic system that is both efficient and sustainable. The findings of this research could have far-reaching implications for environmental remediation, renewable energy conversion, and the development of new catalytic processes.

The introduction provides an overview of the environmental challenges posed by CO₂ emissions, the limitations of conventional reduction methods, and the potential of plasmonic nanoparticles to address these challenges. It also outlines the research objectives, the experimental approach, and the significance of the study, setting the stage for a detailed exploration of the background, objectives, methodology, and structure of this thesis. However, it is important to note that some of the catalytic measurements are only partially complete due to time constraints and limited access to the instrument in a collaborator laboratory, and the results have not been fully quantified. Despite these limitations, this research aims to contribute to the development of innovative solutions for CO₂ reduction, enhancing the sustainability and efficiency of these processes using advanced nanomaterials and catalytic systems.

1.2 Background of the study

The increasing concentration of carbon dioxide (CO₂) in the atmosphere is a significant driver of climate change, contributing to global warming and its associated adverse effects, including extreme weather events, rising sea levels, and ecosystem disruptions. The primary sources of CO₂ emissions are the burning of fossil fuels, deforestation, and various industrial processes. As the global community strives to mitigate the impact of climate change, there is an urgent need for effective and sustainable methods to reduce atmospheric CO₂ levels.

Recent advancements in nanotechnology and catalysis have opened new avenues for CO₂ reduction, particularly through the development of photocatalytic systems that harness solar energy (Chen *et al.*, 2013). Photocatalysis involves the acceleration of a photoreaction in the presence of a catalyst, which can be activated by light. This approach is particularly attractive for CO₂ reduction as it offers the potential to utilize abundant and renewable solar energy to drive the conversion of CO₂ into valuable products such as CO, CH₄, formic acid and ethylene. (Malkhandi et Yeo, 2019).

Among various photocatalytic materials, plasmonic nanoparticles, especially those made of gold (Au), have gained significant attention due to their unique optical properties. Other materials, such as silver (Ag), aluminum (Al), and copper (Cu), also exhibit plasmonic activity and are widely studied for their applications in photocatalysis. Plasmonic nanoparticles exhibit localized surface plasmon resonances (LSPRs), which occur when the conduction electrons on the nanoparticle surface oscillate in resonance with incident light. This resonance leads to the generation of strong electromagnetic fields, primarily in hot spots such as small nanometer gaps or sharp features, making the activity highly dependent on the shape and aggregation level in the nanoparticle dispersion. These properties make plasmonic nanoparticles highly effective in driving photocatalytic reactions (Fong et Yung, 2013).

Gold nanoparticles (AuNPs) are particularly promising in this context due to their stability, and strong plasmonic properties. When exposed to light, AuNPs can absorb and concentrate light energy, creating "hot spots" where the local electromagnetic field is significantly enhanced. This localized energy can facilitate various chemical reactions, including the reduction of CO₂, via the creation of energetic charge carriers (Zhang *et al.*, 2023). The ability to tailor the size, shape, and surface chemistry of AuNPs further allows for optimization of their plasmonic properties and catalytic performance.

The integration of plasmonic AuNPs with other catalytic materials can create hybrid systems with synergistic effects, enhancing the overall catalytic efficiency. In this research, iron tetraphenyl porphyrin (FeTPP), an organometallic catalyst known for its catalytic activity in CO₂ reduction, is combined with AuNPs to form a hybrid catalyst. FeTPP can effectively facilitate the reduction of CO₂, and its combination with plasmonic AuNPs aims to enhance this activity under light irradiation.

The concept of using plasmonic nanoparticles in combination with organometallic catalysts for CO₂ reduction is rooted in the broader field of photocatalysis, which has seen substantial growth over the past few decades. Photocatalytic CO₂ reduction mimics natural photosynthesis, where sunlight drives the conversion of CO₂ and water into glucose and oxygen. However, unlike biological systems, photocatalytic systems can be designed to produce a range of valuable chemicals, such as carbon monoxide (CO), methane (CH₄), methanol (CH₃OH), and other hydrocarbons, which can serve as fuels or feedstocks for chemical industries (Kushnarenko *et al.*, 2024).

In this study, we build upon these advancements by exploring the synthesis and optimization of AuNPs for their integration with FeTPP. The goal is to develop a hybrid catalyst that leverages the plasmonic properties of AuNPs to enhance the photocatalytic reduction of CO₂ by the porphyrin. By investigating various parameters, such as the nanoparticles' size, shape, and surface chemistry, we aim to identify the optimal conditions for maximizing their catalytic performance.

The experimental techniques employed in this research, including UV-Vis spectroscopy, gas chromatography, scanning electron microscopy, atomic force microscopy, dynamic light scattering, and transmission electron microscopy, provide comprehensive insights into the properties and behaviour of the synthesized nanoparticles. These techniques allow us to characterize the optical and structural properties of the AuNPs, assess their stability and dispersion, and evaluate their catalytic performance in CO₂ reduction reactions.

1.3 Research Objectives

The overarching aim of this research is to develop a hybrid catalytic system that leverages the unique properties of plasmonic gold nanoparticles (AuNPs) and an organometallic catalyst, iron tetraphenyl porphyrin (FeTPP), to enhance the efficiency and selectivity of carbon dioxide (CO₂) reduction processes. This section details the project's specific objectives.

1.3.1 Synthesis of Gold Nanoparticles with Different Methods

The first objective is to synthesize gold nanoparticles using various methods to explore the influence of synthesis parameters on the properties of the nanoparticles. The methods investigated include:

1. Turkevich Method:

In the Turkevich method, gold nanoparticles are synthesized by reducing gold chloride (HAuCl_4) using sodium citrate as a reducing agent. This process involves dissolving gold chloride in water, then adding sodium citrate, followed by heating the solution. The reduction of gold ions leads to the formation of AuNPs. The size and shape of the nanoparticles can be precisely controlled by varying key parameters, including the concentration of sodium citrate, temperature, and pH (Facchi *et al.*, s. d.).

As depicted in Figure 1, this method effectively produces AuNPs with tailored properties, which are essential for optimizing the hybrid catalytic system.

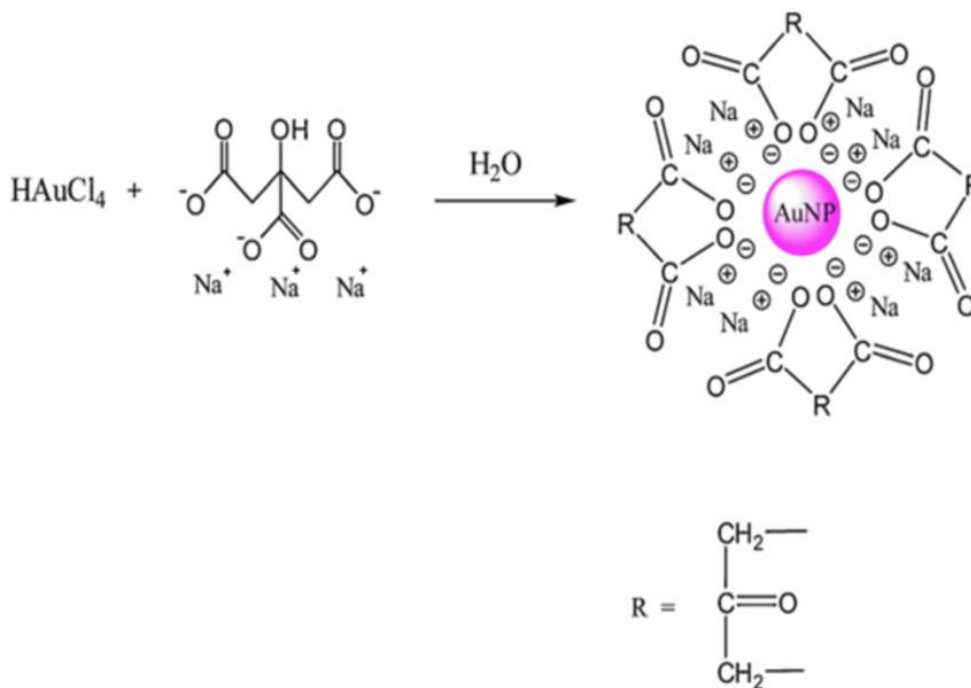


Figure 1.1. Synthesis of gold nanoparticles (AuNPs) via the Turkevich method, where sodium citrate reduces Au^{3+} ions from HAuCl_4 and stabilizes the formed nanoparticles by capping their surface. (Facchi *et al* 2023) reproduced with permission

2. Seed Growth Method:

The seed growth method is a two-step synthesis technique that allows precise control over the size and morphology of gold nanoparticles (Situ *et al.*, 2023). This makes it a valuable approach for producing particles with specific plasmonic properties.

Initially, gold seeds are prepared using cetyltrimethylammonium chloride (CTAC) as a stabilizing agent and citric acid to control particle growth. Chloroauric acid (HAuCl_4) serves as the gold precursor, and sodium borohydride (NaBH_4) acts as a strong reducing agent to facilitate seed formation.

In the subsequent growth phase, the prepared gold seeds are introduced into a solution containing cetyltrimethylammonium bromide (CTAB), which directs and stabilizes the growth of the nanoparticles. Silver nitrate (AgNO_3) regulates the nanoparticle morphology, hydrochloric acid (HCl) adjusts the pH, and additional chloroauric acid provides gold ions. Ascorbic acid, a mild reducing agent, promotes the reduction of these ions at the seed surface, leading to the formation of gold nano bipyramids (Au NBPs) with sharp tips, enhancing their plasmonic activity for photocatalytic CO_2 reduction.

As illustrated in Figure 2, panels (b-e) demonstrate how this method effectively controls the growth mechanism, resulting in various nanoparticle shapes, including Au NPs, Au NRs, and Au NBPs.

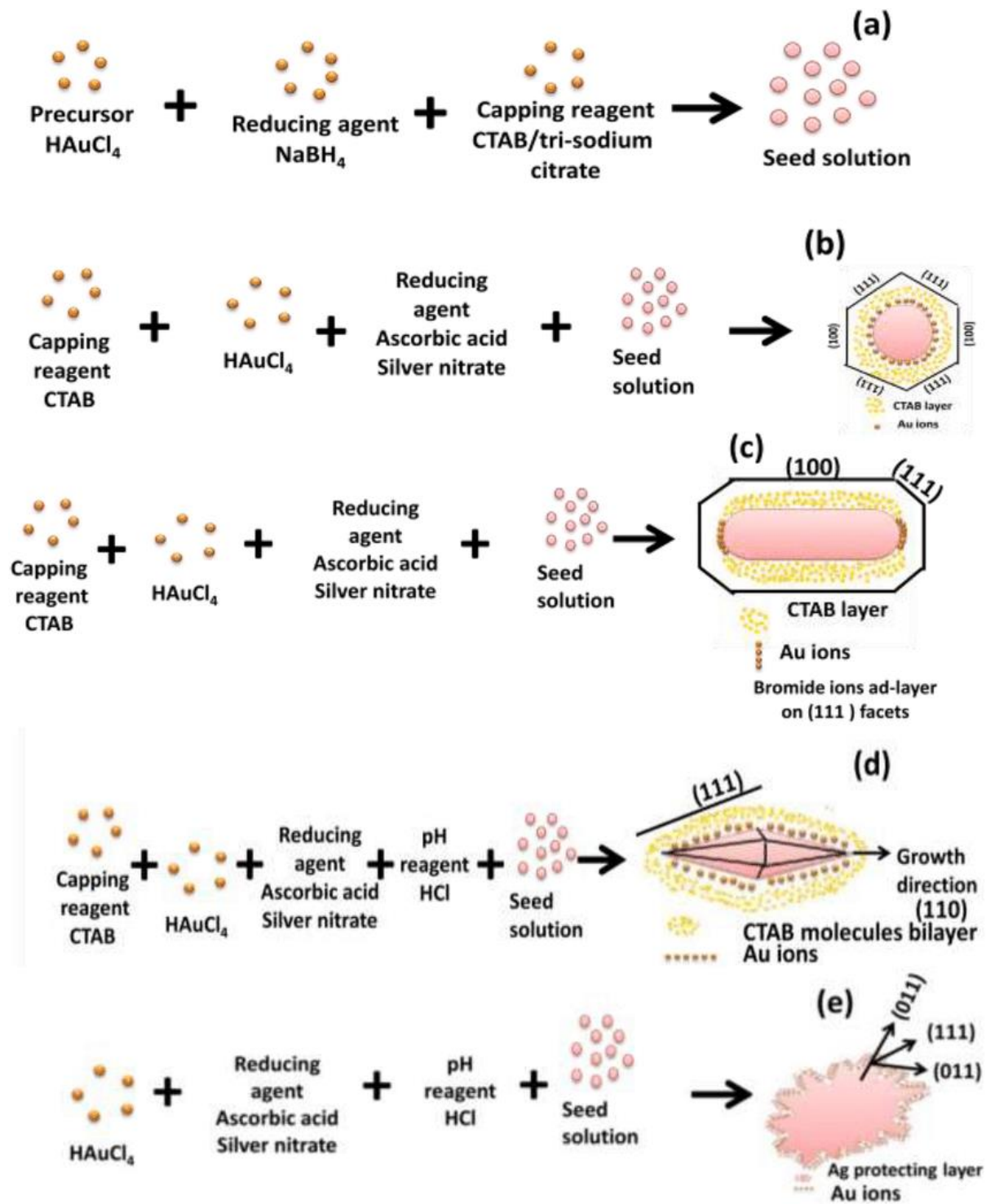


Figure 1.2. Synthesis of gold nanoparticles using seed-mediated growth. (a) Formation of seeds using HAuCl_4 and NaBH_4 . (b-e) Growth of various shapes (spheres, bipyramids, triangles, and stars) by adjusting the capping agents, reducing agents, and pH in subsequent steps. (Meher et Chaur, 2020) reproduced with permission

3. Electrodeposition of Gold Nanoparticles on FTO:

Since one of the main challenges in the previous methods was depositing gold nanoparticles on surfaces like FTO or glass, which was time-consuming and did not result in a uniform deposition, we decided to test electrodeposition. This method ensures that gold nanoparticles are deposited uniformly and consistently on the desired surface (Ma *et al.*, 2009). The electrodeposition method involves depositing gold nanoparticles onto any conductive substrate like fluorine-doped tin oxide (FTO) substrates through an electrochemical process. Gold chloride (HAuCl_4) is used as the precursor, and by applying a specific voltage, gold ions are reduced and deposited onto the FTO surface (Bagheri *et al.*, 2015). This technique allows precise control over the size and distribution of the nanoparticles by adjusting key parameters, such as applied voltage, deposition time, and electrolyte composition. As depicted in Figure 3, this method can produce well-defined AuNPs, crucial for enhancing plasmonic behavior and catalytic activity.

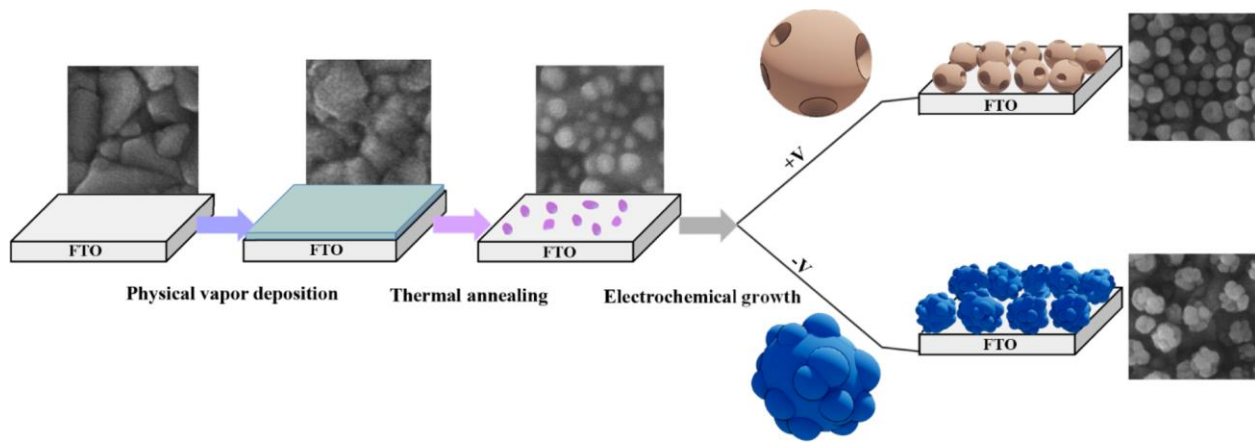


Figure 1.3. Schematic of the fabrication procedure of AuNSs on FTO. (Siampour *et al.*, 2020) reproduced with permission

1.3.2 Investigating the Plasmonic Effect of Gold Nanoparticles in the Photocatalytic CO_2 Reduction

The second objective focuses on exploring the plasmonic effect of gold nanoparticles and its role in enhancing the photocatalytic reduction of CO_2 . This involves:

1. **Optical Characterization:** Using techniques such as UV-Vis spectroscopy to analyze the optical properties of the synthesized nanoparticles. This helps in understanding how different shapes and sizes affect the plasmonic resonance.
2. **Photocatalytic Activity:** Evaluating the photocatalytic performance of the gold nanoparticles in CO₂ reduction under light irradiation. Parameters such as light intensity, wavelength, and duration will be varied to optimize the photocatalytic conditions.
3. **Mechanistic Studies:** Investigating how plasmonic excitation enhances CO₂ reduction. This includes studying the generation of hot electrons and their role in driving the catalytic reactions at the nanoparticle surface.

By comprehensively understanding the plasmonic properties and their impact on catalytic activity, we aim to identify the optimal conditions for maximizing the efficiency of CO₂ reduction.

1.3.3 Combining Gold Nanoparticles with FeTPP to Increase Effectiveness in CO₂ Reduction

The final objective was to integrate the synthesized gold nanoparticles with FeTPP to create a hybrid catalytic system. However, it should be noted that due to experimental limitations, not all objectives in this integration were fully achieved. Despite these challenges, the preliminary results offer valuable insights into the potential effectiveness of such a system for CO₂ reduction.

1. **Hybrid Catalyst Synthesis:** Developing methods to functionalize gold nanoparticles with FeTPP, ensuring strong interaction and optimal spatial arrangement between the two components.
2. **Characterization of Hybrid Catalysts:** Using techniques such as scanning electron microscopy (SEM), transmission electron microscopy (TEM), atomic force microscopy (AFM), and dynamic light scattering (DLS) to characterize the morphology, surface properties, and stability of the hybrid catalysts.
3. **Performance Evaluation:** Testing the hybrid catalysts in photocatalytic CO₂ reduction reactions. The effectiveness of the hybrid system will be compared with that of the individual components (AuNPs and FeTPP) to determine the synergistic effects.
4. **Optimization Studies:** Varying the ratio of AuNPs to FeTPP, light conditions, and other reaction parameters to optimize the catalytic performance of the hybrid system.

Through these objectives, this research seeks to develop a highly efficient and sustainable catalytic system for CO₂ reduction, contributing to the broader goals of mitigating climate change and promoting a circular carbon economy. The findings from this study will provide valuable insights into the design and optimization of advanced catalytic materials for environmental and energy applications.

1.4 Methodology

The methodology of this research involves a systematic approach to synthesizing, characterizing, and evaluating the performance of plasmonic gold nanoparticles (AuNPs) combined with iron tetraphenyl porphyrin (FeTPP) for the photocatalytic reduction of carbon dioxide (CO₂). This section outlines the experimental procedures, analytical techniques, and optimization strategies employed to achieve the research objectives.

1.4.1 Characterization of Gold Nanoparticles:

The synthesized gold nanoparticles will be characterized using a range of analytical techniques to determine their size, shape, surface properties, and optical characteristics.

1.4.1.1 UV-Vis Spectroscopy:

UV-Vis spectroscopy is an analytical technique used to measure the absorption of light in the ultraviolet and visible regions of the electromagnetic spectrum. This method is particularly useful for probing electronic transitions in materials by analyzing the light absorbed at specific wavelengths. In the case of gold nanoparticles, UV-Vis spectroscopy is employed to investigate their plasmonic behavior. As illustrated in Figure 4, light passes through a solution containing the nanoparticles, and the absorption at different wavelengths is measured. The surface plasmon resonance (SPR) peaks observed in the absorption spectra provide crucial information about the nanoparticles' size, shape, and degree of aggregation. These peaks result from the collective oscillation of the nanoparticles' conduction electrons in response to the light, and their characteristics are influenced by the particles' physical properties and the surrounding environment. Understanding these properties is essential for optimizing the nanoparticles' performance in catalysis (Borse et Konwar, 2020).

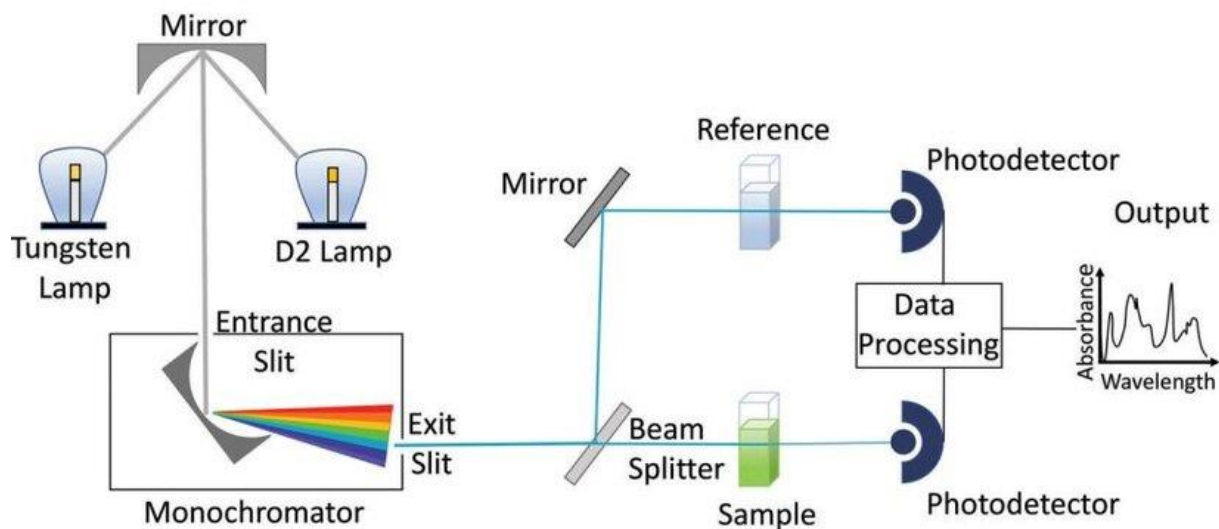


Figure 1.4. Schematic representation of a UV-Vis spectroscopy setup.

1.4.1.2 Scanning Electron Microscopy (SEM):

Scanning Electron Microscopy (SEM) is a powerful analytical technique used to visualize the morphology and surface structure of materials at a very high resolution. As shown in Figure 5, SEM works by directing a focused beam of electrons onto the sample surface, where the electrons interact with the atoms in the sample. This interaction produces various signals, including secondary electrons, which are collected to generate detailed images of the surface topography.

In this project, SEM will be employed to image the gold nanoparticles. The samples will be prepared by depositing nanoparticle solutions onto conductive substrates, ensuring proper electron flow during imaging. SEM will allow us to examine the shape, size, distribution, and surface structure of the nanoparticles with high precision. The ability to observe these properties at the nanoscale is crucial for understanding and optimizing the nanoparticles' performance in catalytic applications. By analyzing these SEM images, we can make informed decisions to enhance the effectiveness of the nanoparticles in CO₂ reduction processes (Aljabali *et al.*, 2018).

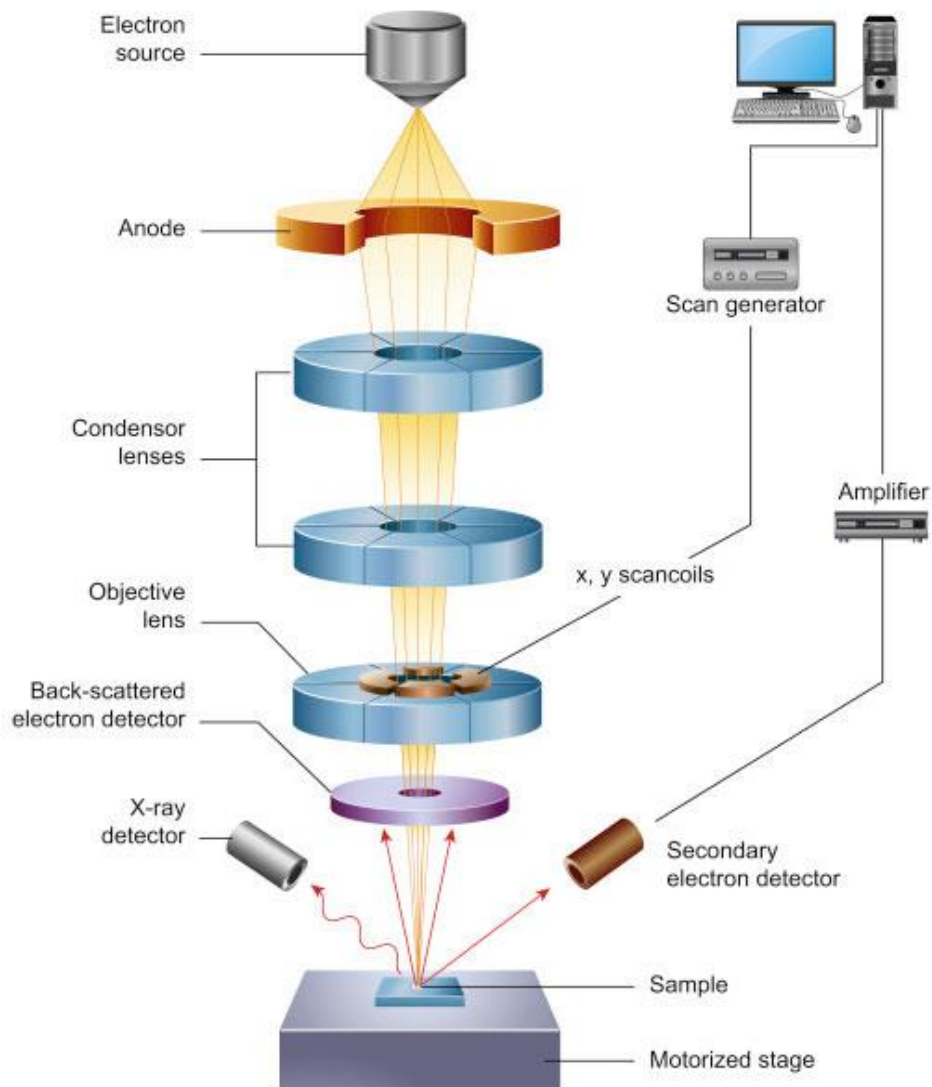


Figure 1.5. Schematic representation of the SEM technique. (Zhou *et al.*, 2007) reproduced with permission

1.4.1.3 Atomic Force Microscopy (AFM):

Atomic Force Microscopy (AFM) is an advanced technique used to obtain high-resolution images and precise measurements of the surface topography of materials at the nanometer scale. AFM works by scanning a sharp probe (also known as a cantilever) across the surface of the sample, as shown in Figure 6. As the probe moves over the surface, it interacts with the atomic forces present on the sample, which causes the cantilever to deflect. These deflections are measured and used to generate detailed topographical images of the surface (Hubenthal *et al.*, 2012).

In this project, AFM was utilized in this thesis to analyze electrodeposited films, providing topographical data to assess their roughness and general surface features. This method is particularly valuable for analyzing nanoparticles because it allows for direct measurement of their physical dimensions and surface features without requiring any special sample preparation. The information obtained from AFM is essential for understanding the physical properties of the nanoparticles and optimizing their performance in catalytic applications. By focusing on these characteristics, the research aims to enhance the efficiency and effectiveness of the nanoparticles in CO₂ reduction processes.

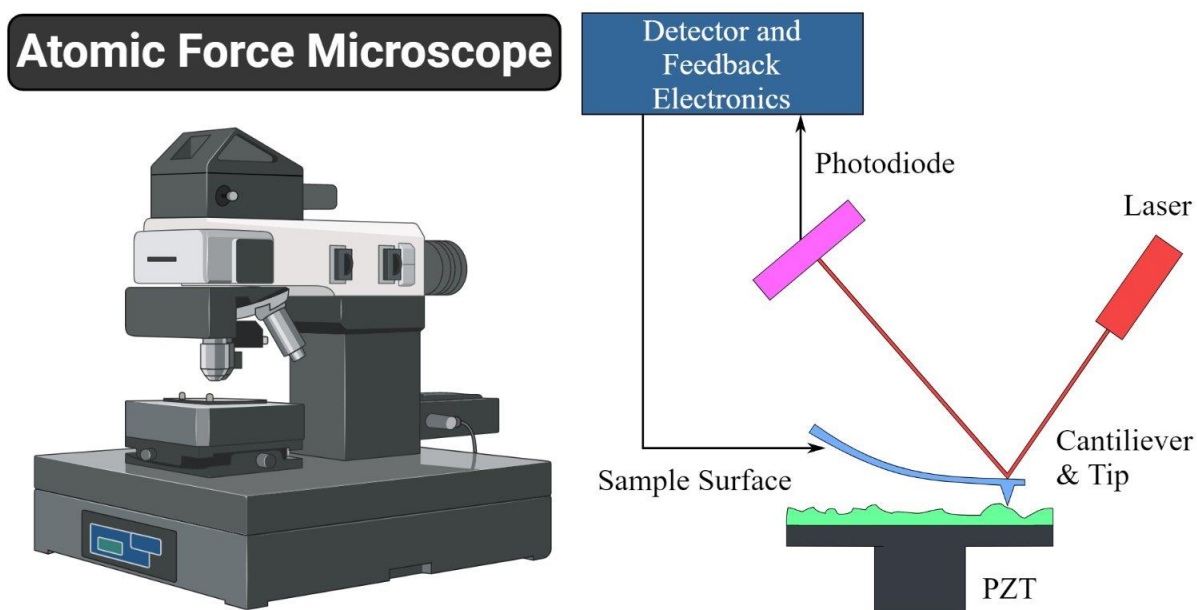


Figure 1.6. Schematic representation of an AFM technique. (Tsenova-Ilieva et Karova, 2020) reproduced with permission

1.4.1.4 Dynamic Light Scattering (DLS):

Dynamic Light Scattering (DLS) is a critical technique for determining the size distribution and stability of nanoparticles in suspension. As shown in Figure 7, DLS works by passing a laser beam through a nanoparticle solution, where the nanoparticles cause the light to scatter. The fluctuations in the intensity of the scattered light, caused by the Brownian motion of the nanoparticles, are measured over time. By analyzing these fluctuations, DLS provides information about the hydrodynamic diameter of the nanoparticles and their polydispersity index, which indicates the size distribution within the sample. In this project, DLS will be employed to measure the size distribution of gold nanoparticles in solution.

The hydrodynamic diameter obtained from DLS reflects how the nanoparticles behave in a fluid, taking into account not only their core size but also the layer of solvent molecules surrounding them. Additionally, the polydispersity index gives insights into the uniformity and stability of the nanoparticle suspension, which is crucial for ensuring consistent performance in catalytic applications. Understanding these properties is essential for optimizing the nanoparticles' effectiveness in CO₂ reduction processes (Jans *et al.*, 2009).

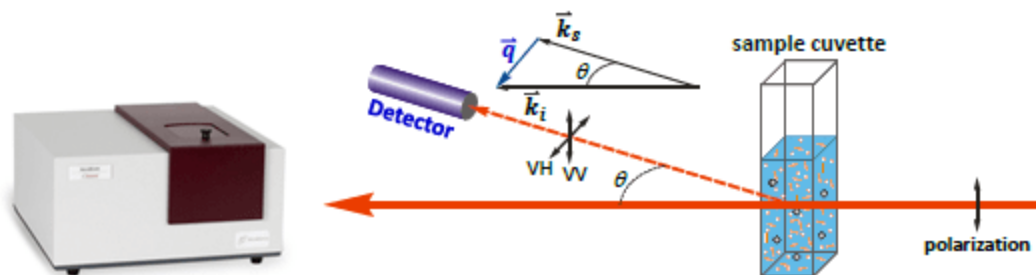


Figure 1.7. Schematic representation of a DLS technique. (Brookhaven Instruments)

1.4.1.5 Transmission Electron Microscopy (TEM):

Transmission Electron Microscopy (TEM) is a powerful technique that provides high-resolution images and detailed analysis of the internal structure and composition of nanoparticles. As shown in Figure 8, TEM works by transmitting a beam of electrons through an ultra-thin sample, with the electrons interacting with the sample's atoms as they pass through. These interactions produce images that reveal the internal structure, size, shape, and morphology of the nanoparticles with exceptional detail.

In this project, TEM will be used to observe and analyze the size, shape, and morphological details of gold nanoparticles. The high-resolution capabilities of TEM make it possible to visualize the fine structural details of nanoparticles, which are crucial for understanding their behavior and properties. Additionally, TEM was employed in this thesis to confirm the shape and size of the gold nanoparticles, rather than to examine lattice fringes or obtain crystallographic information. This level of analysis is essential for comprehensively understanding the fundamental properties of the nanoparticles and optimizing their applications in catalysis, where precise control over particle size and structure can significantly influence catalytic activity (Rattanawongwiboon *et al.*, 2022).

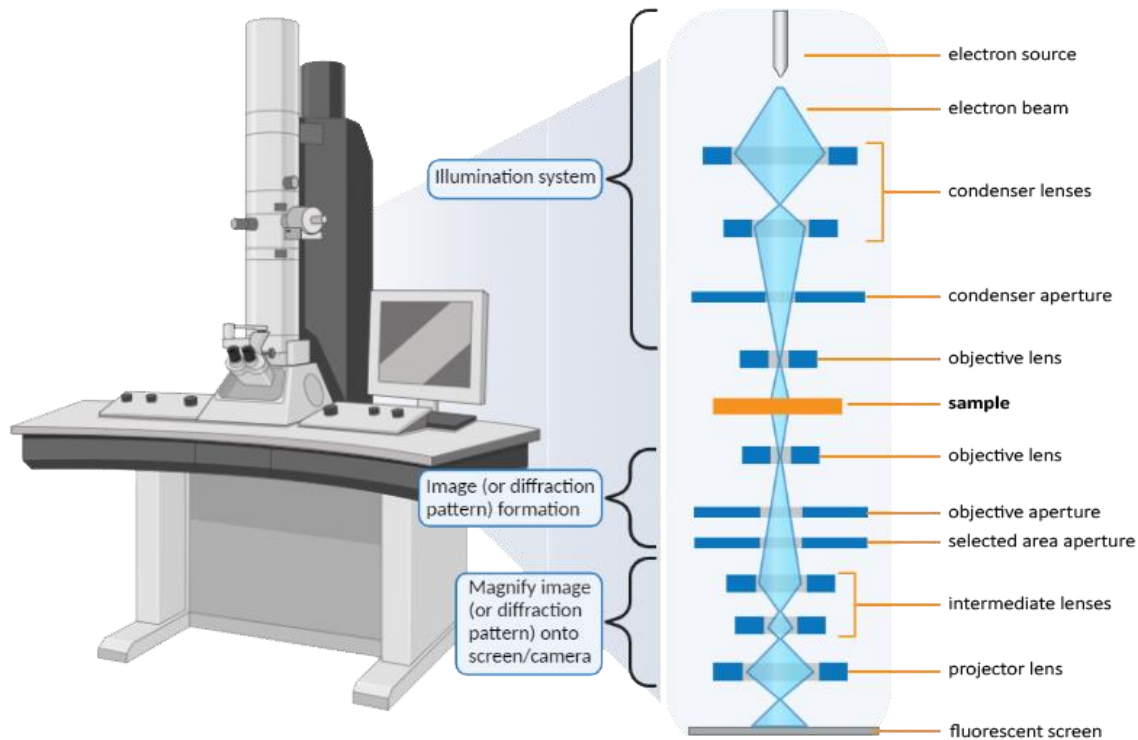


Figure 1.8. Schematic representation of a TEM technology. (NanoScience).

1.4.1.6 Gas Chromatography (GC):

Gas Chromatography (GC) is an analytical technique that separates, identifies, and quantifies components within a gas mixture. In this project, GC will be employed to analyze the composition of gaseous products resulting from the CO₂ reduction process. This analysis is essential for determining the efficiency and selectivity of the catalytic reactions involving the synthesized nanoparticles. In this CO₂ reduction experiment, we use gas chromatography (GC) to detect and quantify the main products, which are carbon monoxide (CO) and hydrogen (H₂). These are key products in the catalytic reduction process, and measuring them is crucial for evaluating the reaction's efficiency.

The process involves injecting the gas sample directly into the GC system, where it is carried by an inert gas (the mobile phase) through a column packed with a stationary phase. As the gas mixture travels through the column, its components separate based on their interactions with the stationary phase. These interactions depend on factors such as molecular size, polarity, and boiling point (though in our case, the focus is on separation based on molecular interactions rather than vaporization).

After separation, the individual components of the gas mixture are detected and quantified by a detector, providing a detailed analysis of the sample's composition, shown in Figure 9. This information is crucial for evaluating the performance of the catalytic system, understanding the chemical properties of the reaction products, and ensuring the quality and consistency of the CO₂ reduction process (Gross *et al.*, 2003).

Gas Chromatography

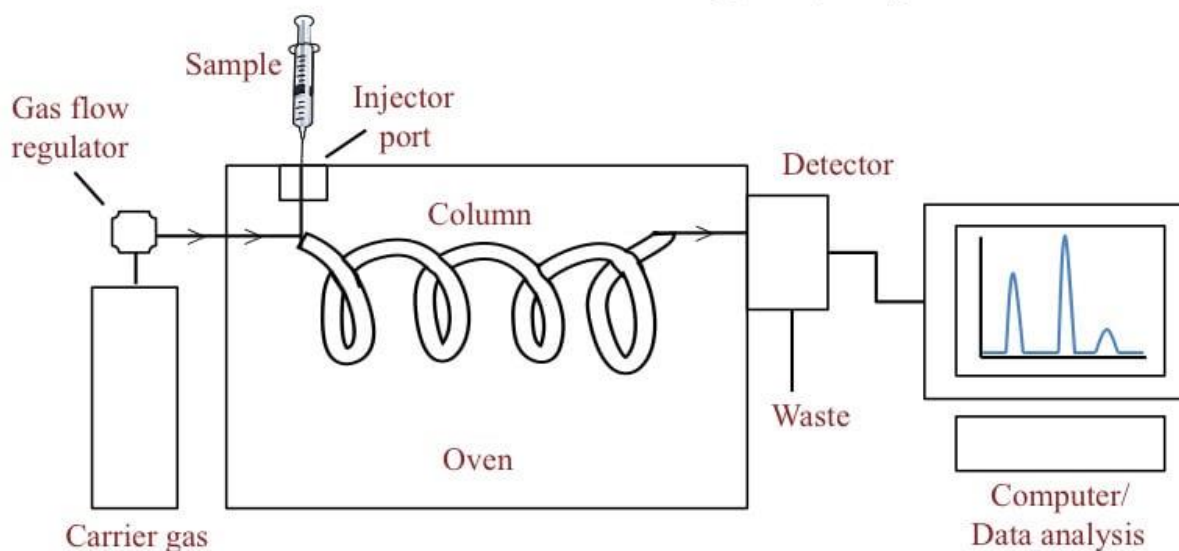


Figure 1.9. Schematic representation of a (GC) Gas Chromatography. (Bitesize Bio)

1.5 Structure of the Thesis

This thesis is organized into several chapters, each addressing a specific aspect of the research on combining plasmonic gold nanoparticles (AuNPs) with iron tetraphenyl porphyrin (FeTPP) for the photocatalytic reduction of carbon dioxide (CO₂). The structure is designed to provide a logical progression from the background and motivation of the study, through the experimental methods and results, to the conclusions and implications of the findings.

Chapter 2: Literature Review: In this chapter, a comprehensive review of the existing literature on CO₂ reduction methods, plasmonic nanoparticles, and hybrid catalytic systems is presented. The review covers fundamental principles, recent advancements, and gaps in the current knowledge that this research aims to address.

Chapter 3: Synthesis and Characterization of AuNP: This chapter details the experimental procedures used to synthesize and characterize gold nanoparticles, investigate their plasmonic properties, and develop the hybrid AuNP-FeTPP catalysts. It includes descriptions of the synthesis methods, characterization techniques, and performance evaluation tests.

Chapter 4: Photocatalyst Experiment: This chapter describes the experimental procedures for depositing gold nanoparticles on various substrates (glass, ITO, and FTO), combining gold nanoparticles with FeTPP, and conducting photocatalysis and photoelectrocatalysis experiments to investigate CO₂ reduction.

CHAPITRE 2

Literature Review

2.1 Introduction

Escalating atmospheric carbon dioxide (CO₂) levels represent one of our time's most pressing environmental challenges. CO₂, a primary greenhouse gas, is a significant driver of global warming and climate change, leading to severe ecological, economic, and social impacts worldwide. The urgent need to mitigate CO₂ emissions has spurred extensive research into innovative and sustainable technologies for CO₂ reduction. Among these, nanomaterials, particularly plasmonic nanoparticles, have emerged as a promising approach due to their unique optical properties and catalytic potential (Li *et al.*, 2021).

This chapter reviews the existing literature on the fundamental principles and recent advancements in the fields of plasmonic materials, organometallic catalysts, and CO₂ reduction techniques. The review aims to contextualize the current research within the broader scientific landscape, highlighting the synergistic potential of combining plasmonic materials with organometallic catalysts to enhance CO₂ reduction processes.

The chapter begins with an overview of plasmonic materials, focusing on their unique properties, mechanisms of action, and applications in catalysis. Plasmonic nanoparticles, especially those made of noble metals like gold and silver, exhibit remarkable optical properties due to their ability to support localized surface plasmon resonances (LSPRs). These resonances lead to enhanced light absorption and electromagnetic field concentration at the nanoparticle surface, which can be harnessed to drive various chemical reactions, including the reduction of CO₂.

Following the discussion on plasmonic materials, the chapter delves into the realm of organometallic catalysts, with a particular emphasis on iron tetraphenyl porphyrin (FeTPP). Organometallic catalysts, which consist of metal atoms coordinated to organic ligands, are known for their high catalytic activity and selectivity in various chemical transformations. FeTPP has shown significant promise in the catalytic reduction of CO₂, owing to its ability to activate CO₂ molecules and facilitate their conversion into valuable products.

The literature review then examines the various techniques developed for CO₂ reduction, ranging from traditional methods such as chemical absorption and biological fixation to advanced approaches like photocatalysis and electrocatalysis. Each method is evaluated in terms of its efficiency, scalability, and environmental impact. The limitations and challenges associated with conventional CO₂ reduction techniques underscore the need for more effective and sustainable solutions.

The synergistic combination of plasmonic materials and organometallic catalysts is exciting for CO₂ reduction. This synergy leverages the strengths of both components: the enhanced light absorption and electron transfer capabilities of plasmonic nanoparticles, and the high catalytic activity of organometallic catalysts. By integrating these materials into hybrid catalytic systems, researchers aim to develop novel photocatalytic processes that are both efficient and sustainable (Cuong et Quang, 2020).

The chapter concludes with a summary of the key findings from the literature review, highlighting the potential of hybrid catalytic systems for CO₂ reduction. The insights gained from this review will inform the current research's subsequent experimental design and methodology, providing a solid foundation for developing advanced catalytic materials for environmental and energy applications.

2.2 Overview of Plasmonic Materials

Plasmonic materials are a class of materials that exhibit unique optical properties due to their ability to support collective oscillations of free electrons, known as plasmons when interacting with light. These materials are typically metals, such as gold, silver, and copper. (Naik *et al.*, 2013)

The most fundamental concept in plasmonics is surface plasmon resonance (SPR), which occurs when light interacts with the free electrons on the surface of a metal, leading to a collective oscillation of these electrons. This phenomenon is particularly pronounced at sharp corners and tips. (Hinman *et al.*, 2017)

The conditions for SPR are highly dependent on the frequency of the incident light, the optical properties of the materials involved, and the geometry of the metal surface. When SPR is excited, it leads to a dramatic increase in the local electromagnetic field at the surface, which is confined to a region much smaller than the wavelength of the incident light (Zhou *et al.*, 2018). This confinement enhances light-matter interactions, making SPR a powerful tool in various scientific and technological applications,

however the focus here remains on the fundamental aspects. Figure 2.1 shows surface plasmon resonance (SPR).

One of the most striking features of plasmonic materials is their ability to confine electromagnetic fields to nanoscale dimensions, far below the diffraction limit of light. This confinement is a direct consequence of the interaction between light and the free electrons in the metal. (Piazza *et al.*, 2015)

Smaller particles tend to have more pronounced field enhancements due to the higher surface-to-volume ratio, which increases the concentration of free electrons at the surface.

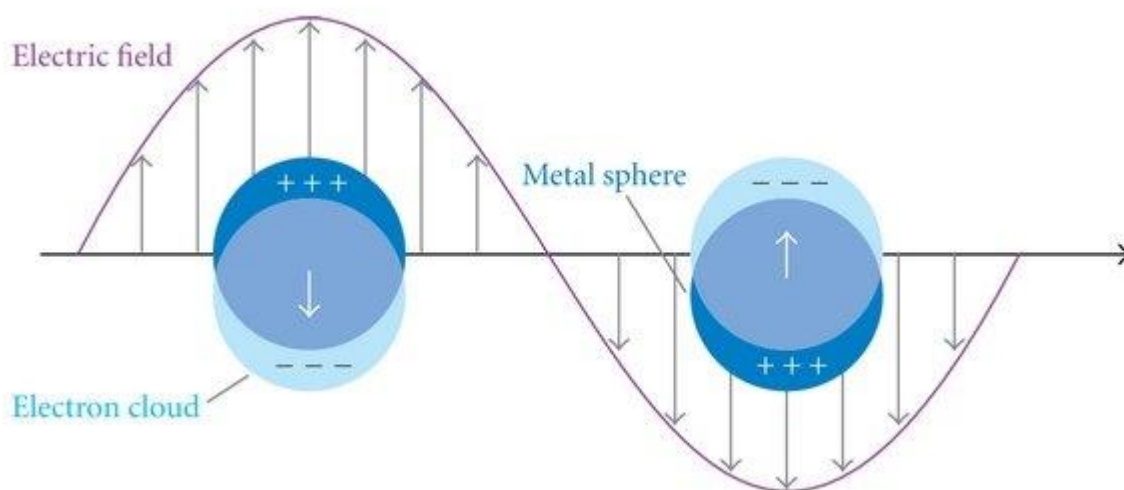


Figure 2.1. Illustrations of (a) surface plasmon resonance (SPR) and (b) localized surface plasmon resonance (LSPR), resulting from the collective oscillations of delocalized electrons in response to an external electric field. (Hong *et al.*, 2012) reproduced with permission

2.2.1 Hot electron and Plasmonic Effects in Catalysis

Hot electrons are generated when light interacts with plasmonic materials. When surface plasmons are excited by incident light, the energy from the electromagnetic field can be transferred to the free electrons within the metal, elevating them to higher energy states. These energized electrons, known as "hot electrons," possess kinetic energies higher than the Fermi level of the metal, making them more reactive. (Park *et al.*, 2015). In plasmonic catalysis, these hot electrons play a critical role by providing the necessary energy to drive chemical reactions that might require high activation energy. The generation of hot electrons is particularly efficient in noble metals like gold, silver, and copper, commonly used in plasmonic applications due to their favourable electronic properties. These hot electrons are not just a byproduct;

they are the key to unlocking the chemical potential of AuNPs in catalysis. Specifically, in CO₂ reduction, the hot electrons generated by AuNPs can be transferred to CO₂ molecules that are adsorbed onto the surface of the nanoparticles. This electron transfer is crucial as it weakens the robust carbon-oxygen bonds within the CO₂ molecule, facilitating its conversion into more valuable products, such as carbon monoxide (CO) or hydrocarbons, which can serve as precursors for industrial applications.. This process not only helps mitigate CO₂ emissions, a major contributor to global warming, but also enables the production of useful chemicals with wide industrial applications (Zeng *et al.*, 2020).

Gold nanoparticles are particularly efficient in this regard due to their strong plasmonic resonance in the visible spectrum and their ability to generate hot electrons that can efficiently interact with CO₂. Moreover, the surface properties of AuNPs can be tuned (e.g., by size, shape, or functionalization) to enhance the interaction between the hot electrons and the CO₂ molecules, improving the overall catalytic efficiency.(Ghosh et Pal, 2007)

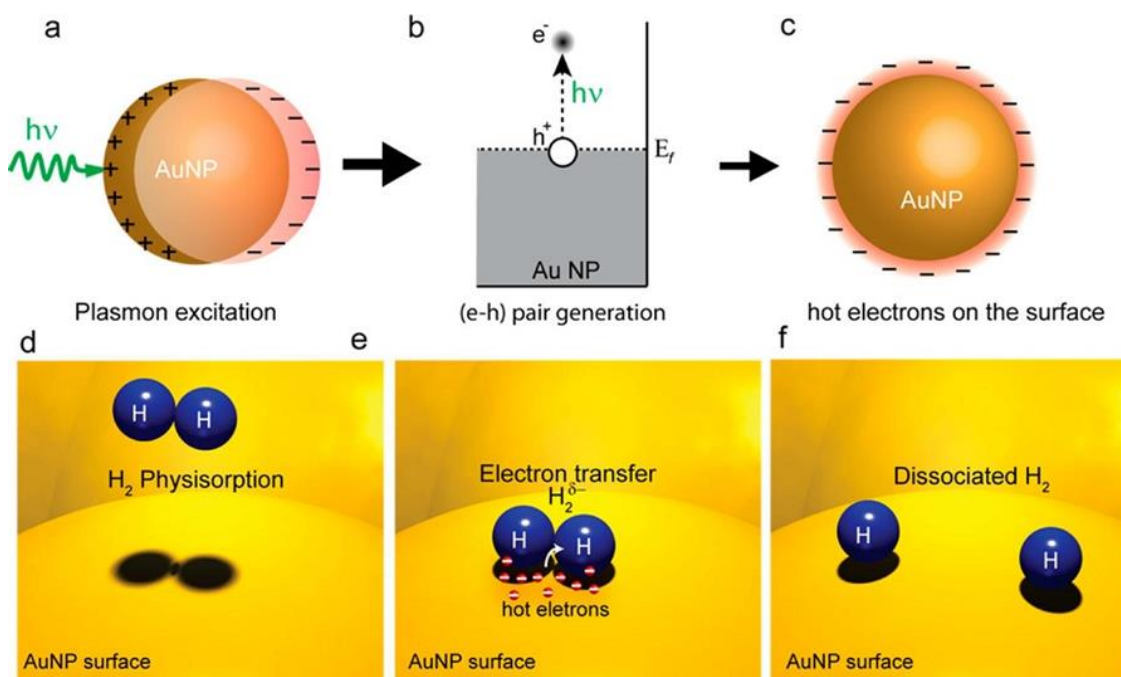


Figure 10. Schematics of plasmon-induced hot electron generation on AuNP and mechanistic representation of H₂ dissociation on the AuNP surface. (Mukherjee *et al.*, 2013) reproduced with permission

When a plasmonic nanoparticle absorbs light, it creates a collective oscillation of its conduction electrons. This oscillation can decay via two primary mechanisms: The energy is re-emitted as photons and the energy is transferred to the conduction electrons, producing hot electrons. The non-radiative decay process is more relevant in catalysis, as it directly leads to the formation of hot electrons. These hot electrons are usually generated within femtoseconds and can either thermalize rapidly or be extracted before thermalization to participate in chemical reactions.(Wang *et al.*, 2019)

In the context of catalysis, hot electrons can be injected into adsorbed molecules on the nanoparticle surface, activating chemical bonds. This can reduce the activation energy required for a reaction, effectively lowering the reaction barrier. For instance, in CO₂ reduction, hot electrons can help break the strong C=O bonds in CO₂ molecules, facilitating their conversion into more valuable products like CO or hydrocarbons (Chu *et al.*, 2020).

One of the major advantages of gold is its remarkable chemical stability. Unlike silver or copper, which can tarnish or corrode over time due to oxidation, gold remains stable and retains its plasmonic and electronic properties even in harsh environments. This stability is essential for long-term applications where maintaining consistent performance is critical, such as in environmental sensors, where the material may be exposed to reactive gases or liquids over extended periods.

2.2.2 Influence of Size and Shape on Gold Nanoparticles (AuNPs) in Plasmonic Catalysis:

Size of Gold Nanoparticles: The size of gold nanoparticles (AuNPs) plays a critical role in determining their plasmonic properties, which directly influences their efficiency in catalysis, including CO₂ reduction.

The resonance frequency of LSPR, which is the specific wavelength at which the oscillation of surface electrons is maximized, depends on the size of the nanoparticles. Smaller nanoparticles generally exhibit LSPR in the visible range of the spectrum, which is ideal for applications requiring visible light activation, such as photocatalysis. As the size of AuNPs decreases, the LSPR peak typically shifts towards shorter wavelengths (blue shift), and the peak becomes broader. Smaller AuNPs tend to generate hot electrons more efficiently due to the increased surface-to-volume ratio. This means that a higher proportion of the atoms in smaller nanoparticles are at the surface, where they can directly interact with incident light and adsorbed molecules like CO₂. The increased surface area also enhances the probability of hot electron

transfer to adsorbed molecules, making smaller AuNPs more effective for catalytic processes that rely on hot electrons (Panigrahi *et al.*, 2007).

Shape of Gold Nanoparticles: The shape of gold nanoparticles also significantly impacts their plasmonic behavior and catalytic performance. Different shapes of AuNPs, such as spheres, rods, cubes, and stars, exhibit distinct plasmonic properties.

Anisotropic AuNPs, such as gold nanorods or nanostars, exhibit multiple plasmon resonance modes due to their non-spherical shapes. For instance, gold nanorods have two LSPR peaks: one corresponding to the transverse mode (shorter wavelength) and the other to the longitudinal mode (longer wavelength). The longitudinal mode, in particular, can be tuned to the near-infrared region, which is advantageous for catalysis under longer wavelength light. The aspect ratio (length-to-width ratio) of nanorods directly affects the position of the longitudinal LSPR peak. Higher aspect ratios shift the peak to longer wavelengths, enabling the tuning of plasmonic properties to match specific light sources (Zhang *et al.*, 2007).

Non-spherical shapes, like nanostars or nanocubes, can create plasmonic "hot spots" at their sharp edges, tips, or corners. These hot spots are regions where the electromagnetic field is highly concentrated, leading to significantly enhanced local electric fields.(Hentschel *et al.*, 2011)

These enhanced fields can increase the generation of hot electrons at specific sites on the nanoparticle surface, which can then be transferred to CO₂ molecules more effectively, boosting the catalytic reaction's efficiency.

The shape of AuNPs also affects their surface reactivity. Nanoparticles with more complex shapes (e.g., stars or branched structures) have a higher density of reactive sites (like edges and corners) where chemical reactions are more likely to occur. These sites often exhibit lower coordination numbers, meaning the atoms at these sites have fewer neighbouring atoms, which makes them more reactive. For CO₂ reduction, having a higher density of reactive sites can enhance the interaction between the gold surface and CO₂ molecules, facilitating their activation and subsequent reduction.(Carnovale *et al.*, 2016)

2.3 Organometallic Catalyst

Organometallic catalysts are a unique class of catalysts that contain metal atoms bonded to organic ligands, combining the reactivity of metal centers with the versatility of organic chemistry. These catalysts play a crucial role in various industrial and environmental processes due to their ability to facilitate a wide range of chemical transformations with high efficiency and selectivity. This section provides an overview of organometallic catalysts, focusing on their properties, mechanisms, and applications, with a particular emphasis on their use in CO₂ reduction. (Apaydin *et al.*, 2017)

2.3.1 Fundamental Properties of Organometallic Catalysts

Organometallic catalysts are characterized by several key properties that make them highly effective for catalytic applications:

The coordination of metal atoms with organic ligands forms the basis of organometallic chemistry. This metal-ligand interaction allows for fine-tuning of the electronic and steric properties of the catalyst, enabling precise control over its reactivity and selectivity.

The electronic properties of the metal center can be modulated by the nature of the ligands attached to it. Electron-donating or electron-withdrawing ligands can alter the electron density at the metal center, affecting its catalytic activity and the types of reactions it can facilitate. (Steinborn, 2011)

Organometallic catalysts are known for their ability to activate small molecules, such as CO₂, H₂, and O₂, and facilitate their conversion into more valuable products. The presence of both metal and organic components allows for a high degree of selectivity in these transformations, often leading to fewer side products and higher yields.

2.3.2 Iron Tetraphenyl Porphyrin (FeTPP) as a Catalyst for CO₂ Reduction

Iron tetraphenyl porphyrin (FeTPP) is a prominent organometallic catalyst known for its efficiency in catalyzing the reduction of CO₂. FeTPP consists of an iron (Fe) atom coordinated to a porphyrin ring, which is further substituted with phenyl groups. This structure mimics the active sites of natural enzymes such as cytochromes and provides a robust platform for catalytic activity (Mondal *et al.*, 2019).

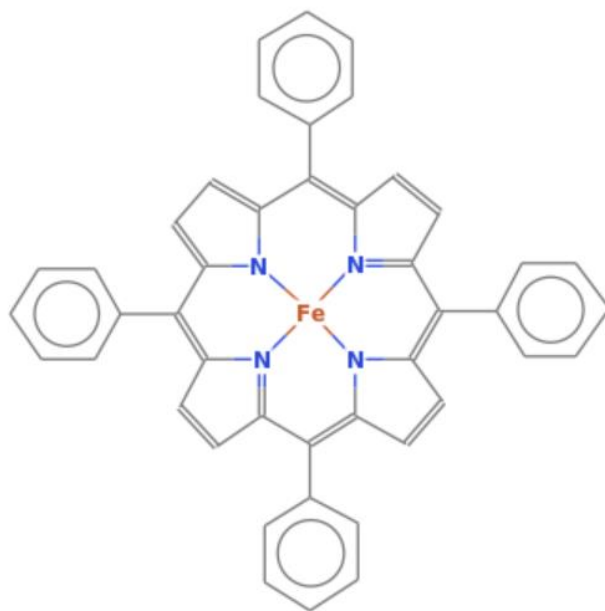


Figure 11. Iron tetraphenyl porphyrin structure.

Structure and Properties: The porphyrin ring in FeTPP provides a stable and planar environment for the central iron atom, enhancing its ability to coordinate and activate CO_2 molecules. The phenyl groups attached to the porphyrin ring can be modified to adjust the electronic and steric properties of the catalyst, optimizing its performance for specific reactions.

Mechanism of CO_2 Reduction: The catalytic cycle for CO_2 reduction using iron tetraphenyl porphyrin (FeTPP) involves several key steps that include CO_2 activation, electron transfer, and product release. The cycle can be understood through the following detailed steps, supported by both theoretical and experimental data:

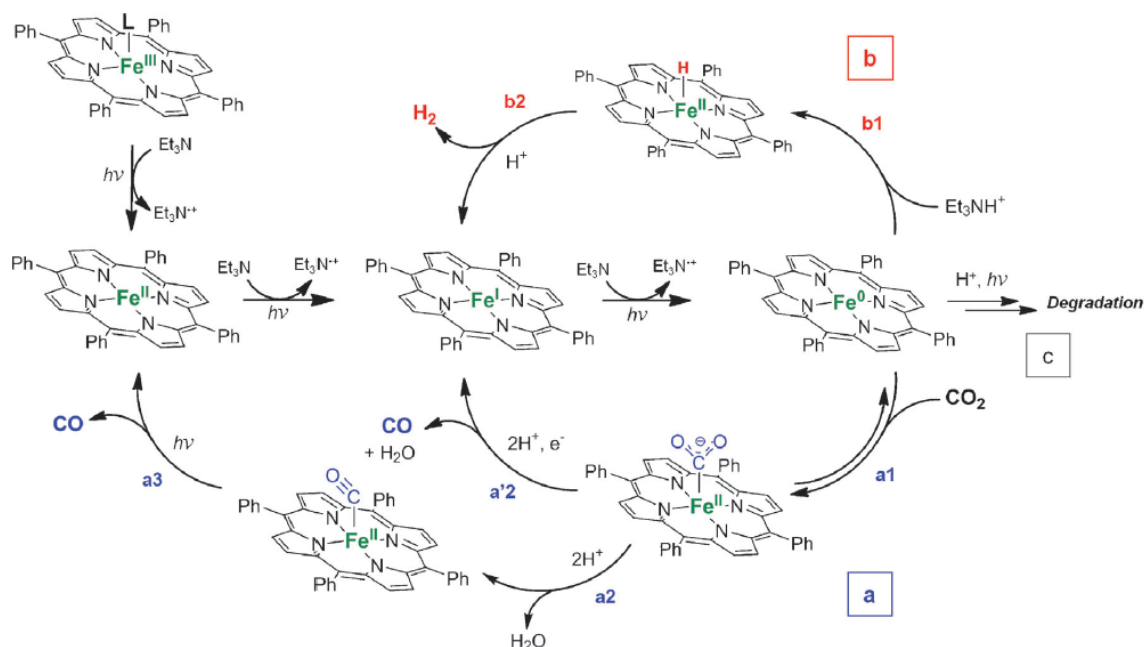


Figure 2.4. Proposed mechanism for the photochemical catalytic reduction of CO₂ to a) CO and b) H₂ with PFe catalysts. (Bonin *et al.*, 2014) reproduced with permission

1. CO₂ Binding and Activation:

The first step in the catalytic cycle involves the coordination of a CO₂ molecule to the iron center of FeTPP, which typically starts in the Fe(0) oxidation state. This coordination is crucial as it activates the otherwise inert CO₂ molecule, making it susceptible to subsequent reduction. The binding of CO₂ to the iron center results in the formation of a Fe(II)-CO₂ adduct, where the CO₂ is bound in a bent geometry. This activation process is often the rate-determining step (RDS) of the reaction, as it involves a significant change in the coordination environment of the iron center (Amanullah *et al.*, 2024).

2. Electron Transfer and Reduction:

Following CO₂ binding, electron transfer to the CO₂ molecule occurs. The iron center in FeTPP undergoes a series of redox changes, cycling between Fe(0), Fe(I), and Fe(II) states. This electron transfer is facilitated by the iron's ability to stabilize different oxidation states, which is a key characteristic of Fe porphyrins. During this step, the coordinated CO₂ is progressively reduced. The reaction may proceed through the

formation of intermediates such as a Fe(II)-CO_2^{2-} species, which can be further reduced to form Fe(II)-CO . This intermediate is then converted to Fe(I)-CO as more electrons are supplied. The Fe(I)-CO species is a crucial intermediate, indicating the reduction of CO_2 to CO , the final product of the catalytic cycle.

The figure 14. provided in the image shows the relationship between the Gibbs free energy of binding ($\Delta G_{\text{binding}}$) and the energy barrier (ΔG^\ddagger) for different intermediates (Shome *et al.*, 2024). The strong correlation ($R^2 = 0.998$) between these values indicates the efficiency of the catalytic process, with lower energy barriers leading to more favorable CO_2 reduction.

3. Role of Scavengers:

In the solution, electron and proton scavengers such as ascorbate or sacrificial donors like triethylamine play an essential role in the catalytic cycle. These scavengers provide the necessary electrons and protons to facilitate the reduction process, helping to maintain the iron in its reduced state and enabling the continuous cycling of FeTPP. Without these scavengers, the catalytic efficiency would decrease, as the Fe center might not return to its active state as readily.

4. Product Release and Catalyst Regeneration:

The final step in the cycle involves the release of the reduced CO product from the FeTPP complex. This step regenerates the active FeTPP species, typically in the Fe(0) or Fe(I) state, ready to participate in another cycle of CO_2 reduction. The release of CO is a critical step, as it frees the iron center to bind another CO_2 molecule and continue the catalytic cycle. (Wang et Lai, 2024)

The schematic diagram 2.5 provided shows the overall cycle, emphasizing the importance of the different redox states of iron and the binding and release of CO_2 and CO . This visual representation helps to clarify the stepwise reduction of CO_2 and the regeneration of the catalyst.

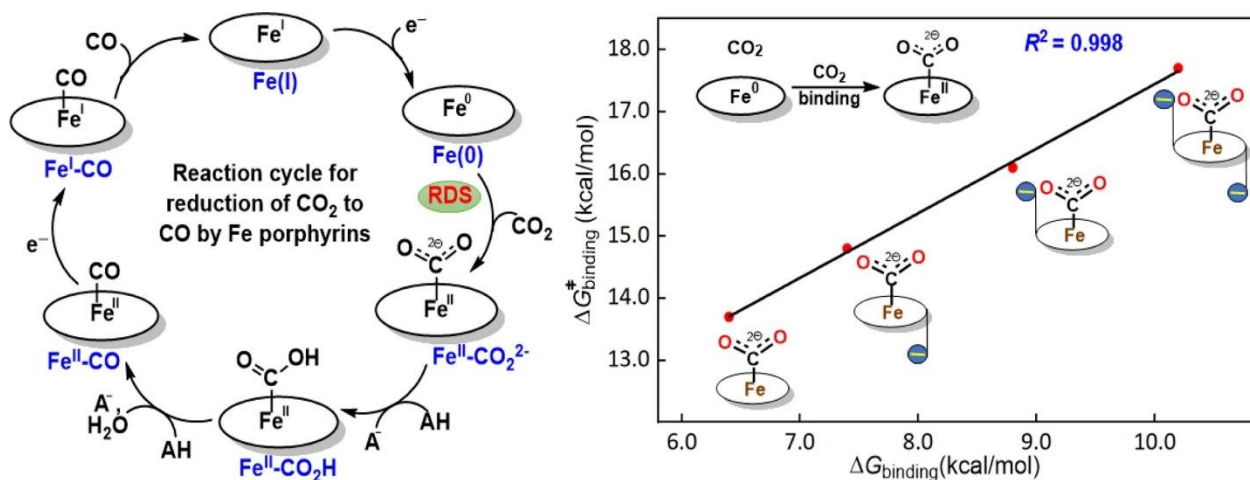


Figure 2.5. Catalytic Cycle for CO₂ Reduction to CO by Iron Porphyrin Complexes. (Wang et al., 2024) reproduced with permission

2.4 CO₂ Reduction Techniques

The rising concentration of carbon dioxide (CO₂) in the atmosphere has prompted the development of various techniques aimed at reducing CO₂ emissions and converting CO₂ into valuable products. These techniques span a broad spectrum, from traditional methods to advanced catalytic processes, each with its own set of advantages and challenges. This section provides a comprehensive overview of the main CO₂ reduction techniques, highlighting their principles, effectiveness, and potential applications. (Zhang *et al.*, 2020)

2.4.1 Chemical Absorption and Adsorption

Chemical absorption involves the capture of CO₂ by reactive solvents, typically amine-based solutions such as monoethanolamine (MEA) or diethanolamine (DEA). CO₂ reacts with the amine to form a carbamate or bicarbonate, which can be regenerated by heating to release pure CO₂. Recent advancements have introduced the use of blended amines, ionic liquids (ILs), and nanofluids to improve CO₂ capture capacity and reduce energy requirements. For instance, the use of mixed amines like MEA with methyl diethanolamine (MDEA) has shown promising results in enhancing CO₂ absorption while minimizing energy consumption (Sattari *et al.*, 2021).

This method is widely used in industrial applications due to its high capture efficiency and relatively simple technology. However, it is energy-intensive and can lead to solvent degradation and corrosion issues. The use of amine blends, such as MEA with piperazine (PZ), has been shown to reduce energy consumption by up to 20%, while maintaining high capture efficiency. Chemical absorption is commonly employed in post-combustion carbon capture from power plants and industrial emissions. The deployment of CO₂ capture using MEA in large-scale power plants has been well-documented, with ongoing research focusing on reducing operational costs and improving solvent stability. (Koronaki *et al.*, 2015)

Adsorption techniques use solid materials, such as zeolites, metal-organic frameworks (MOFs), or activated carbon, to capture CO₂ from gas streams. CO₂ molecules adhere to the surface of the adsorbent through physical or chemical interactions. The development of new adsorbent materials, such as amine-functionalized MOFs, has significantly enhanced CO₂ capture capacity and selectivity, particularly under low-pressure conditions. (Petrovic *et al.*, 2021)

Adsorption offers advantages such as low energy requirements for regeneration and the potential for high selectivity and capacity. However, the development of cost-effective and stable adsorbents remains a challenge. Advanced materials like MOFs have demonstrated CO₂ adsorption capacities of up to 10 mmol/g, making them highly competitive for large-scale applications.

Adsorption is used in pre-combustion and post-combustion carbon capture and in direct air capture technologies. MOFs and zeolites have been successfully integrated into CO₂ capture systems in various industrial settings, with ongoing research focusing on improving the scalability and economic feasibility of these technologies (Soo *et al.*, 2024).

2.4.2 Biological Fixation

Photosynthetic organisms, such as plants, algae, and cyanobacteria, naturally convert CO₂ into organic compounds using sunlight. This process is fundamental to the global carbon cycle and offers a renewable method for CO₂ fixation. Microalgae, in particular, have been extensively studied for their potential to serve as a sustainable source of biofuels and biochemicals due to their rapid growth rates and high photosynthetic efficiency. For instance, microalgae like *Chlorella vulgaris* and *Spirulina platensis* have shown considerable potential in capturing CO₂ and converting it into valuable bio-products such as bioethanol and biodiesel. (Liu *et al.*, 2024)

While biological fixation is sustainable and environmentally friendly, it is generally limited by the slow growth rates of natural organisms and their relatively low CO₂ uptake capacity. However, advancements in genetic engineering have led to the development of modified algae strains that exhibit enhanced CO₂ absorption and faster growth rates. For example, genetically engineered strains of *Synechococcus elongatus* have demonstrated increased CO₂ fixation and biomass production, making them more efficient for large-scale applications.

Enhancing photosynthesis through genetic engineering and optimizing growth conditions can significantly improve CO₂ capture. Applications include bioenergy production, biofuels, and biomass-based carbon sequestration. Specifically, open pond systems and photobioreactors have been deployed for large-scale microalgae cultivation, with some systems achieving biomass yields as high as 70 metric tons per hectare per year in ideal conditions. These systems have been integrated into carbon capture and utilization (CCU) frameworks, where the captured CO₂ is utilized for algal growth, leading to the production of biofuels and other high-value chemicals. (Li *et al.*, 2016)

2.4.3 Chemical and Electrochemical Reduction

Thermochemical Reduction: Thermochemical processes employ high temperatures to convert CO₂ into CO, methane (CH₄), or other hydrocarbons, often using catalysts such as metal oxides or carbides. A widely studied example is the CO₂ methanation process, which uses catalysts like nickel-based compounds to achieve high conversion rates. The reverse water-gas shift (RWGS) reaction is another example, where CO₂ is reduced to CO at high temperatures in the presence of metal catalysts such as iron or cobalt oxides. Thermochemical reduction can achieve high conversion rates and yields. For instance, in the methanation of CO₂, catalytic systems using nickel-based catalysts have shown high efficiency in converting CO₂ to methane under optimized conditions. However, these processes require significant energy input, which is often derived from non-renewable sources, limiting their sustainability (Komarala *et al.*, 2023).

This method is utilized in producing synthetic fuels and chemical feedstocks, particularly through processes like the reverse water-gas shift reaction and CO₂ methanation. Recent advancements in catalyst development have improved the energy efficiency of these reactions, making them more viable for industrial applications.

Electrochemical Reduction: Electrochemical reduction involves applying an external electrical current to reduce CO₂ at the surface of a catalyst within an electrochemical cell. Depending on the catalyst and reaction conditions, the reduction products can include CO, formic acid, methanol, and other hydrocarbons. For example, copper.(Jin *et al.*, 2021)based catalysts have been shown to produce hydrocarbons such as ethylene and methane, while tin-based catalysts favor the production of formic acid. Electrochemical reduction offers the advantage of being powered by renewable electricity sources, making it a sustainable option. Recent research has focused on developing catalysts that are both efficient and durable, such as using bimetallic combinations like Cu-Sn or using innovative electrode designs to improve the selectivity and efficiency of the reduction process.

This technique has potential applications in producing renewable fuels, chemicals, and energy storage materials. A notable example is the production of formic acid using tin-based catalysts, which has demonstrated high Faradaic efficiency and selectivity under specific conditions. Ongoing research aims to optimize these systems for large-scale industrial applications, focusing on enhancing catalyst stability and reducing energy consumption. (Hua *et al.*, 2019)

2.4.4 Photocatalytic Reduction

Photocatalytic reduction utilizes light-absorbing materials, typically semiconductors like titanium dioxide (TiO₂), to drive the reduction of CO₂. Upon illumination, the photocatalyst generates electron-hole pairs that participate in redox reactions, leading to the reduction of CO₂ into various products such as methanol, methane, and oxalic acid. For instance, copper-loaded TiO₂ supported on molecular sieve 5A has been shown to enhance the selectivity and yield of products like oxalic acid by promoting charge separation and improving the adsorption properties of CO₂.(Karamian et Sharifnia, 2016)

Photocatalytic reduction is a promising approach due to its ability to harness solar energy, a renewable and abundant resource. However, challenges such as low quantum efficiency, poor selectivity, and stability of photocatalysts must be addressed. Recent studies, such as the one involving Cu-TiO₂ on molecular sieve 5A, have demonstrated the potential for increased photocatalytic activity and selectivity, particularly in alkaline conditions where the solubility of CO₂ is higher and recombination of electron-hole pairs is minimized.

The applications of photocatalytic reduction include the conversion of CO₂ into fuels (e.g., methane, methanol), chemicals, and integration into solar fuel production systems. Research focuses on developing novel photocatalysts with enhanced activity and stability. For example, the Cu-TiO₂/molecular sieve 5A composite has been shown to selectively produce oxalic acid, methanol, and acetic acid, with maximum yields observed under specific reaction conditions. These advancements highlight the ongoing efforts to improve the viability of photocatalytic CO₂ reduction for sustainable energy and chemical production. (Srinivas *et al.*, 2011)

2.4.5 Hybrid Catalytic Systems

Hybrid catalytic systems combine different types of catalysts, such as plasmonic nanoparticles and organometallic complexes, to leverage synergistic effects for improved CO₂ reduction. In these systems, the plasmonic component, typically composed of metals like gold or silver, enhances light absorption and generates hot electrons, which can then transfer to the organometallic catalyst. The organometallic catalyst, often a complex containing transition metals like ruthenium or rhenium, facilitates the chemical conversion of CO₂ into valuable products such as CO, formic acid, or methanol. For example, semiconductor photocathodes combined with ruthenium complexes have demonstrated improved selectivity and efficiency in CO₂ reduction processes. (Mohan *et al.*, 2020)

Hybrid systems offer significant enhancements in catalytic efficiency and selectivity by combining the strengths of each component. The plasmonic nanoparticles boost the overall light absorption, while the organometallic complexes ensure that the absorbed energy is effectively used for the multi-electron reduction of CO₂. The design and optimization of these systems, such as matching the energy levels between the semiconductor and the metal complex, are crucial for achieving optimal performance. Recent studies have shown that hybrid systems can achieve higher Faradaic efficiencies and selectivities compared to standalone catalytic systems, particularly when integrated into photoelectrochemical cells.

Applications of hybrid catalytic systems include advanced photocatalytic processes for CO₂ reduction, with potential for integration into solar fuel production, environmental remediation, and sustainable chemical manufacturing. For instance, combining semiconductor light harvesters like InP with metal complexes such as ruthenium-based catalysts has shown promise in converting CO₂ into formate with high efficiency. These hybrid systems are also being explored for their potential to produce more highly reduced chemicals

like methanol, which is a key goal in the development of sustainable energy solutions.(Zhao *et al.*, 2014b)
This topic will be explained in more detail in the next section.

2.4.5.1 Catalytic solution

Role of FeTPP as a Catalyst and Gold Nanoparticles as Photosensitizers in the Electrolyte Solution: In the context of photocatalytic and photoelectrocatalytic CO₂ reduction, the choice of electrolyte components is crucial for ensuring effective and stable catalytic reactions. Each component in the electrolyte solution plays a specific role, contributing to the overall efficiency and stability of the catalytic system.

Solvents: Acetonitrile (ACN) and Dimethylformamide (DMF) (Schneider *et al.*, 2016)

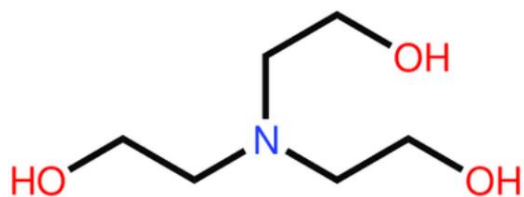
Both ACN and DMF are widely used solvents in photochemical and electrochemical systems due to their ability to dissolve a wide range of organic and inorganic compounds. ACN is particularly valued for its high dielectric constant and low viscosity, which facilitate efficient charge transfer and improve the solubility of CO₂. DMF, on the other hand, offers a polar environment that supports the stabilization of reactive intermediates during the reduction process. The selection between these solvents depends on the specific reaction dynamics and the interaction of the solvent with both the catalyst and the photosensitizer.

Sacrificial Electron Donors: Triethanolamine (TEA), Triethylamine (TEOA), and 1,3-Dimethyl-2-phenyl-1,3-dihydrobenzimidazole (BIH) (Lowe, 2023)

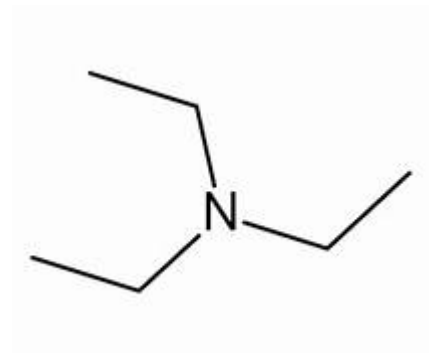
Sacrificial electron donors are essential in maintaining the continuous flow of electrons necessary for the reduction of CO₂, effectively preventing the recombination of photogenerated electron-hole pairs in the system.

TEA is commonly used in photocatalytic systems due to its ability to donate electrons while forming stable radicals that do not interfere with the catalytic process. Its high reducing power makes it effective in driving CO₂ reduction reactions. TEOA offers a similar function to TEA but with a slightly different molecular structure that can lead to variations in electron donation efficiency and the stabilization of intermediate states in the catalytic cycle. BIH is a more complex sacrificial electron donor that provides both stability and high electron donation capacity. Its incorporation alongside TEA and TEOA can enhance the overall

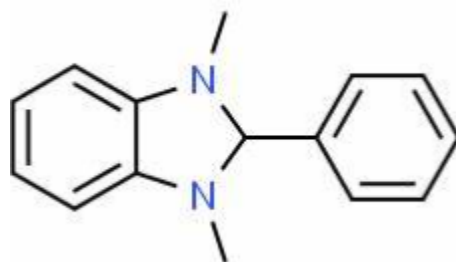
efficiency of the system by providing multiple pathways for electron transfer, which can prevent bottlenecks in the catalytic process.



(a)



(b)



(c)

Figure 2.6. Structure of a) Triethanolamine (TEA), b) Triethylamine (TEOA), and c) 1,3-Dimethyl-2-phenyl-1,3-dihydrobenzimidazole (BIH)

Synergistic Effects of Combined Components

When combined, these components create a highly effective catalytic environment where the gold nanoparticles enhance light absorption and electron generation, the sacrificial electron donors provide a steady supply of electrons, and the FeTPP catalyst efficiently reduces CO_2 . The use of different solvents, such as ACN and DMF, further optimizes the reaction environment, ensuring the highest possible efficiency and stability of the system.

2.5 Synergy between Plasmonic Materials and Organometallic Catalysts

The integration of plasmonic materials with organometallic catalysts represents a cutting-edge approach in photocatalysis, aiming to enhance the efficiency and selectivity of catalytic processes, particularly for CO₂ reduction. The synergistic combination of these two types of materials leverages plasmonic nanoparticles' unique properties and organometallic complexes' catalytic capabilities, leading to improved performance in light-driven chemical transformations. This section explores the mechanisms and advantages of this synergy and its applications and potential for future development.

2.5.1 Mechanisms of Synergy

The synergy between plasmonic materials and organometallic catalysts, particularly in CO₂ reduction, is rooted in the complementary functionalities of these two components.

Electron Transfer Dynamics in Plasmonic-Organometallic Systems: The integration of plasmonic materials, such as gold nanoparticles (AuNPs), with organometallic catalysts like iron tetraphenylporphyrin (FeTPP), creates a unique catalytic environment that enhances electron transfer processes crucial for CO₂ reduction. The AuNPs, when exposed to light, induce an electric field that affects nearby FeTPP molecules. This field facilitates the transfer of electrons from the FeTPP complex to CO₂, lowering the energy barrier for the reaction and increasing the reaction rate (Bin *et al.*, 2022).

For example, in a system where AuNPs are coupled with FeTPP, the hot electrons generated by AuNPs upon light absorption can be directly transferred to FeTPP. This transfer process is facilitated by the overlap of energy states between the excited electrons in AuNPs and the LUMO (Lowest Unoccupied Molecular Orbital) of FeTPP, thereby enhancing the CO₂ reduction process.

Structural Effects and Catalyst Efficiency: The structure of the catalyst plays a crucial role in determining its efficiency. Studies have shown that modifications to the FeTPP (iron tetraphenylporphyrin) structure, such as changing the substituents on the phenyl groups or altering the coordination environment of the iron center, can significantly influence its catalytic behavior. These modifications can affect the electron density on the iron center, making the catalyst more effective in catalyzing CO₂ reduction. (Sun *et al.*, 2024)

For example, introducing electron-donating or electron-withdrawing groups on the phenyl rings of FeTPP can shift the electronic properties of the catalyst, thereby enhancing its reactivity towards CO₂. These

structural changes can improve the overall catalytic performance by making the iron center more reactive or by stabilizing key reaction intermediates during the CO₂ reduction process. However, these modifications can also introduce complexities in the electron transfer process, potentially affecting the stability of intermediates and the selectivity of the catalytic reaction.

2.5.2 Applications and Future Development

The synergy between plasmonic materials and organometallic catalysts has been explored in various applications beyond CO₂ reduction, including the synthesis of fine chemicals and the degradation of environmental pollutants. This approach is highly versatile, making it valuable in a broad range of catalytic processes.

Synthesis of Fine Chemicals: One of the primary applications of plasmonic-organometallic hybrid catalysts is in the selective oxidation of organic substrates. The combination of gold nanoparticles (AuNPs) with iron porphyrin catalysts, for example, has been extensively studied for its ability to catalyze oxidation reactions under visible light. This is particularly useful in the synthesis of fine chemicals, where precise control over reaction pathways and product selectivity is essential. For instance, hybrid catalysts have been shown to improve the oxidation of alcohols to aldehydes and ketones, achieving high yields and selectivities. (Peng, 2019)

Degradation of Environmental Pollutants: Another critical application area for these hybrid catalysts is in the degradation of environmental pollutants, such as nitrophenols and chlorinated organic compounds. For example, iron porphyrin catalysts supported on zeolites or other porous materials have been utilized in the photocatalytic degradation of 4-nitrophenol, a common industrial pollutant. The plasmonic effect enhances the generation of reactive oxygen species, which are crucial for breaking down these pollutants into less harmful compounds. (Gu *et al.*, 2023)

CO₂ Conversion to Value-Added Products: While CO₂ reduction to CO is a primary focus, there is significant interest in expanding this process to produce more complex value-added chemicals, such as methanol or hydrocarbons. Advances in the design of plasmonic-organometallic catalysts are driving this research forward. For example, by fine-tuning the interaction between the plasmonic material and the organometallic catalyst, researchers aim to control the reaction environment more precisely, leading to higher selectivities for specific products. (Zou *et al.*, 2020)

Integration with Photovoltaic and Electrochemical Systems: Another exciting avenue for future development is the integration of plasmonic-organometallic catalysts with photovoltaic or electrochemical systems. This integration could enable the direct use of sunlight or electrical energy to drive chemical reactions, thereby enhancing the overall efficiency and sustainability of the process. For example, coupling these catalysts with water oxidation anodes through a proton-exchange membrane could facilitate the production of syngas (a mixture of CO and H₂) under controlled conditions. (Bonin *et al.*, 2017)

Tailoring Catalyst Structures for Specific Reactions: The ability to tailor the structure of these hybrid catalysts at the molecular level will be key to expanding their applicability. This includes not only adjusting the physical properties of the nanoparticles but also modifying the chemical environment of the organometallic catalyst to optimize its performance for specific reactions. For instance, the development of water-soluble catalysts for CO₂ reduction in aqueous environments is an area of active research, which could lead to more practical and scalable solutions. (Wang *et al.*, 2021)

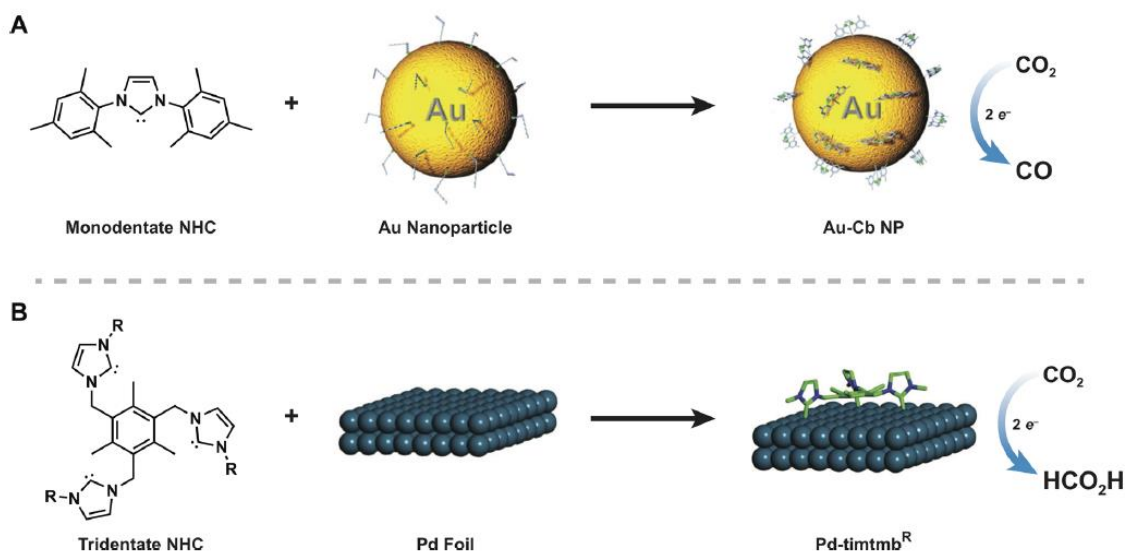


Figure 2.7. (A) Monodentate NHC coordination to Au nanoparticles for CO₂ reduction into CO and (B) tridentate NHC coordination to Pd foil for CO₂ reduction into formate, highlighting the ability of ligands to tune product selectivity of materials catalysts. (Zhao *et al.*, 2014b) reproduced with permission

Figure 2.7 illustrates the role of plasmonic and organometallic catalysts in CO₂ reduction, showcasing how gold nanoparticles (Au NPs) coordinated with monodentate NHC ligands enhance the selective conversion of CO₂ to CO, while tridentate NHC ligands coordinated to palladium foil direct the reduction of CO₂ to

formate. This highlights the tunable nature of catalyst design, where the choice of metal and ligand influences both the efficiency and selectivity of the catalytic process.

2.6 Deposition Techniques

The deposition of gold nanoparticles (AuNPs) onto various substrates is a critical step in the preparation of efficient heterogenous photocatalysts. The choice of deposition technique significantly impacts the distribution and aggregation of nanoparticles, which in turn affects their photocatalytic performance. This section describes various deposition techniques, including drop casting, electrodeposition, the sol-gel method, physical vapor deposition (PVD), and dip coating. Each technique is explored in terms of its process, advantages, and applications, providing a comprehensive understanding of their role in enhancing the photocatalytic activity of AuNPs (Khashayar *et al.*, 2016).

2.6.1 Drop casting

Drop casting is an accessible and widely used technique for creating thin films, particularly when working with nanoparticle suspensions. It involves depositing a controlled amount of solution onto a clean substrate and allowing it to air dry or dry under controlled conditions. This method was chosen for its simplicity, as it requires minimal specialized equipment, making it highly suitable for early-stage experiments or rapid prototyping.

In this study, drop casting was employed to deposit gold nanoparticles synthesized by both the seed-mediated and citrate reduction methods. The process allowed for a uniform layer of nanoparticles to form, as observed in the case of gold nano bipyramids, which created a continuous and homogeneous film. This method was critical for experiments involving photocatalytic CO₂ reduction, as the films needed to maintain structural integrity when immersed in electrolytes.

Despite its advantages, the films created by drop casting exhibited varying degrees of stability depending on the nanoparticles' synthesis route. For instance, the citrate-reduced nanoparticles dissolved entirely in water, while those produced by the seed method adhered better to the substrate but required securing with lacquer to remain intact in solution. These observations highlight the need for optimization of the method for improved film stability and uniformity in photocatalytic applications (Zhao *et al.*, 2014a).

2.6.2 Electrodeposition

Electrodeposition is a process in which a material is deposited onto a conductive surface from a solution containing the material's ions, through the application of an electric potential. This technique is widely used in the fabrication of nanostructures and coatings, offering precise control over the thickness and morphology of the deposited layer. Electrodeposition is used to create a layer of gold nanoparticles on the surface of an electrode. This process begins with the electrode being immersed in a solution containing gold ions. When an electric current is applied, these ions are reduced and deposited as gold nanoparticles onto the electrode surface. The size and density of the deposited nanoparticles can be controlled by varying the conditions of the electrodeposition process, such as the voltage applied and the duration of the process. The Figure 2.8 illustrates three different scenarios where gold nanoparticles of varying sizes (184 nm, 91 nm, and 52 nm) are deposited onto the electrode. (Chiang *et al.*, 2019)

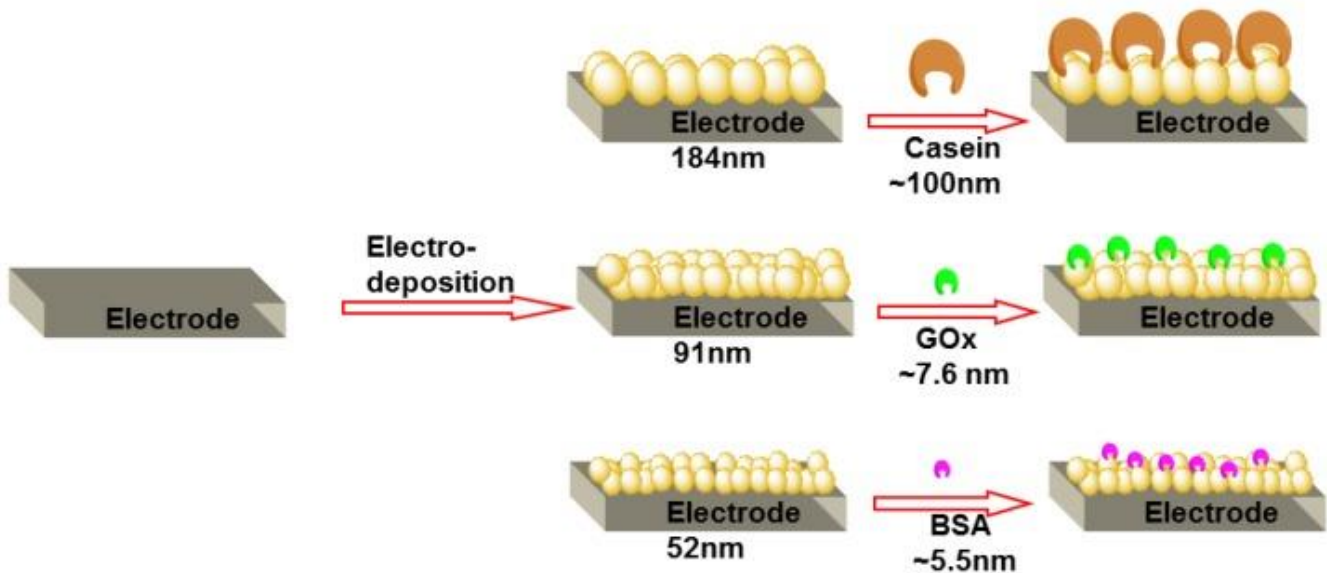


Figure 2.8. Schematic presentation of the adsorption of proteins on surfaces with different sizes of AuNPs. (Chiang *et al.*, 2019) reproduced with permission

2.6.3 Sol-Gel Method

The sol-gel method is a versatile and widely used technique for producing nanoparticles and thin films. This method involves the transition of a system from a liquid "sol" into a solid "gel" phase. The process begins with the preparation of a precursor solution by mixing metal alkoxides with a solvent. This solution

undergoes hydrolysis and condensation reactions to form a gel. The gel can then be applied to a substrate and subsequently heated to form nanoparticles. The sol-gel method is highly versatile and can be used to produce a wide range of materials, including ceramics, glasses, and hybrid materials. This technique allows for precise control over the composition and structure of the final material, making it suitable for producing uniform and high-purity films. The sol-gel method is commonly employed in the production of thin films, optical coatings, and nanoparticles for various applications. As shown in Figure 2.9, the sol-gel process involves chemical solution deposition following the order of hydrolysis and condensation, gel formation, aging process, removing the solvent from materials by evaporation/calcination, and finally obtaining crystallization. However, this precursor method is costly with lower production and the possibility of dangerous conditions. (Azam et Mupit, 2022)

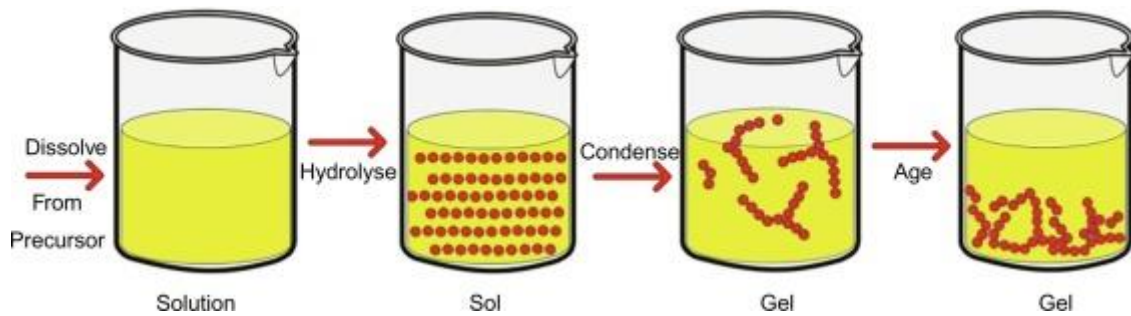


Figure 2.9. The basic process of the sol-gel method.(Azam et Mupit, 2022) reproduced with permission

2.6.4 Dip Coating

Dip coating is a straightforward and cost-effective technique for depositing thin films onto substrates. In dip coating, a substrate is repeatedly dipped into a solution or suspension of nanoparticles and then withdrawn to deposit a thin film. The process involves immersing the substrate into the nanoparticle solution, where capillary forces cause the solution to adhere to the substrate surface. After multiple dips and drying cycles, a uniform film is formed on the substrate. Dip coating is advantageous due to its simplicity and ability to coat large areas uniformly. This technique is particularly suitable for applications requiring thin films, such as anti-reflective coatings, protective layers, and the fabrication of thin films for various industrial applications. (Yin-Fen *et al.*, 2023)

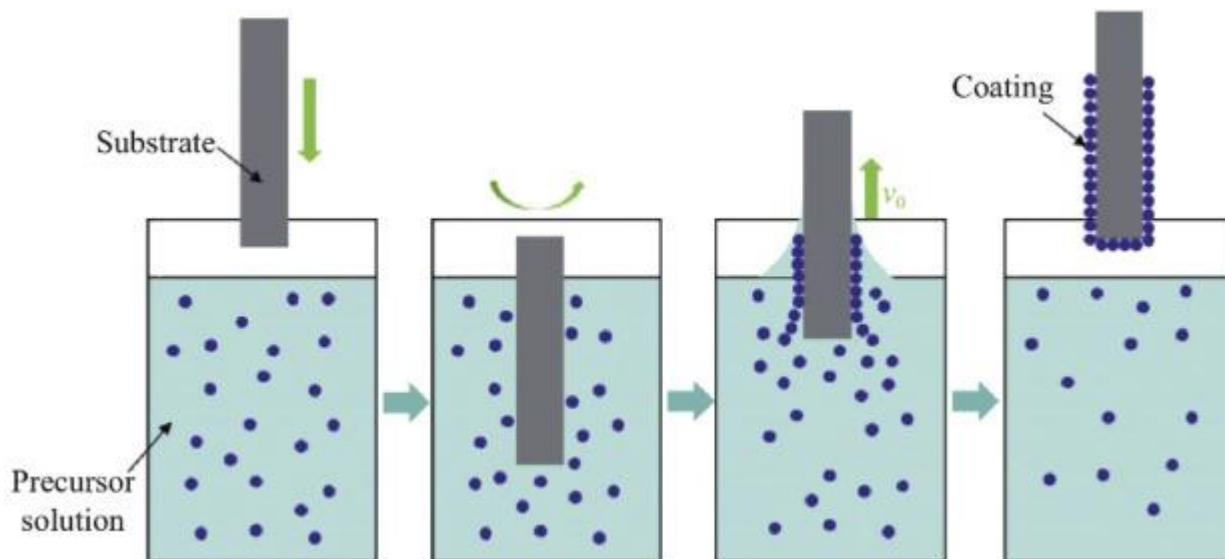


Figure 12. Dip coating method. (Yin-Fen *et al.*, 2023) reproduced with permission

Each of these deposition techniques offers unique advantages and is suited to different applications and requirements. For instance, chemical deposition and dip coating are highly accessible and cost-effective, making them ideal for large-scale production. Electrodeposition and PVD, on the other hand, provide precise control over film properties, which is essential for high-performance applications.

By optimizing the deposition process, we aim to enhance the photocatalytic activity of the nanoparticles, thereby improving their efficiency in CO₂ reduction processes. This research provides valuable insights into the design and fabrication of high-performance photocatalysts, contributing to the advancement of sustainable energy technologies and environmental protection.

CHAPITRE 3

Synthesis and Characterization of AuNP

3.1 Introduction

This chapter focuses on the synthesis and characterization of AuNPs with varying shapes and sizes, tailored to optimize their plasmonic properties for catalytic applications. By systematically varying these parameters, we aim to explore how different morphologies influence the generation of hot electrons and, consequently, the efficiency of the photocatalytic process.

This chapter delves into the methodologies employed for the controlled synthesis of AuNPs, followed by a comprehensive characterization of their optical and electronic properties. Understanding these aspects is essential for optimizing the nanoparticles' performance in plasmonic catalysis, laying the groundwork for their application in more complex catalytic systems.

3.2 Synthesis of gold nanoparticles with seed growth method

There are two steps for the synthesis of AuNP with this method:

Synthesis of Gold Seeds: Gold seeds were synthesized using a reduction method, following the procedures described by (Grzelczak *et al.*, 2008). The synthesis began by diluting 0.25 ml of a 10 mmol/l HAuCl₄ solution with 10 ml of water, which served as the gold source. At this stage, gold ions existed in the form of Au(III) ions (Au³⁺), giving the solution a pale yellow colour indicative of these ions. Next, citric acid was prepared as both a reducing and stabilizing agent by dissolving 0.960 g in 10 ml of water, and this solution was added to the gold precursor. The citric acid reduced the Au(III) ions to Au(0), leading to the formation of very small gold particles, or seeds. This reduction process was accompanied by a color change in the solution to a pale pink, indicating the formation of gold nanoparticles at the nanoscale.

Following this, cetyltrimethylammonium chloride (CTAC) was introduced as a surfactant. At a concentration of 0.05 mol/l, 1.65 ml of the CTAC solution was added to 100 ml of water. CTAC attached to the surface of the gold nanoparticles, stabilizing them and playing a crucial role in controlling the final shape of the nanoparticles. While no significant color change occurred at this stage, the solution became more transparent and homogeneous due to the presence of CTAC.

The reduction reaction was then initiated by adding 500 microliters of a 25 mmol/l NaBH_4 solution (0.0094 g in 10 ml water). Sodium borohydride acted as a strong reducing agent, further reducing any remaining Au(III) ions to Au(0) . This step accelerated the growth of the initial seeds, increasing the size of the gold nanoparticles and helping them attain their final shape and size. After the addition of NaBH_4 , the solution changed to a dark red or burnt red color, indicating the formation of gold nanoparticles with the desired size. Finally, the reaction mixture was incubated at 80°C for 90 minutes. This heating step enhanced the stability of the nanoparticles and completed their growth process. During this phase, the nanoparticles reached their final shape and size, and the solution adopted a stable red color. As shown in Figure 3.1, you can see the changes in color throughout the process. Throughout this synthesis, the role of the seeds is critical, as controlling the initial conditions allows for precise control over the final shape and size of the gold nanoparticles, as outlined by Grzelczak et al. (Grzelczak *et al.*, 2008).



Figure 13. The color changes after adding the first reducing agent (a), and again after 90 minutes at 80 degrees (b).

Synthesis of Gold Nano bipyramids: The synthesis of gold nano bipyramids begins with a CTAB solution. Initially, CTAB (Cetyltrimethylammonium Bromide) is introduced at a concentration of 0.1 mol/l (3.64 g in 100 ml water). CTAB acts as a surfactant, stabilizing the nanoparticles and controlling their size and shape during growth. Then 500 microliters of a 10 mmol/l HAuCl_4 solution is added, which serves as the gold source. Due to the relatively high concentration of gold ions in this step, the solution exhibits a deep yellow color, indicating the presence of a significant concentration of Au(III) ions (Au^{3+}).

Next, 100 microliters of a 10 mmol/l AgNO_3 solution (0.033 g in 20 ml water) are added. Silver nitrate (AgNO_3) plays a crucial role in directing the growth of the nanoparticles along a single twinning axis,

essential for achieving the bipyramidal shape. The pH of the solution is then adjusted by adding 200 microliters of 1 mol/l HCl. This acidic environment is crucial for maintaining the stability of the gold ions and promoting controlled growth of the bipyramids.

Following the pH adjustment, 80 microliters of ascorbic acid (0.352 g in 20 ml water) are added as a reducing agent. Ascorbic acid reduces Au(III) ions to Au(0), initiating the growth of nanoparticles from the seeds. This reduction process leads to a visible color change from deep yellow to white.

After approximately 10 minutes of stirring, a carefully measured volume (X microliters) of the pre-prepared seed solution is introduced to the reaction mixture. The exact volume of seeds added is varied in different experiments to determine the optimal seed concentration for efficient growth of the bipyramids. Following the addition of the seeds, the solution transitions from white to a pale pink color, indicating the initial stages of nanoparticle growth.

The reaction mixture is then left to proceed at 30°C overnight. During this time, the gold nanoparticles continue to grow, and the color of the solution deepens to a rich, intense pink. This final color change signifies the successful formation of gold nano bipyramids with the desired structure. Various seed concentrations are tested to evaluate which amount yields the most efficient and effective nanoparticle growth.

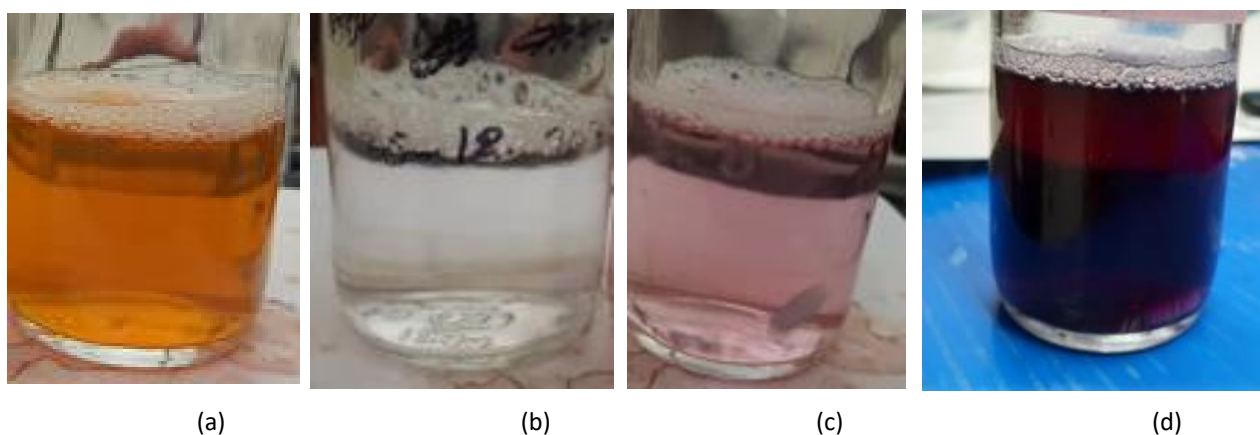


Figure 3.2. Sequential color changes during the synthesis of gold nano bipyramids. (a) Deep yellow due to Au³⁺ ions, (b) white after reduction with ascorbic acid, (c) pale pink after adding seeds, and (d) deep pink indicating successful formation of gold nano bipyramids after overnight stirring.

3.3 Synthesis of Gold Nanoparticles by Citrate Reduction Method

Gold nanoparticles were synthesized using the citrate reduction method, a widely recognized approach for producing spherical nanoparticles. This method was explored after initial experiments with gold nanobipyramids, which were synthesized through a seed-mediated method. These nanobipyramids were deposited onto glass substrates, forming a homogeneous and continuous film. This film was then used in a photocatalytic CO₂ reduction experiment. Although the results were promising, it was essential to investigate whether using a different nanoparticle synthesis method could yield improved or varied outcomes. Therefore, the citrate reduction method was employed as an alternative approach.

The procedure began with preparing a 1.0 mM HAuCl₄ solution by diluting 0.4 ml of a 50 mmol/l HAuCl₄ stock solution into 20 ml of distilled water. This gold precursor solution was then transferred to a 50 ml Erlenmeyer flask equipped with a magnetic stir bar (Ojea-Jiménez et Campanera, 2012).

The solution was heated on a stirring hot plate until it reached a rolling boil. At this point, 2 ml of a 1% trisodium citrate solution—freshly prepared by dissolving 0.5 g of Na₃C₆H₅O₇·2H₂O in 50 ml of distilled water—was rapidly added to the boiling gold solution. The sudden addition of citrate serves as both a reducing and stabilizing agent, initiating the reduction of Au(III) ions to Au(0) and leading to the formation of gold nanospheres.

The color of the solution initially appears yellow due to the presence of Au(III) ions. As the reduction proceeds, the solution darkens, indicating the reduction to Au(I) and the nucleation of gold atoms. Finally, as the nanoparticles grow, the solution transitions to a deep red color, characteristic of colloidal gold, signifying the successful synthesis of gold nanoparticles.

After the citrate was added, the solution was allowed to boil for another 10 minutes. The heat was then turned off, and the reaction mixture was left to cool down to room temperature while stirring continuously. Stirring was maintained for 1 hour post-cooling to ensure complete reaction and stabilization of the nanoparticles.

The key difference between the citrate reduction method and the seed-mediated method lies in the morphology and application of the nanoparticles. While the seed-mediated method produces gold nanobipyramids that form a homogeneous and continuous film upon deposition, the gold nanospheres

produced by the citrate method do not exhibit the same film-forming properties. The nanospheres are less likely to form a uniform film, which can negatively impact their effectiveness in applications such as photocatalytic CO₂ reduction. The seed-mediated method is particularly advantageous when specific nanoparticle shapes and a controlled deposition process are required, leading to better performance in catalytic applications.

In contrast, the citrate reduction method is more straightforward, but it may not provide the same level of control over the nanoparticle shape and deposition behavior. The choice of method thus depends on the specific requirements of the application, with the citrate method serving as a useful comparison to evaluate the influence of nanoparticle shape and film formation on the overall performance.

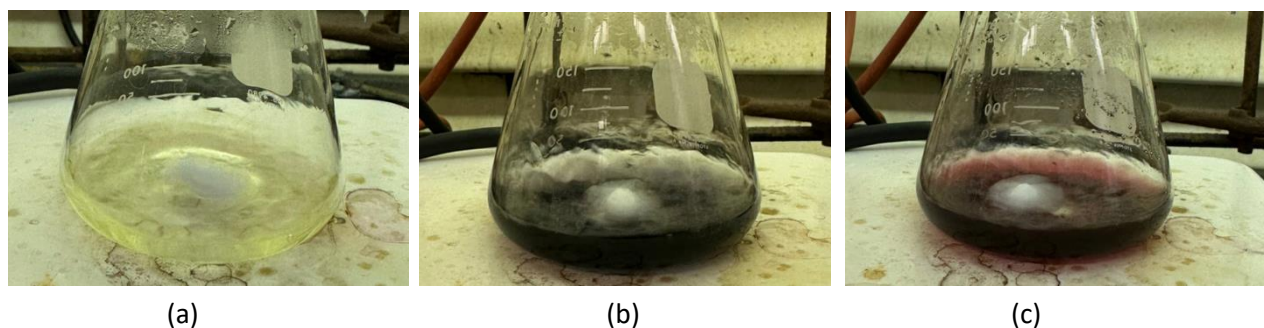
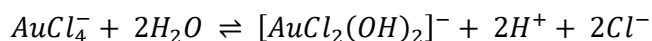
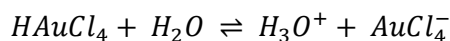


Figure 14. Stages of gold nanoparticle synthesis via citrate reduction: (a) Au(III) ions in yellow solution, (b) nucleation with darkening color, (c) formation of colloidal gold with deep red color.

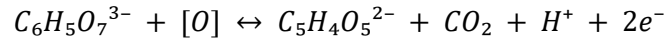
Chemical reactions involved in the citrate reduction method for the synthesis of gold nanoparticles. The hydrolysis of AuCl₄⁻, oxidation of citrate, reduction of Au(III) to Au(I), and the overall process, culminating in the formation of colloidal gold nanoparticles, are outlined.

Hydrolysis of AuCl₄⁻:

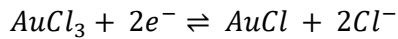
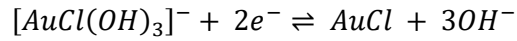
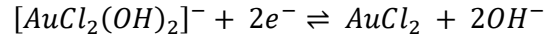
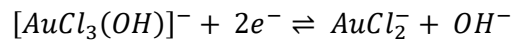
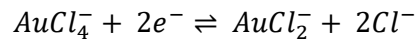




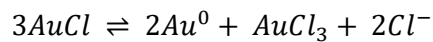
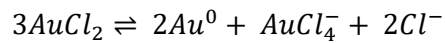
Oxidation of Citrate to Dicarboxy Acetone:



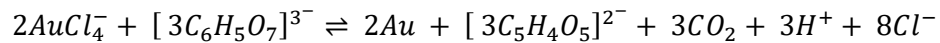
Reduction of Au(III) to Au(I):



Disproportionation of Au(I) to Metallic Au:



Overall Reaction:



3.4 Electrodeposition of gold nanoparticles on FTO

Gold was electrodeposited on fluorine-doped tin oxide (FTO) coated glass substrates using a potentiation method. The electrolyte solution was prepared by dissolving 1 mM HAuCl_4 in a 0.1 M potassium phosphate buffer solution. The buffer solution, with a target pH of ~ 6.7 , was prepared by mixing K_2HPO_4 and KH_2PO_4 . Specifically, 8.71 g of K_2HPO_4 was dissolved in 500 ml of distilled water, and 6.80 g of KH_2PO_4 was dissolved separately in another 500 ml of distilled water. The KH_2PO_4 solution was then added to the K_2HPO_4 solution gradually until the pH of the combined solution reached 6.7 and the total volume was adjusted to 500 ml. This buffer solution was stored at 4°C to maintain its stability.

A three-electrode system was set up for the electrodeposition process. Platinum was used as the counter electrode, and a saturated Ag/AgCl electrode served as the reference electrode. The FTO-coated glass was used as the working electrode. The gold and buffer solution acted as the electrolyte for the deposition process.

The electrodeposition was carried out using a potential with the potential cycled between -1.25 V to -0.75 V versus Ag/AgCl . The scan rate was maintained at 10 mV/s . To investigate the effect of the number of cycles on the deposition process, experiments were conducted for 4, 8, and 12 redox cycles. Each cycle was expected to increase the thickness and change the morphology of the gold nanoparticle layer deposited on the FTO substrate. (Yang *et al.*, 2015)

Upon completion of the electrodeposition, the FTO substrates with deposited gold nanoparticles were carefully rinsed with distilled water to remove any remaining electrolytes and then dried at room temperature. The substrates were subsequently characterized to assess the morphology and coverage of the gold nanoparticles on the FTO surface.

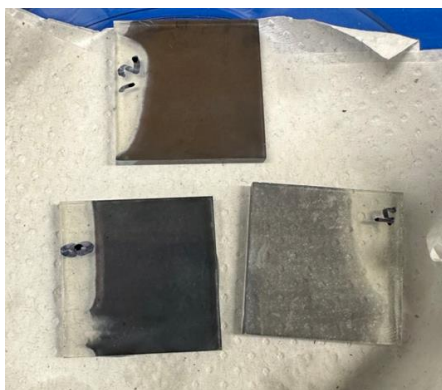


Figure 15. Electrodeposition of Au on FTO with 4,8,12 cycles

3.5 Result and Discussion

Synthesis of gold nanoparticles with seed growth method:

In the synthesis of gold nanoparticles using the seed growth methods (Figure 3.5), the characterization of the nanoparticles was primarily conducted using Ultraviolet-Visible (UV-Vis) spectroscopy and Dynamic Light Scattering (DLS).

UV-Vis Spectroscopy Results:

In this study, UV-Vis spectroscopy was employed to analyze both the gold seed solution and the subsequent gold bipyramid nanoparticles synthesized by adding varying amounts of these seeds to a CTAB-based growth solution. The primary objective was to understand how the quantity of gold seeds influences the size distribution and optical properties of the resulting nanoparticles, and ultimately, to determine which configuration might yield the best performance in photocatalytic CO₂ reduction. However on the fact that some spectra have been acquired too quickly and some of them have an unusual form/background.

Gold Seed Solution: The first UV-Vis spectrum corresponds to the gold seed solution synthesized using CTAC. This solution shows a single, sharp surface plasmon resonance (SPR) peak centred around 530 nm, which is typical for small, spherical gold nanoparticles. The narrowness of this peak indicates a uniform size distribution, with the nanoparticles being relatively small and consistent in size. This well-defined peak confirms that the gold seeds are monodisperse, forming a stable and homogeneous population of small nanoparticles. These seeds serve as the nucleation sites for the subsequent growth of gold bipyramids in the CTAB-based growth solutions.

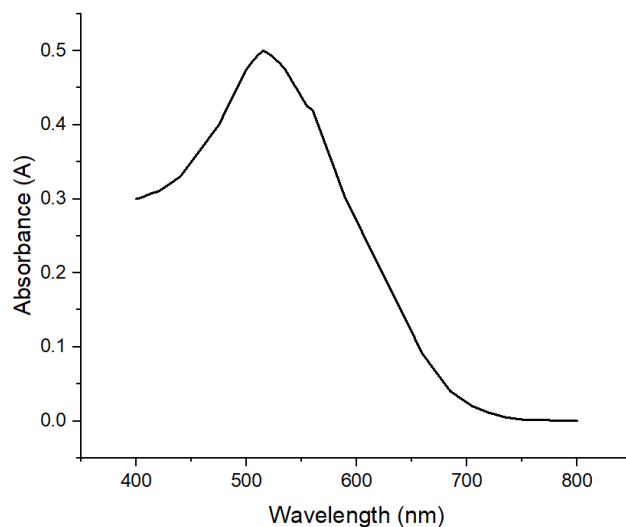


Figure 3.5. The UV-Vis spectrum of gold seeds particle.

Growth Solutions with Varying Seed Amounts: To investigate the effect of varying the amount of gold seeds on the nanoparticle growth process, four different growth solutions were prepared, each with a different volume of gold seed solution added to the CTAB-based growth medium. The seed volumes tested were 0.3 ml, 3 ml, 7 ml, and 12 ml. The UV-Vis spectra for these solutions reveal critical insights into how seed concentration affects nanoparticle size distribution and morphology.

Nanoparticles with 0.3 ml of Gold Seeds added: The UV-Vis spectrum of this solution exhibits two distinct peaks. The first peak, around 530 nm, corresponds to the original gold seeds, indicating their persistence in the solution. The second, broader peak appears at a much longer wavelength, approximately 800 nm, suggesting the formation of significantly larger nanoparticles or even aggregates. The large distance between these peaks indicates a bimodal distribution, where the low seed concentration led to uncontrolled growth of some nanoparticles, resulting in a population of larger, less uniform particles. This scenario arises because there are fewer nucleation sites, allowing some nanoparticles to grow extensively, leading to variability in size. On this figure, there is a plasmon resonance above 800nm as we can guess from the increase at the right of the spectrum. It is the most right-shifted one.

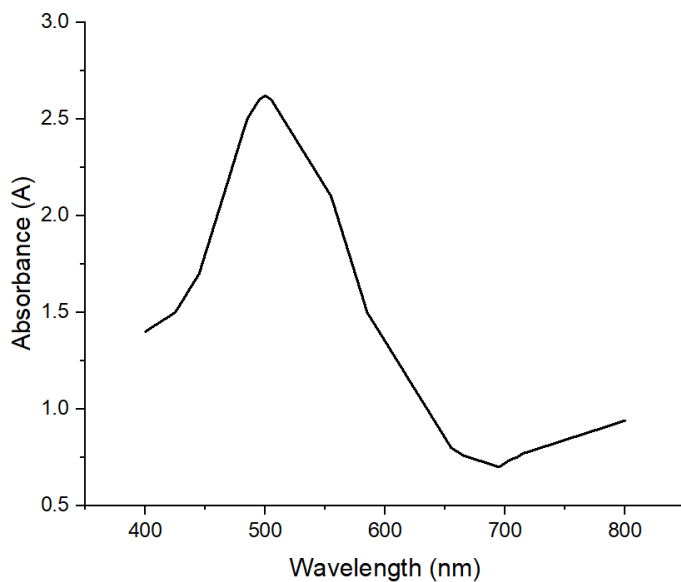


Figure 16. The UV-Vis spectrum of 0.3 ml of Gold Seeds added to growth solution.

Nanoparticles with 3 ml of Gold Seeds added: For the 3 ml sample, the UV-Vis spectrum still shows two peaks, but they are closer together compared to the 0.3 ml sample. The first peak remains near 520 nm, while the second peak shifts to a shorter wavelength, around 680 nm. This shift suggests that although larger nanoparticles are forming, the overall size distribution is more uniform than the 0.3 ml sample. The increase in the number of seeds provides more nucleation sites, which helps to control the growth of nanoparticles, reducing the formation of excessively large particles.

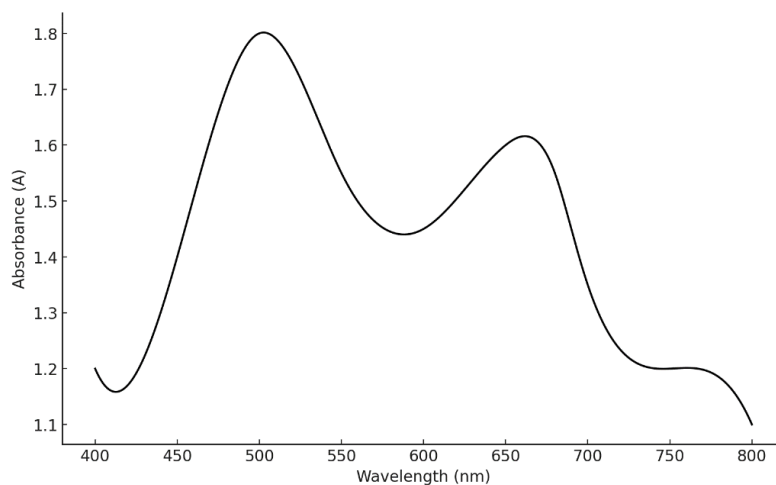


Figure 17. The UV-Vis spectrum of 3 ml of Gold Seeds was added to the growth solution.

Nanoparticles with 7 ml of Gold Seeds added: In the 7 ml sample, the UV-Vis spectrum shows a further convergence of the two peaks. The primary peak around 540 nm remains, while the second peak is less pronounced and close to the first, at approximately 720 nm. This indicates that the nanoparticle growth is becoming even more controlled, with fewer large particles forming. The closer proximity of the peaks suggests a narrower size distribution, with the growth process favoring smaller, more uniform nanoparticles due to the increased seed concentration.

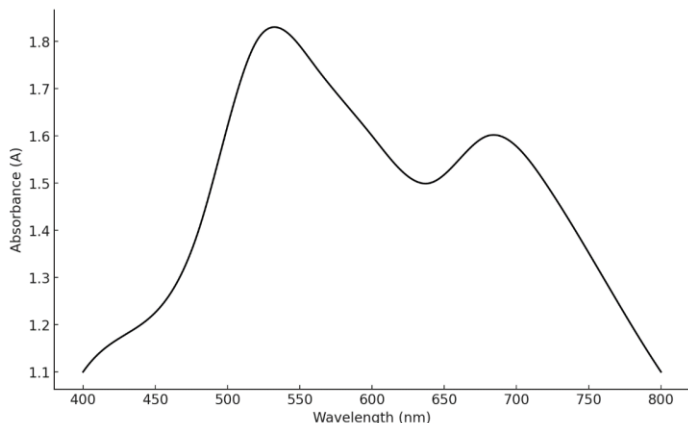


Figure 3.8. The UV-Vis spectrum of 7 ml of Gold Seeds was added to the growth solution.

Nanoparticles with 12 ml of Gold Seeds added: The UV-Vis spectrum for the 12 ml sample reveals that the two peaks have nearly merged into a single, broad peak centered around 530-550 nm. This result suggests a highly uniform nanoparticle size distribution, dominated by smaller nanoparticles. The merging of the peaks indicates that the majority of the nanoparticles are now similar in size, as the high concentration of seeds provided ample nucleation sites, limiting the growth of any individual nanoparticle and resulting in a more homogeneous particle population. The second peak is very close to the one at 520-540 nm, it is the most blue-shifted because the nanoparticles are smaller.

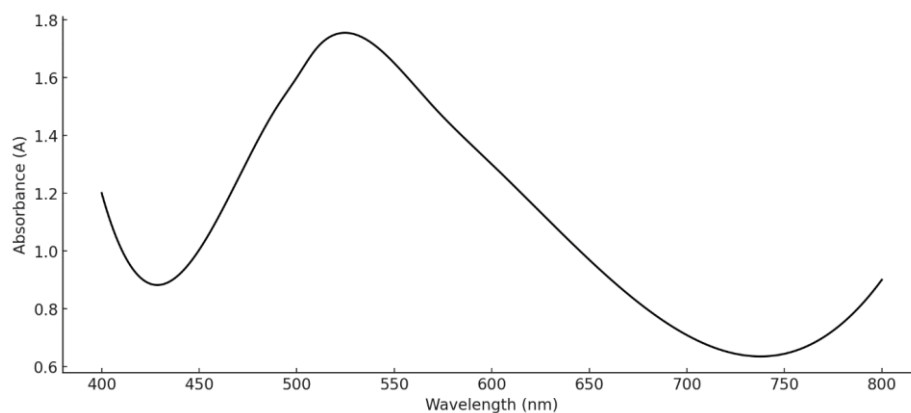


Figure 18. The UV-Vis spectrum of 12 mL of gold seeds, which was added to the growth solution.

The absorption spectra showed a redshift in the SPR peak as the seed volume increased, suggesting a growth in the size of the nano bipyramids. Typically, using a larger seed volume can result in more available nucleation sites, promoting the formation of smaller bipyramids.

Size Characterization Using Dynamic Light Scattering (DLS)

To verify the size of the synthesized nanoparticles, Dynamic Light Scattering (DLS) was employed. DLS is a widely used technique for determining the size distribution of particles in colloidal solutions. Due to its high accuracy and quick analysis, it serves as a crucial tool in nanoparticle characterization. These measurements provide precise information about the size distribution of the nanoparticles, helping to confirm the accuracy of the UV-Vis spectroscopy results.

As shown in Figure 3.10, DLS measurement was conducted to assess the size of the gold seed nanoparticles used in the synthesis process. The figure below shows the size distribution of the gold seed nanoparticles. As seen, the majority of the particles fall within a specific size range in average of 8 nm, indicating uniformity and homogeneity of the synthesized nanoparticles. The measurements reveal that the average size of these nanoparticles is within the nanometer range, consistent with the findings from the UV-Vis spectroscopy analysis.

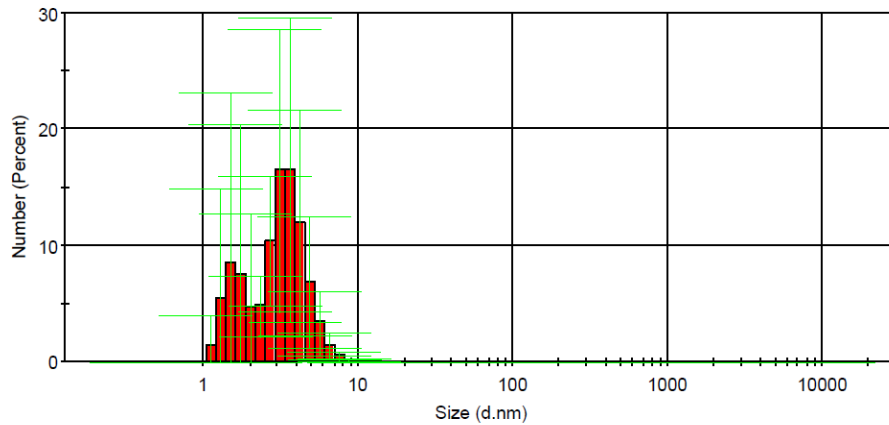


Figure 19. DLS for Au seeds.

The Dynamic Light Scattering (DLS) measurements for the gold nano bipyramids synthesized with varying volumes of Au seed (0.3, 3, 7, and 12 ml) showed a clear trend in particle size distribution. The DLS data indicated that the hydrodynamic diameter of the nano bipyramids decreased with the volume of the seed used. The smallest seed volume (0.3 ml) produced nano bipyramids with the largest average hydrodynamic diameter, while the largest seed volume (12 ml) resulted in the smallest nano bipyramids. Shown in Figure 30-33.

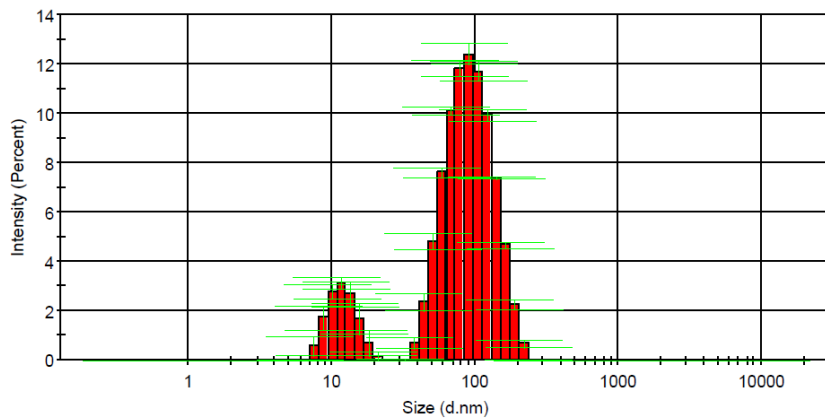


Figure 20. DLS for 0.3 ml seed in growth solution. The average size of nano bipyramids is 100nm.

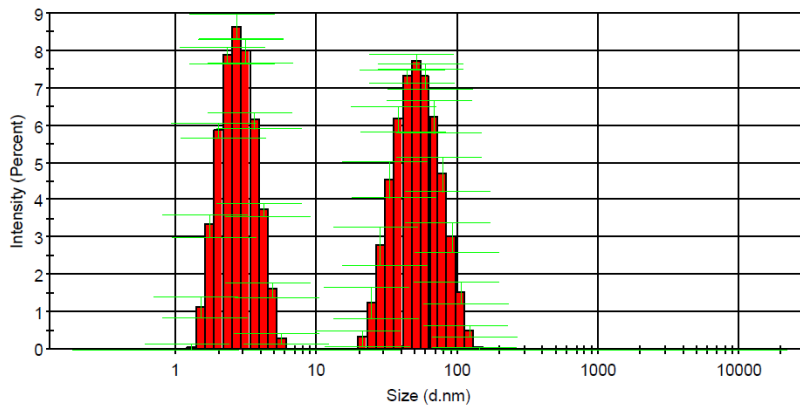


Figure 3.12. DLS for 3 ml seed in growth solution. The average size of nano bipyramids is 70nm, 5nm.

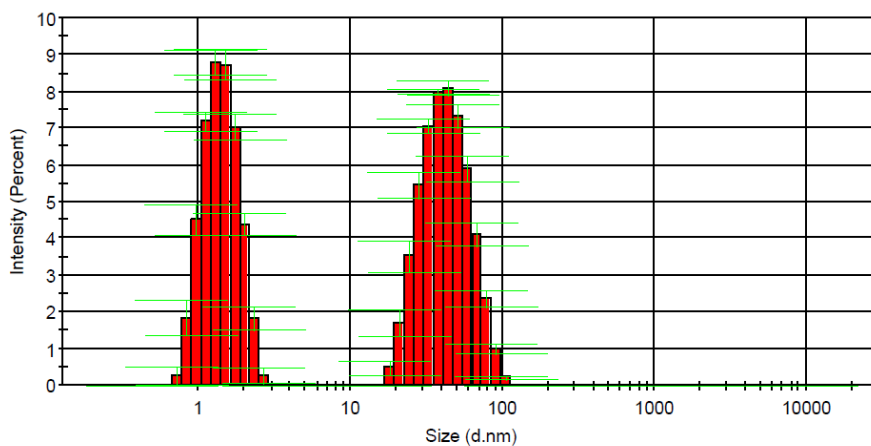


Figure 21. DLS for 7 ml seed in growth solution. The average size of nano bipyramids is 60nm, 3nm.

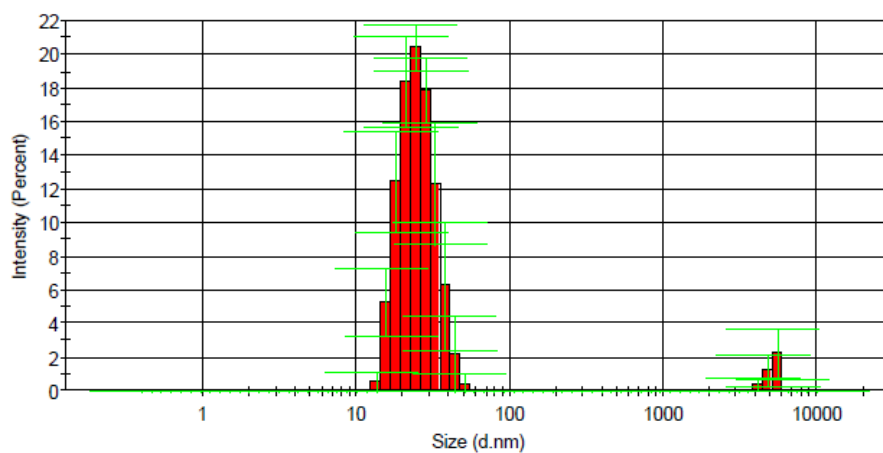


Figure 3.14. DLS for 12 ml seed in growth solution. The average size of nano bipyramids is 12 nm.

Transmission Electron Microscopy (TEM) Results: The TEM analysis provided detailed insights into the size and morphology of the gold nanoparticles synthesized with varying seed volumes. For the sample synthesized with 0.3 ml of seed, the nanoparticles exhibited an average size of approximately 100 nm along the major axis, predominantly forming nano bipyramids, as shown in Figure 3.15.

When the seed volume was increased to 3 ml, the nanoparticles became more spherical with an average size of around 50 nm Figure 3.16.

Further increasing the seed volume to 7 ml resulted in nanoparticles with an average size of about 44 nm, displaying a mix of spherical and slightly elongated shapes, as illustrated in Figure 3.17.

Finally, the highest seed volume of 12 ml produced the smallest nanoparticles, averaging around 10 nm, which were mostly uniform spherical particles Figure 3.18.

The TEM images confirm that increasing the seed volume consistently leads to a decrease in the size of the nanoparticles. This trend is significant because it demonstrates that the seed-mediated growth method allows for precise control over the nanoparticle size, which is crucial for applications where specific particle dimensions are required. The shift from larger, elongated bipyramids to smaller, spherical nanoparticles with increased seed volume highlights the impact of seed concentration on the growth dynamics of the particles.

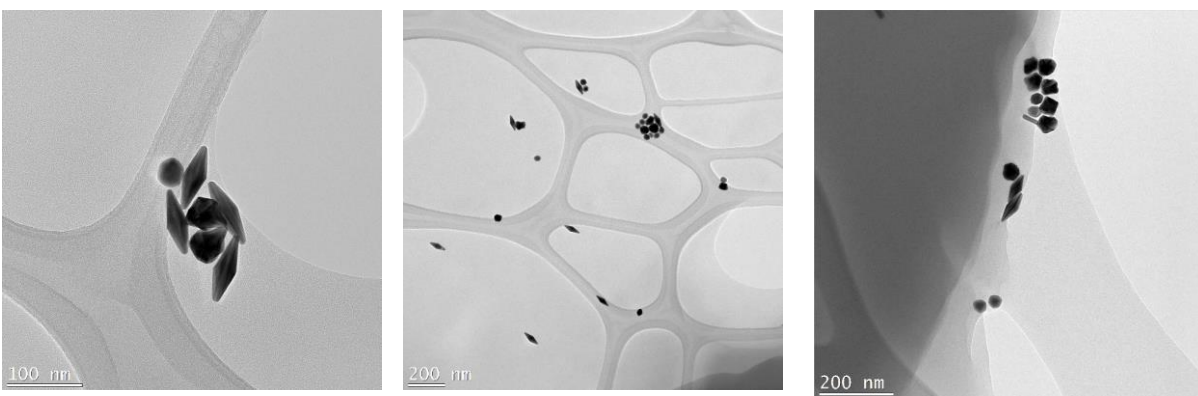


Figure 22. TEM images of gold nanoparticles synthesized with 0.3 mL seed solution, showing bipyramidal and smaller aggregated particles. Scale bars: 100 nm (left), 200 nm (center and right).

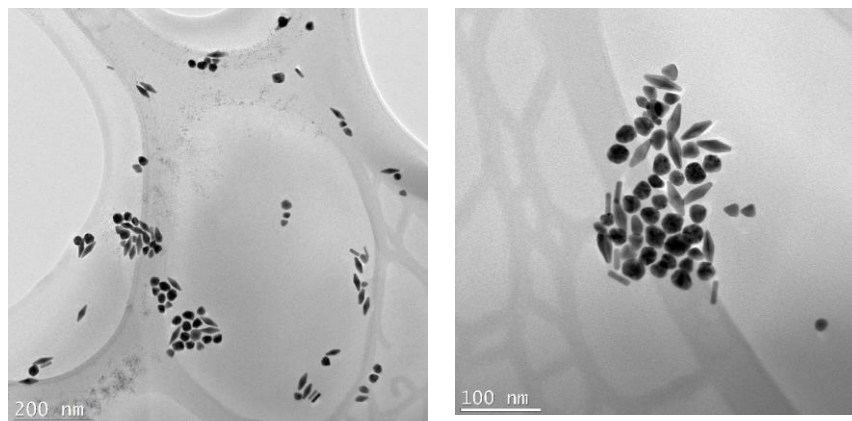


Figure 23. TEM images of gold nanoparticles synthesized with 3 mL seed solution, showing clusters of bipyramidal nanoparticles. Scale bars: 200 nm (left), 100 nm (right).

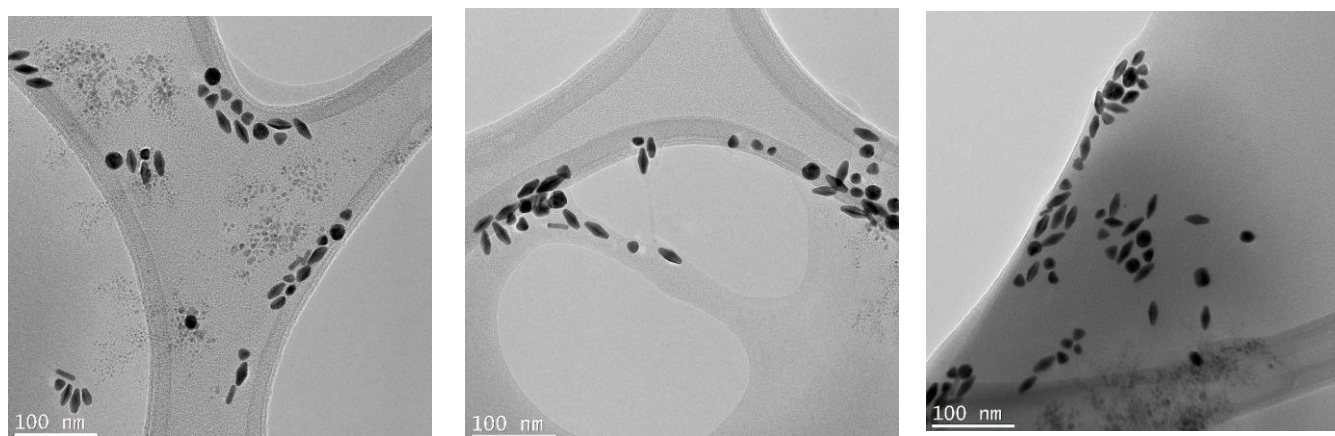


Figure 3.17. TEM images of gold nanoparticles synthesized with 7 mL seed solution, showing dispersed bipyramidal nanoparticles. Scale bars: 100 nm (all images).

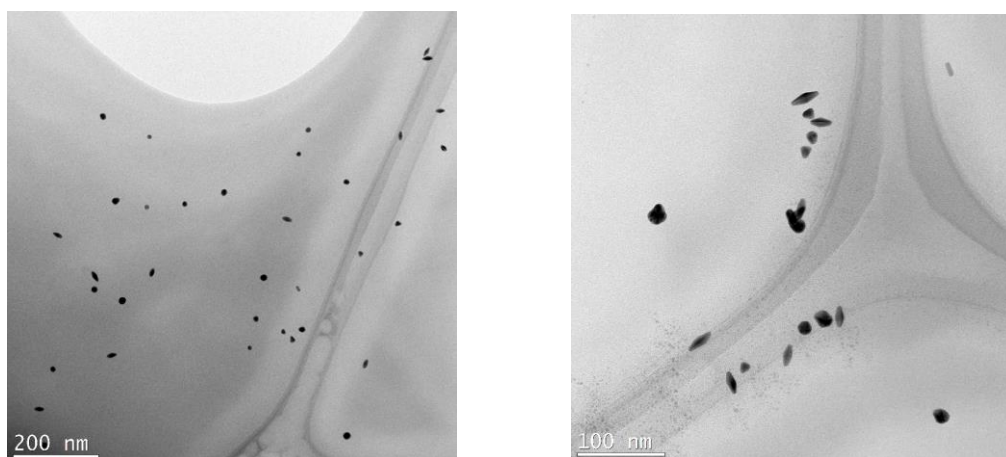


Figure 3.18. TEM images of gold nanoparticles synthesized with 12 mL seed solution, showing smaller, dispersed particles. Scale bars: 200 nm (left), 100 nm (right).

The results from UV-Vis spectroscopy, Dynamic Light Scattering (DLS), and TEM demonstrate the significant influence of the seed volume on the size and distribution of gold nanoparticles. The smaller and more uniform nanoparticles observed at higher seed volumes can be attributed to a more effective nucleation process, where the increased number of seed particles promotes the formation of smaller gold nanoparticles and this one gives the better nanoparticles.

Synthesis of Gold Nanoparticles by Citrate Reduction Method:

In this study, we employed the simplest system: Au NPs synthesized using the citrate reduction method. This method was selected as a starting point due to its straightforward approach and the ability to produce small, spherical nanoparticles suitable for forming films on substrates. Initially, the plan was to study more complex nanostructures, such as gold nanopyramids, for their catalytic properties. However, due to time constraints, we focused solely on the simpler citrate-stabilized nanoparticles—characterization of gold nanoparticles synthesized by the citrate reduction method.

Dynamic Light Scattering (DLS) Analysis: The size distribution of gold nanoparticles synthesized via the citrate reduction method was analyzed using Dynamic Light Scattering (DLS), as shown in Figure 35. The DLS data reveals a broad size distribution, with a primary peak centred around 100 nm, indicating that the majority of the nanoparticles fall within this size range. Additionally, a secondary peak at larger sizes suggests the presence of nanoparticle aggregates, which could result from partial agglomeration during the synthesis process.

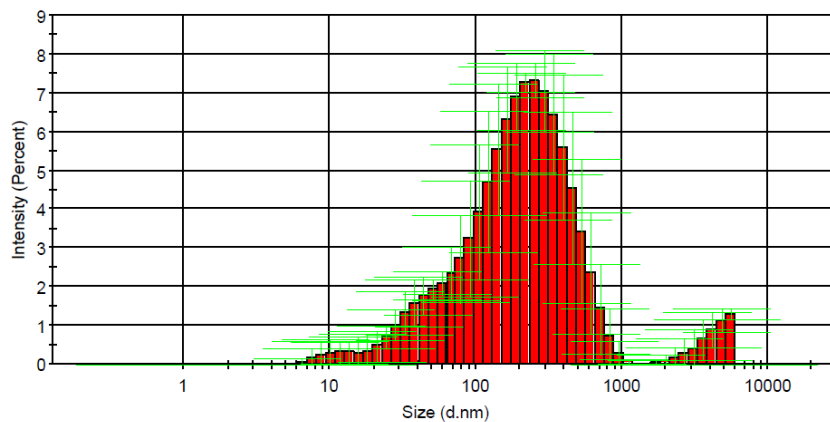


Figure 3.19. DLS for Gold Nanoparticles synthesized by Citrate Reduction Method

UV-Vis Spectroscopy Analysis: The UV-Vis absorption spectrum of the synthesized gold nanoparticles is presented in Figure 39. The spectrum features a broad surface plasmon resonance (SPR) peak centered around 530 nm, characteristic of gold nanoparticles. The breadth of the SPR peak, compared to the sharper peaks observed in gold nano bipyramids, suggests a broader size distribution and potential anisotropy in particle shapes. The broadening of the SPR peak may also indicate the presence of gold-citrate aggregates, as these aggregates can affect the homogeneity and stability of the nanoparticles in solution.

The combination of DLS and UV-Vis spectroscopy results confirms the successful synthesis of gold nanoparticles using the citrate reduction method.

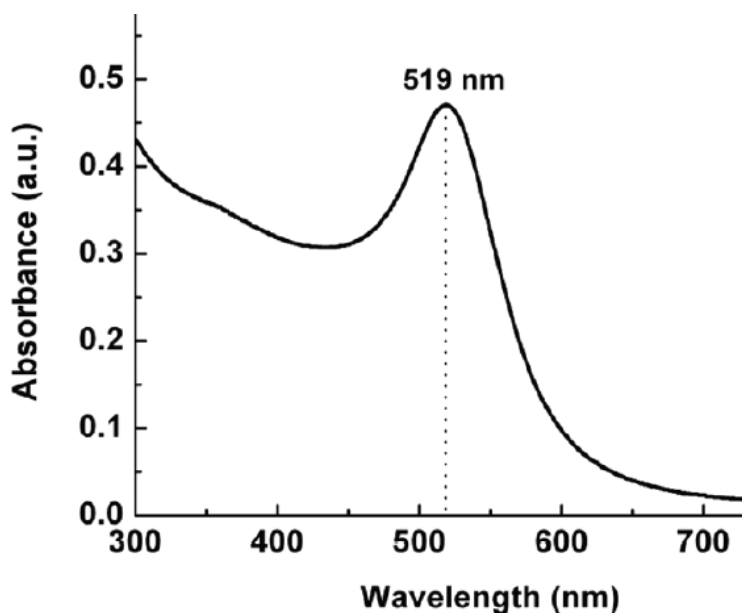


Figure 24. UV-VIS for Gold Nanoparticles Synthesized by Citrate Reduction Method

3.6 Electrodeposition gold nanoparticles

Electrodeposition is a widely used technique to deposit a thin layer of material onto an electrode surface by applying an electric current. In the context of gold nanoparticles, this process involves the reduction of gold ions (Au^{3+}) present in the solution to form metallic gold (Au) on the electrode surface. This is achieved by applying a potential that is sufficiently negative to drive the reduction reaction.

Before the actual deposition, cyclic voltammetry (CV) is often employed to identify the optimal potential range for gold reduction. CV involves sweeping the potential of the working electrode in a cyclic manner

while recording the resulting current. This allows for the observation of the reduction and oxidation processes of the gold ions in solution. From the CV curve, the potential at which gold ions begin to reduce (known as the reduction potential) can be identified.

Once the appropriate reduction potential is determined, the electrodeposition process can proceed in one of two ways. One method is to apply a potential that cycles around the reduction potential, which helps to control the growth of gold nanoparticles on the electrode surface. This cycling approach can promote the formation of nanoparticles with more uniform size and distribution.

Alternatively, a constant potential, held at a value sufficiently negative to ensure continuous reduction of gold ions, can be applied. This method simplifies the process by maintaining a steady driving force for the reduction reaction, leading to the gradual buildup of gold on the electrode surface.

Cyclic Voltammetry (CV) Results: The electrochemical behavior observed during cyclic voltammetry (CV) provided insights into gold nanoparticles' nucleation and growth mechanisms on the FTO substrate. As the number of cycles increased from 4 to 8, there was a clear increase in current density, indicating the progressive accumulation of gold on the electrode surface. The first few cycles displayed a typical nucleation loop, suggesting the initial formation of discrete gold nuclei. The total charge passed during the CV cycles directly correlates with the amount of gold deposited. As the number of cycles increased, the nucleation sites grew, eventually leading to the formation of a continuous gold film.

To calculate the charge passed, which correlates with the amount of gold (Au) deposited, it is necessary to integrate the current over time for each cycle. The charge Q passed is given by the equation:

$$Q = \int I(t), dt$$

Where:

$I(t)$ is the current as a function of time during the deposition.

dt is the differential time interval.

The progressive increase in current density across cycles further emphasizes the accumulation of gold on the electrode surface (see Figure 3.21 for 4 cycles). The calculated charge passed during these 4 cycles is approximately 2.45 μC , which correlates with the amount of gold deposited.

Similarly, for 8 cycles, the continuous increase in current density further indicates enhanced accumulation of gold on the electrode surface (see Figure 3.22 for 8 cycles). The calculated charge passed during these 8 cycles is approximately 4.9 μC , reflecting the increased deposition of gold with additional cycles.

Increase in Charge Passed: The comparison of charges passed during 4 and 8 cycles shows an increase from 2.45 μC to 4.9 μC . This indicates that more gold was deposited on the FTO substrate as the number of CV cycles increased.

Growth Mechanism: The initial few cycles suggest nucleation, where discrete gold nuclei form on the substrate. As cycles progress, these nuclei grow into larger particles, and eventually, a continuous gold film forms.

Preparation: Prepare 1 mM of HAuCl_4 in 0.1 M potassium phosphate buffer solution as a supporting electrolyte with a pH of ~ 6.7 .

For preparing buffer: 8.71 g of K_2HPO_4 in volume 500 ml distilled water/6.80 g of KH_2PO_4 in volume 500 ml distilled water/ To 400 mL of the KH_2PO_4 solution, gradually add the K_2HPO_4 solution until the pH reaches 6.7 and volume is 500 ml. Store the buffer at 4°C for stability. Use platinum as a counter electrode, gold and buffer solution as an electrolyte, FTO as a working electrode, and Ag/AgCl as a reference electrode.

The rate was 10 mVs⁻¹, the potential from -1.25 to -0.75 V, and the number of redox cycles 4,8,12. (Elgrishi *et al.*, 2018)

Film Formation: The higher charge passed during 8 cycles compared to 4 cycles suggests that the gold film becomes denser and more continuous as the deposition process continues.

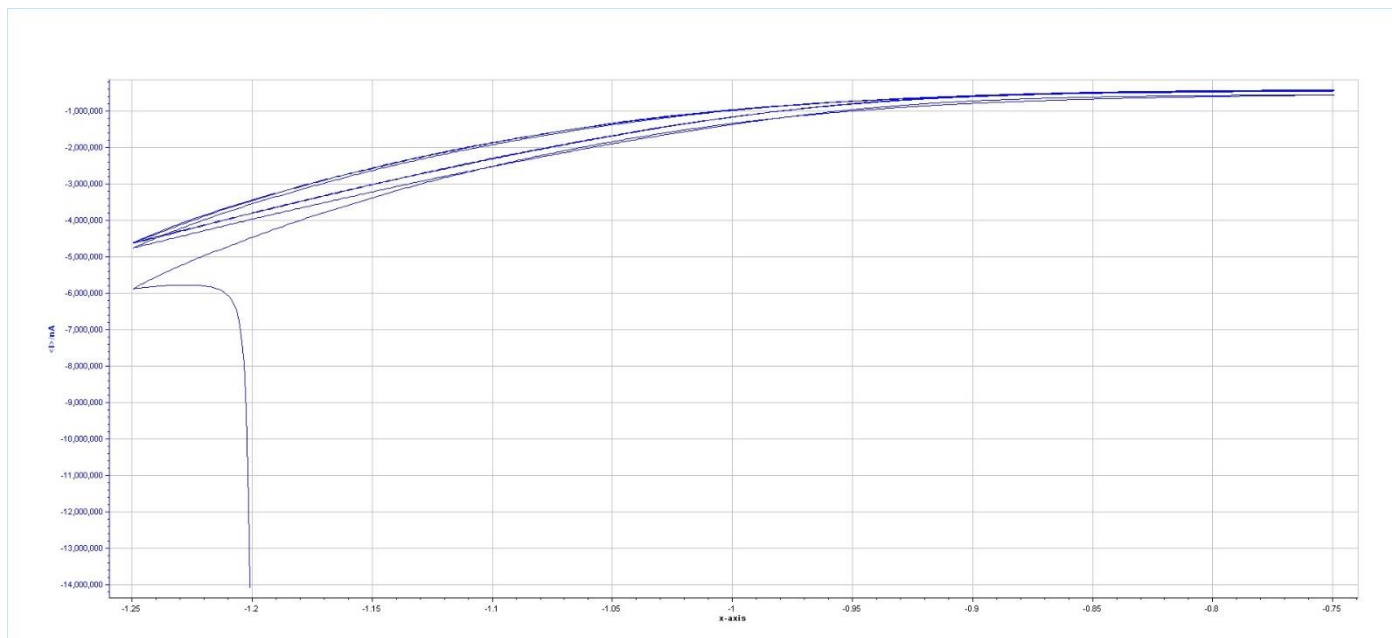


Figure 3.21. Cyclic Voltammetry (CV) results for 4 cycles of electrodeposition of gold on FTO substrate with Ag/AgCl reference electrode and potassium phosphate buffer solution as a supporting electrolyte.

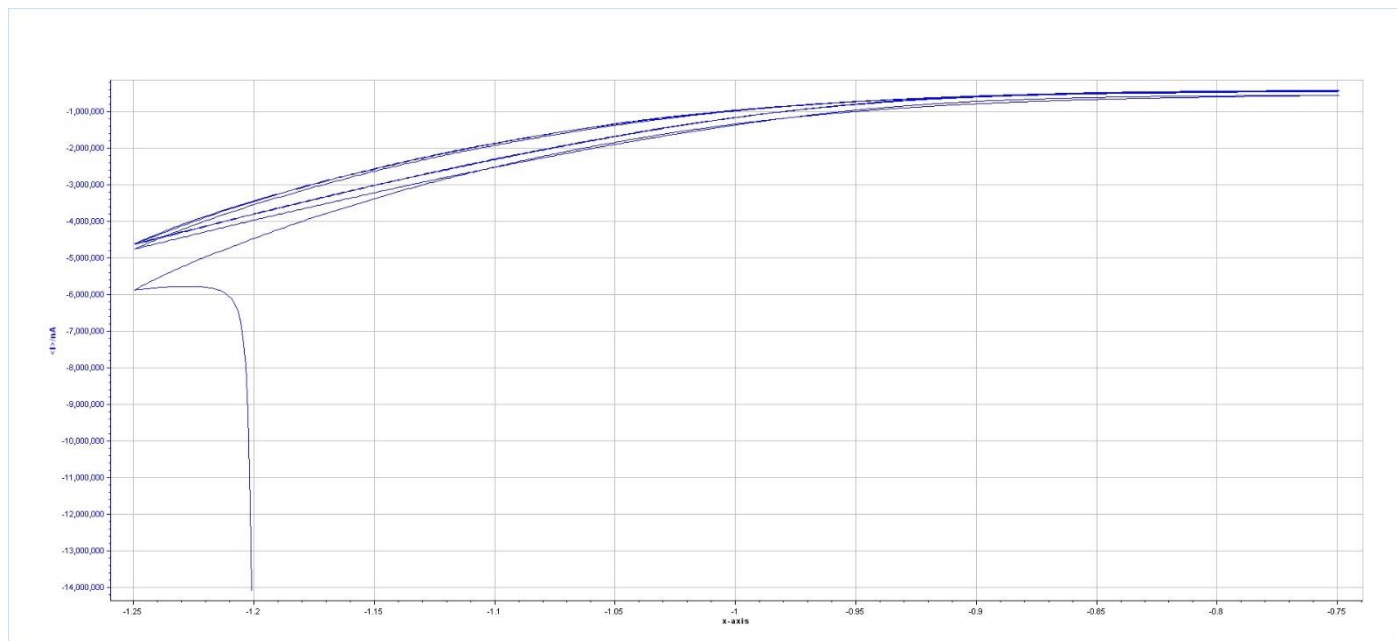


Figure 25. Cyclic Voltammetry (CV) results for 8 cycles of electrodeposition of gold on FTO substrate with Ag/AgCl reference electrode and potassium phosphate buffer solution as a supporting electrolyte.

Scanning Electron Microscopy (SEM) Analysis:

Detailed SEM analysis post-deposition revealed significant changes in morphology corresponding to the number of cycles. After 4 cycles, the SEM images displayed a rough film completely covered with gold nanoparticles, with average diameters of approximately 20-30 nm. The nanoparticles were well-separated, with little to no aggregation, indicating a successful initial nucleation phase. This suggests that the gold nanoparticles formed a uniform layer on top of the underlying film, effectively covering the electrode surface. Since SEM only probes the surface, the images demonstrate that the electrode is fully coated with these nanoparticles.

At 8 cycles, the SEM images showed a transition from discrete nanoparticles to larger aggregates. In this phase, individual nanoparticles were no longer easily distinguishable, indicating the onset of coalescence where nanoparticles begin to merge, forming larger and more irregular structures. This transition marks the beginning of a more continuous and denser gold layer, reflecting the progression from initial nucleation to growth and aggregation phases as more cycles were applied.

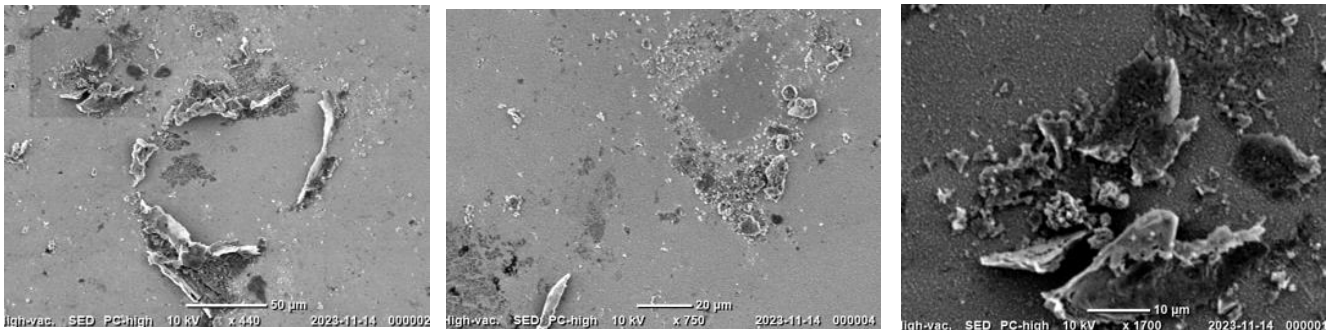


Figure 3.23. SEM image of the gold nanoparticles deposited after 4 cycles of cyclic voltammetry

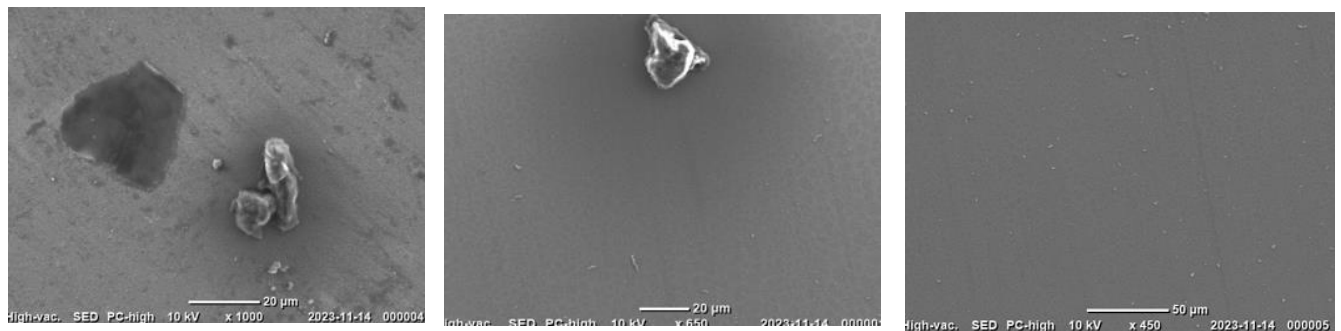


Figure 3.24. SEM image of the gold nanoparticles deposited after 8 cycles of cyclic voltammetry

Atomic Force Microscopy (AFM) Analysis:

AFM topography analysis confirmed the observations made through SEM and provided quantitative measurements of surface roughness. After 4 cycles of cyclic voltammetry, the surface appeared relatively smooth with a low RMS roughness value, as shown in Figure 45. The AFM phase images at this stage displayed a homogenous phase contrast, which is consistent with the distribution of similarly sized nanoparticles across the surface.

As the number of cycles increased to 8, the RMS roughness value increased, indicating the transition to a more textured surface. This change is visually supported by the AFM phase images in Figure 46, which show greater variations in phase contrast. These variations reflect the increased topographical variance, likely due to the coalescence of nanoparticles as they merge into larger, more irregular structures.

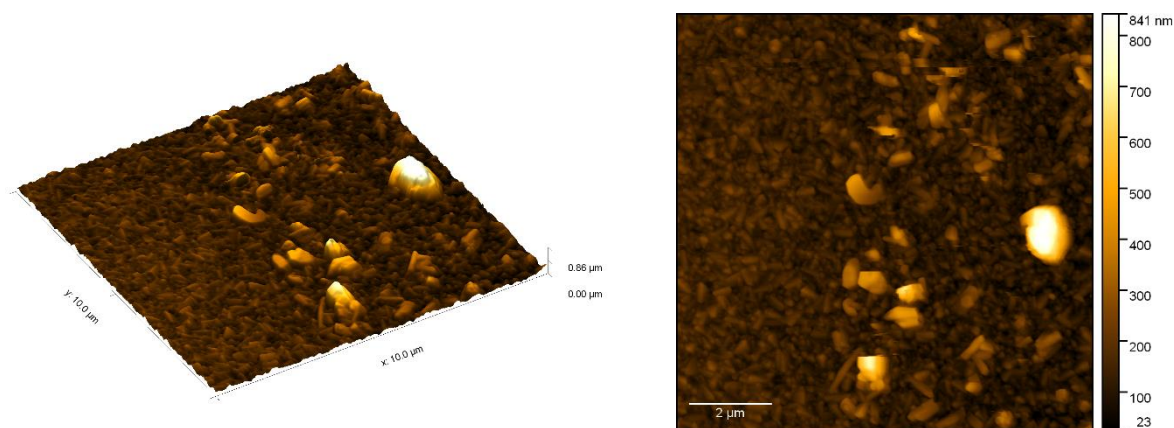


Figure 3.25. AFM image of the gold nanoparticles deposited after 4 cycles of cyclic voltammetry

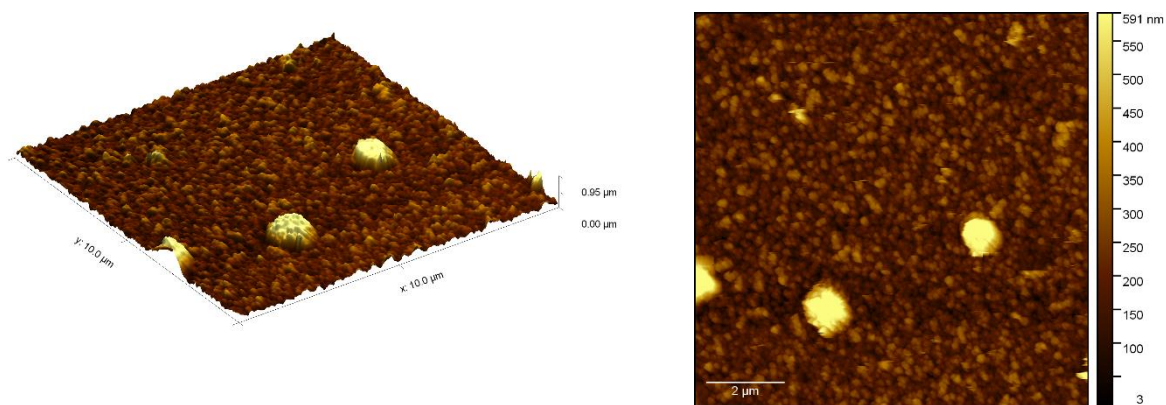


Figure 3.26. AFM image of the gold nanoparticles deposited after 8 cycles of cyclic voltammetry

Isolated nucleation sites lead to the formation of discrete nanoparticles. As the deposition continues, these nanoparticles grow and start to coalesce, leading to the formation of larger aggregates and eventually a continuous film. This gradual growth from discrete particles to a film is crucial for applications that rely on specific nanostructures, such as localized surface plasmon resonance (LSPR)-based sensors or catalytic beds.

CHAPITRE 4

Photocatalysis experiments

4.1 Introduction

The primary objective of the photocatalyst experiments described in this chapter is to explore, optimize, and enhance the deposition of gold nanoparticles (AuNPs) on various substrates, and to improve their photocatalytic and photoelectrocatalytic performance when combined with iron (III) meso-tetraphenylporphyrin chloride (FeTPP). These efforts are crucial in advancing the efficiency of carbon dioxide (CO₂) reduction processes, contributing significantly to developing sustainable energy solutions and environmental remediation strategies.

Unlike typical semiconductor catalysts, where light absorption is enhanced through localized surface plasmon resonance (LSPR), our focus is on utilizing the hot electrons generated in the plasmonic metal (AuNPs) under light irradiation. These hot electrons can be efficiently transferred to the adsorbed CO₂ molecules on the catalyst's surface, driving the reduction of CO₂ into valuable chemicals such as methane, CO, methanol, and other hydrocarbons.

However, the performance of AuNPs as photocatalysts is highly dependent on several factors, including their size, shape, and the method of deposition onto the substrate. The interaction between AuNPs and the substrate can influence the overall catalytic activity, stability, and durability of the photocatalyst. In this chapter, we investigate multiple deposition techniques, including dip coating, electrodeposition, drop casting, to identify the most effective method for anchoring AuNPs onto substrates such as glass, indium tin oxide (ITO), and fluorine-doped tin oxide (FTO). Each of these substrates offers distinct advantages in terms of electrical conductivity, optical transparency, and compatibility with various photocatalytic systems, choosing substrate a critical factor in the overall efficiency of the photocatalyst.

Optimization of these deposition techniques is essential for achieving uniform, stable, and efficient nanoparticle coatings. Uniformity in nanoparticle distribution ensures consistent photocatalytic activity across the entire substrate surface, while stability and durability are crucial for long-term operation and practical applications. The deposition process must be finely tuned to control the thickness, morphology, and dispersion of the AuNPs, as these characteristics directly impact the light absorption and electron transfer capabilities of the photocatalyst.

In addition to optimizing the deposition of AuNPs, this chapter explores the synergistic combination of AuNPs with FeTPP, a well-known porphyrin-based catalyst. FeTPP can facilitate electron transfer and provide additional catalytic sites for CO₂ reduction, potentially enhancing the overall photocatalytic efficiency. By integrating AuNPs with FeTPP, we aim to create a composite material that leverages the strengths of both components. The combined photocatalyst is expected to exhibit superior performance due to enhanced light absorption, and increased availability of active catalytic sites.

This research focuses on the systematic investigation, optimization, and characterization of photocatalysts composed of gold nanoparticles (AuNPs) coupled with porphyrin molecules. By exploring various deposition techniques—such as drop casting, electrochemical deposition, and dip coating—this study aims to optimize the interaction between AuNPs and porphyrins to enhance the generation and utilization of hot electrons for CO₂ reduction. The findings will provide critical insights into the effective integration of plasmonic metals with molecular catalysts, guiding the design of high-performance photocatalytic systems. This work will contribute to advancing photocatalysis for sustainable energy production and environmental protection by demonstrating a targeted approach for maximizing catalytic efficiency in AuNP-porphyrin systems.

4.2 Deposition Optimization

Optimizing the deposition process is crucial to achieving uniform, stable, and efficient coatings of gold nanoparticles (AuNPs) on substrates such as glass, indium tin oxide (ITO), and fluorine-doped tin oxide (FTO). This section presents a comprehensive overview of the various deposition techniques explored in this research, including drop casting, electrodeposition, and dip-coating. While electrodeposition and dip-coating were initially considered, these methods did not yield the desired results; electrodeposition led to uneven coatings and poor adhesion, and dip-coating failed to produce consistent films. Consequently, the focus shifted to drop casting, a simpler and cost-effective method that provided more uniform and stable coatings. The section details the experimental setup for optimizing drop casting, analyzes the resulting film characteristics, and examines the impact of ethanol on the deposition process and its outcomes.

4.2.1 Experimental Setup

The experimental setup for optimizing the deposition process primarily involved the drop-casting method, which was identified as the most effective among the various techniques tested. The drop-casting process involves carefully placing a controlled volume of gold nanoparticle (AuNP) suspension onto the substrate

surface, such as glass, indium tin oxide (ITO), or fluorine-doped tin oxide (FTO). This method was chosen due to its simplicity, cost-effectiveness, and ability to achieve thicker, higher-concentration AuNP coatings, which are essential for effective photocatalytic CO₂ reduction.

In addition to drop-casting, two other deposition techniques were explored: dip coating and electrodeposition. However, these methods were found to be less effective for our specific application:

Dip Coating:

The substrates were immersed in a suspension of AuNPs and then slowly withdrawn, allowing a thin film to form as the solvent evaporated. Dip coating proved to be time-consuming and ineffective for several reasons: the concentration of AuNPs deposited on the surface was too low, resulting in a film that was not sufficiently gold-rich for our photocatalytic experiments. Moreover, the adhesion of the nanoparticles to the substrates was poor, leading to unstable and non-uniform coatings. For the deposition to be effective in our photocatalytic reduction experiments, a thicker, higher-concentration gold film is necessary, which dip coating could not achieve.

Electrodeposition:

This method was detailed in Chapter 3, where an electric current was applied to deposit gold nanoparticles (AuNPs) onto the substrate from an aqueous solution containing gold ions. While electrodeposition allows for precise control over the deposition process, it was found unsuitable for our application. According to the results presented in Chapter 3, electrodeposition primarily produced smooth films with very large particles, in the micrometer (μm) range rather than the nanometer (nm) scale. These large particles lack localized surface plasmon resonance (LSPR), which is essential for generating hot electrons, a critical requirement for effective photocatalytic reduction. This structural limitation, rather than the amount of deposited gold, rendered the electrodeposition method ineffective for our experiments. The SEM and AFM images in Chapter 3 illustrate these characteristics clearly, further supporting our decision to focus on alternative deposition methods. Given these challenges, the drop-casting method emerged as the most suitable technique, enabling the creation of uniform, stable, and sufficiently thick AuNP coatings required for our experiments. The detailed setup and optimization process for drop casting is described in the following sections, including an analysis of the film characteristics and the impact of ethanol on the deposition process and outcomes.

1. Materials:

Gold nanoparticles (AuNPs): Various synthesis methods were explored, including seed-growth method, citrate reduction method, and electrodeposition, to produce AuNPs with different sizes and properties. While all synthesized nanoparticles were initially tested, the seed-growth method proved to be the most effective, leading us to focus on optimizing this approach further. Adjustments were made to the concentrations and conditions for the seed-growth method to enhance the performance in our photocatalytic experiments.

Ethanol: Ethanol was used as a solvent to mix with the AuNP solution, playing a crucial role in achieving a homogeneous distribution of nanoparticles during deposition. Through trial and error, we discovered that without ethanol, the nanoparticle solution would gather in one corner of the surface and dry unevenly. However, when ethanol was included, the solution dried uniformly across the entire surface, resulting in more consistent coatings.

Substrates: Glass, ITO (Indium Tin Oxide), and FTO (Fluorine-Doped Tin Oxide) were employed as substrates to evaluate the effectiveness of the various deposition processes, with a focus on achieving uniform, stable coatings suitable for photocatalytic applications.

2. Procedure:

Preparation of AuNP Solution: The gold nanoparticles were dispersed in water, and ethanol was added to the solution to improve dispersion. According to articles, the optimal ethanol concentration was determined to be 3 times by volume.(Hashemi *et al.*, 2018)

Drop-Casting Process: A micropipette dispensed a few microliters of the AuNP solution onto the substrate. The volume of the solution varied depending on the substrate size, with typical volumes ranging from 5 to 10 microliters.

Drying: The substrate with the AuNP solution was placed in an oven at 50°C to allow the solvent to evaporate. This temperature was chosen to ensure that the nanoparticles adhered well to the substrate without burning or degrading about 10 minute for each time.

Repetition: The drop-casting process was repeated multiple times, typically 10 to 12 times, to build a thick, uniform layer of AuNPs. After each application, the substrate was allowed to dry completely before applying the next layer.

4.2.2 Optimization Results

4.2.2.1 Uniformity and Stability of Coatings

The uniformity and stability of the AuNP coatings were critical factors in ensuring their effectiveness in photocatalytic and photo-electrocatalytic applications. These aspects were evaluated through repeated deposition and testing in various solutions.

Uniformity: The deposition process was carried out using multiple drop-casting steps, where small volumes of the nanoparticle solution were repeatedly applied to the substrate surface. This method allowed the solvent to evaporate between each application, leading to the gradual buildup of a visibly pink layer as you can see in Figure 48. The pink color indicated the presence of gold nanoparticles. Although no precise imaging techniques, such as SEM, were employed to confirm the uniformity, the consistent color across the surface suggested that the nanoparticles were relatively evenly distributed. This even coverage was visually assessed by observing the absence of color variation or patchiness, indicating non-uniform deposition.

Stability: Initial stability tests indicated that the film remained intact in electrolytes, but it would unexpectedly detach and fall into the solution, revealing a lack of long-term stability. To address this issue, a layer of nail polish was applied around the film on the substrate surface, which effectively secured the film and allowed it to be used in subsequent experiments.



Figure 4.1. Left: The film has detached and fallen into the electrolyte, demonstrating its instability. Right: The film remains intact and adhered to the surface after being stabilized with a surrounding application of Transparent nail polish is a film formed from a nitrocellulose-based polymer in solution.

Two comparative images (Figure 4.1) illustrate the stability differences between the films: one shows a film after detachment in the electrolyte, and the other demonstrates a film secured by lacquer, which initially adhered to the surface but began tearing during the experiment. Both the citrate-reduced and electrodeposited nanoparticles detached from the surface in less than a minute. The citrate-reduced nanoparticles dispersed into the water as a powder, whereas the electrodeposited nanoparticles detached as a complete layer. Although the application of lacquer helped the electrodeposited film remain adhered, it eventually began tearing under experimental conditions, compromising its integrity.

For the citrate-reduced nanoparticles, it was necessary to use freshly synthesized samples, as they destabilized quickly in solution, leading to phase separation. In contrast, while the electrodeposited nanoparticles initially adhered better, their smooth films with larger particle sizes lacked the plasmonic properties required for catalytic applications, and they also detached within a short timeframe.

While logistical constraints at Université de Montréal prevented extensive catalytic activity testing with gas chromatography (GC), further experiments remain feasible. Freshly synthesized nanoparticles could be prepared, and their catalytic activity assessed using GC, particularly if efforts are made to address the instability and detachment issues observed in both deposition methods.

4.2.3 Effect of Deposition Parameters

4.2.3.1 Temperature Control

Temperature was a critical parameter in the deposition process. It was found that maintaining the oven temperature at 45°C was ideal for allowing the solvent to evaporate without causing the AuNPs to burn or degrade. This temperature also ensured the nanoparticles adhered well to the substrate, forming a stable layer.

Optimal Temperature: Through trial and error, it was determined that 45°C was the optimal temperature for drying the AuNP solution. Lower temperatures resulted in incomplete solvent evaporation, while higher temperatures risked damaging the nanoparticles. As can be seen in Figure 48 on the left side, we used both ethanol, which resulted in a uniform deposition across the surface, and a temperature of 45°C in an oven, allowing each layer to dry in one minute before applying the next drop cast. This process created a pink deposition layer, indicating the presence of our nanoparticles. In the right image, we did

not use ethanol, leading to deposition only in one corner of the surface. The temperature was around 55°C, causing the film to burn after ten minutes.

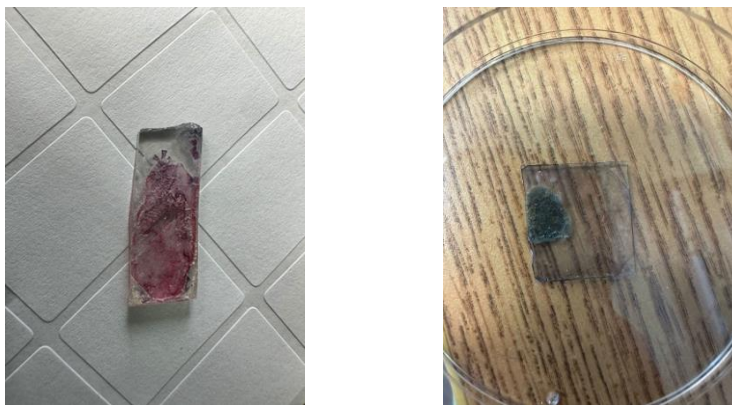


Figure 4.2. (Left) Uniform deposition achieved using ethanol and 45°C drying, forming a pink nanoparticle layer. (Right) Uneven deposition without ethanol, with overheating at 55°C causing film damage.

4.3 Catalysis tests

In this section, we discuss the experimental setups and results of various catalysis tests performed to evaluate the effectiveness of different catalysts and photosensitizers in CO₂ reduction. The focus is on understanding the interplay between different materials and their impact on the efficiency and stability of the catalytic process.

4.3.1 Ru as a photosensitizer and Gold as a catalyst in the solution

Reference Experiment Setup and Objective

To establish a reliable baseline for our catalysis tests, we conducted a reference experiment using Tris(bipyridine)ruthenium(II) chloride as the photosensitizer and gold nanoparticles (AuNPs) as the catalyst. The primary objective of this experiment was to ensure that all experimental conditions were optimal and that any subsequent changes in results could be attributed solely to the variations in experimental variables.

Tris(bipyridine)ruthenium(II) chloride was selected due to their well-known efficiency in absorbing visible light and transferring electrons to AuNPs, thereby facilitating the reduction of CO₂. By using this

combination, we aimed to confirm that the setup was capable of driving CO₂ reduction and producing measurable products, specifically carbon monoxide (CO) and hydrogen (H₂).

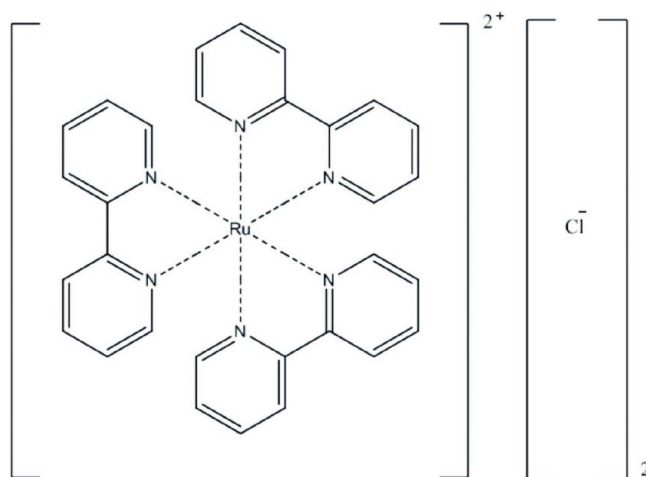


Figure 26. Structure of tris (bipyridine) ruthenium (II) chloride.

Experimental Conditions and Procedure

In this experiment, I maintained consistent conditions across two separate testing channels (Channel 4 and Channel 8) within the experimental setup, which were used to conduct parallel measurements. These channels refer to independent pathways within the gas chromatography system (or other analytical equipment, if applicable) that allow for simultaneous analysis of multiple samples. By using these two channels, we aimed to validate the reproducibility of the results, ensuring that any variations observed were not due to inconsistencies in the equipment or experimental conditions. The solution comprised DMF and H₂O in a 9:1 ratio, with a 5 ml/min flow rate. The electrolyte solution contained 0.5 M TEOA and 0.05 M BIH as sacrificial electron donors, along with Ru(trisbipyridine) at a concentration of 2×10^{-4} M. Gold nanoparticles of varying sizes (labeled Gold 4 and Gold 2) were used as the catalyst. The solution was irradiated with light at 480 nm and 445 nm to activate the Ru complexes.

Gold 2: nanoparticles synthesized with 0.3 ml seed as we present it earlier the size of this nanoparticle is about 100 nm

Gold 4: nanoparticles synthesized with 3 ml seedas we present it earlier the size of this nanoparticle is about 70 nm

Results and Analysis

The experiment successfully resulted in the reduction of CO₂, producing both CO and H₂ as measured by gas chromatography. The results, summarized in the table, indicate that the setup was effective in achieving CO₂ reduction under the given conditions. However, as mentioned earlier, we do not have access to the specific quantities of CO and H₂ produced, as this data has not been provided to us by the University of Montreal. Both channels produced comparable amounts of CO and H₂, demonstrating the consistency of the experimental setup.

Channel	Wavelengths(nm)	Solvent	Flow Rate	Electron Donors	Ru Concentration	Gold Catalyst	Products Detected
4	480, 445	DMF/H ₂ O 9:1	5 ml/min	TEOA 0.5 M, BIH 0.05 M	2 x 10 ⁻⁴ M	Gold 4	CO, H ₂
8	480, 445	DMF/H ₂ O 9:1	5 ml/min	TEOA 0.5 M, BIH 0.05 M	2 x 10 ⁻⁴ M	Gold 2	CO, H ₂

Table 4.1. Experimental conditions and detected products for CO₂ reduction using Ru as a photosensitizer and gold as a catalyst in solution.

These results confirmed that the Ru complexes effectively transferred electrons to the AuNPs, leading to the reduction of CO₂ and the formation of CO and H₂.

4.3.2 FeTPP as a catalyst and Gold as a Photosensitizer in the solution

Experimental Setup and Objective

In this experiment, we explored the catalytic performance of iron porphyrin (FeTPP) in combination with gold nanoparticles (AuNPs) serving as photosensitizers. The primary objective was to investigate how the

interaction between FeTPP and AuNPs under specific light irradiation could enhance the efficiency of CO₂ reduction, focusing particularly on the effects of different AuNP sizes (Gold 2 vs. Gold 4).

FeTPP is a well-known catalyst for multi-electron reduction reactions, making it a suitable candidate for CO₂ reduction. Meanwhile, AuNPs, due to their unique plasmonic properties, can absorb light and generate hot electrons, which can then be transferred to the FeTPP to drive the catalytic process. The experiment was designed to compare the effectiveness of different sizes of AuNPs in this context, with the expectation that nanoparticle size might significantly influence the catalytic outcome.

Experimental Conditions

The experiment was carried out under carefully controlled conditions to ensure accurate comparisons:

Irradiation: The solution was exposed to light at wavelengths of 480 nm and 445 nm for initial tests, and then 480 nm and 525 nm for subsequent tests. These wavelengths were chosen to match the plasmonic resonance of the AuNPs and maximize their electron-generating efficiency.

Solvents: Two solvent systems were tested: acetonitrile (acn) and a DMF/H₂O mixture in a 9:1 ratio. Acetonitrile is known for its good solubility and stability, while the DMF/H₂O mixture provides a polar environment that can influence the behavior of the catalytic species.

Flow Rate: A flow rate of 5 ml/min was maintained across all tests to ensure consistent exposure of the reactants to the light source and catalytic materials.

Sacrificial Electron Donors (SED): The electron donors tested were TEA (0.5 M), TEOA (0.5 M), and BIH (0.05 M) in various combinations. These donors are crucial as they supply the necessary electrons to the AuNPs, preventing recombination of electron-hole pairs and enhancing the reduction process.

Photocatalyst Concentration: FeTPP was used at a concentration of 5×10^{-6} M, ensuring a sufficient number of catalytic sites for the reaction.

Photosensitizer: The gold nanoparticles used as photosensitizers were of two types, Gold 2 and Gold 4, differing in size and volume. This variation allowed for the investigation of how nanoparticle size affects catalytic efficiency.

Results and Analysis

The results from the GC analysis provided insightful data regarding the effectiveness of the catalytic system under different conditions:

CO Detection: Across all tested conditions, CO was detected, indicating successful CO₂ reduction. The consistent detection of CO suggests that the catalytic system was effective in facilitating the multi-electron reduction of CO₂ to CO, with FeTPP as the active catalyst.

H₂ Detection: Interestingly, hydrogen was detected only in the presence of Gold 4, not Gold 2, particularly when using the DMF/H₂O solvent system under 480 nm and 525 nm irradiation. This finding is significant as it highlights the impact of nanoparticle size on the catalytic process.

Channel	Irradiation(nm)	Solvent	Flow Rate	Sacrificial Donors	Photocatalyst	Photosensitizer	Products Detected
4	480, 445 (2 light sources)	ACN	5 ml/min	TEA 0.5M	FeTPP 5 x 10 ⁻⁶ M	N/A	small detection of CO
8	480, 445	ACN	5 ml/min	TEOA 0.5 M	FeTPP 5 x 10 ⁻⁶ M	N/A	small detection of CO
4	480, 445	ACN	5 ml/min	TEOA 0.5 M, BIH 0.05 M	FeTPP 5 x 10 ⁻⁶ M	N/A	small detection of CO
8	480, 445	ACN	5 ml/min	TEA 0.5 M, BIH 0.05 M	FeTPP 5 x 10 ⁻⁶ M	N/A	small detection of CO
4	480, 525	DMF/H2 O 9:1	5 ml/min	TEOA 0.5 M, BIH 0.05M	FeTPP 5 x 10 ⁻⁶ M	Gold 2	small detection of CO
8	480, 525	DMF/H2 O 9:1	5 ml/min	TEOA 0.5 M, BIH 0.05M	FeTPP 5 x 10 ⁻⁶ M	Gold 4	small detection of CO and H2

Table 4.2. Experimental conditions and detected products for CO₂ reduction using FeTPP as a catalyst and Gold as a Photosensitizer in the solution.

The most noteworthy result is that hydrogen was detected exclusively in the presence of Gold 4, which was not the case with Gold 2. This suggests that Gold 4 was more effective as a photosensitizer. The higher effectiveness of Gold 4 can be attributed to the larger volume of seed used, leading to the formation of smaller nanoparticles with a greater surface area-to-volume ratio. Smaller nanoparticles are reported to exhibit enhanced plasmonic properties, which may allow them to generate more hot electrons upon light absorption. These electrons could potentially be transferred to FeTPP to drive the catalytic reduction of CO₂. In contrast, larger nanoparticles tend to reradiate more light, which can reduce the efficiency of hot electron generation. (Li *et al.*, 2017) This finding aligns with the observations made in Chapter 3, where it

was discussed that smaller nanoparticles often exhibit higher catalytic activity due to their increased surface area and improved electron transfer capabilities.

The results from this experiment underscore the critical role of nanoparticle size in catalytic efficiency. The superior performance of Gold 4, as evidenced by the successful detection of both CO and H₂, suggests that optimizing the size and surface properties of AuNPs can significantly enhance the effectiveness of CO₂ reduction systems. The combination of FeTPP as a catalyst and Gold 4 as a photosensitizer proved to be highly effective, particularly under the tested conditions with DMF/H₂O as the solvent. Moving forward, further research could focus on fine-tuning the size and concentration of AuNPs, as well as exploring other solvent systems, to maximize the production of CO and H₂, thereby advancing the development of more efficient and scalable CO₂ reduction technologies.

This expanded analysis not only provides a detailed understanding of the experiment and its outcomes but also offers insights into the potential avenues for future research and optimization.

4.3.3 Gas phase CO₂ Reduction

Experimental Setup and Objective

In this experiment, we aimed to investigate the effectiveness of different catalysts and photosensitizers in the gas-phase reduction of CO₂. Unlike liquid-phase reactions, gas-phase CO₂ reduction more closely mimics industrial processes, where CO₂ is typically present as a gas. The goal was to test the catalytic performance under simulated sunlight conditions using a sun simulator, replicating the solar spectrum, and to analyze the reduction products using gas chromatography (GC).

The experimental setup involved bubbling CO₂ through water at different flow rates, with the catalysts deposited on glass substrates. The sun simulator provided a controlled and consistent light source, ensuring that the catalysts were exposed to the same intensity and spectrum of light throughout the experiment.

Experimental Conditions

The experiment was conducted under the following conditions:

Light Source: A sun simulator was used, providing irradiation similar to natural sunlight with a wavelength centered around 580 nm.

CO₂ Flow Rate: Three different flow rates were tested—5 ml/min, 3 ml/min, and 5 ml/min—to assess the impact of CO₂ concentration on the reduction process.

Catalyst Deposition: The catalysts were deposited on glass substrates. In the first two tests, 200 µl of the catalyst solution (Gold 2 alone and Gold 2 with FeTPP) was deposited. In the third test, a larger volume (1000 µl) was deposited, using Gold 6 (the AuNPs which synthesis by seed growth method with adding 12 ml seeds) in combination with FeTPP.

Reaction Environment: CO₂ was bubbled through water, which was then exposed to the sun simulator's light to activate the catalysts.

Results and Analysis

The results from the GC analysis showed the following:

Test 1 (Gold 2): No detection of CO or H₂, indicating that Gold 2 alone was not effective under these conditions for CO₂ reduction. Test 2 (Gold 2 and FeTPP): Similarly, no CO or H₂ was detected, suggesting that the combination of Gold 2 and FeTPP did not enhance the reduction process under these specific conditions. Test 3 (Gold 6 and FeTPP): A small amount of CO and CH₄ was detected, indicating some level of CO₂ reduction. The detection of methane (CH₄) is particularly interesting, as it suggests a different pathway for CO₂ reduction compared to previous experiments.

Light Source	CO ₂ Flow Rate	Catalyst Deposition	Catalyst Combination	Detection Results
580 nm Sun Simulator	5 ml/min	200 µl deposition on glass	Gold 2	No detection of CO, H ₂ , or CH ₄
580 nm Sun Simulator	3 ml/min	200 µl deposition on glass	Gold 2 with FeTPP	No detection of CO, H ₂ , or CH ₄
580 nm Sun Simulator	5 ml/min	1000 µl deposition on glass	Gold 6 with FeTPP	Small detection of CO and CH ₄

Table 4.3. Experimental conditions and detected products for Gas-phase CO₂ Reduction

The results indicate that the catalyst combination involving a larger volume of Gold 6 and FeTPP was more effective in reducing CO₂ to CO and CH₄ because it has smaller nanoparticle, as we mentioned in DLS measurement the size are about 12nm This suggests that the increased catalyst loading and the specific properties of Gold 6, potentially forming smaller and more active nanoparticles, contributed to the observed catalytic activity. The detection of methane is particularly noteworthy as it implies a potential shift in the reaction mechanism when the catalyst loading is increased.

Unfortunately, we do not have the exact data for the amounts of carbon monoxide, hydrogen, and methane produced in the reactions. Due to limitations with our initial gas chromatography system, we conducted these measurements using the gas chromatography (GC) facilities at the University of Montreal. However, we encountered difficulties in accessing the results from those experiments from our collaborator after the experiments were performed, as well as the inability to conduct additional tests. As a result, we were unable to obtain or retain the data necessary for further, and more quantitative, analysis. This limits the conclusions we can draw from our results, which have to stay qualitative.

Figure 49 illustrates the visual Setup of the experimental setup. The image on the left shows the sun simulator, with a glass container used to expose the CO₂-water mixture to simulated sunlight for photocatalytic reactions. The image on the right presents the blue light setup, containing multiple reactors, potentially for parallel experimental runs or comparisons, with a sampling line connected to the GC, which is not visible in the image.

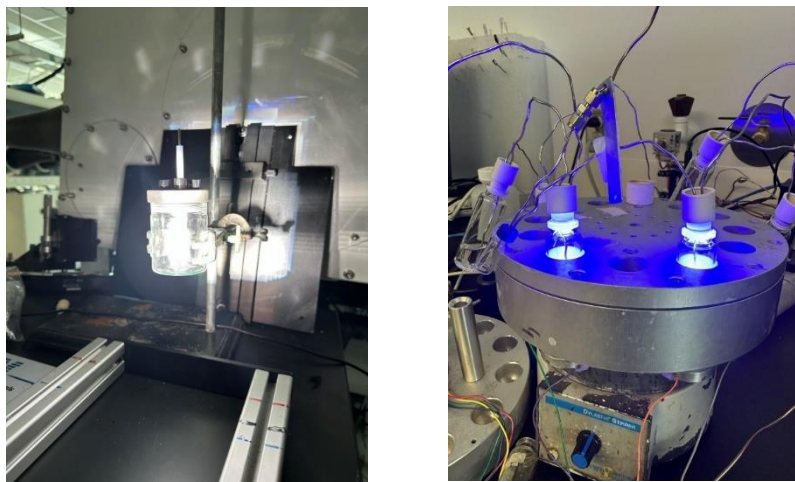


Figure 27. (Left) Sun simulator used for photocatalytic experiments. (Right) Blue light illumination setup with a sampling line leading from the reactor to the GC (not visible).

The gas-phase CO₂ reduction experiments revealed that increasing the volume of catalyst deposited on the glass substrates and using a more active form of gold nanoparticles (Gold 6) in combination with FeTPP resulted in detectable levels of CO and CH₄. These findings suggest that catalyst loading and the specific nature of the AuNPs play critical roles in the effectiveness of the reduction process.

Future experiments could focus on further optimizing the catalyst composition, loading, and reaction conditions to maximize CO and CH₄ production. Additionally, exploring the underlying mechanisms that lead to methane formation could provide valuable insights into developing more efficient catalytic systems for CO₂ reduction.

4.3.4 Photocathode gold nanoparticle and FeTPP

Experimental Setup and Objective

This section of the experiment focuses on evaluating the performance of a photocathode composed of gold nanoparticles (AuNPs) and iron porphyrin (FeTPP) for CO₂ reduction under simulated sunlight conditions. The photocathode was constructed by depositing AuNPs synthesis by seed growth method onto a fluorine-doped tin oxide (FTO) electrode, followed by the addition of FeTPP. The aim was to assess the catalytic activity of this setup in generating photoelectrochemical currents and driving the reduction of CO₂ to products such as CO and H₂.

Experimental Conditions

The experiment was conducted under the following conditions:

Electrolyte: Potassium bicarbonate (KHCO_3) at a concentration of 0.1 M was used as the electrolyte. The preparation involved dissolving 1 g of KHCO_3 in 100 ml of water.

Electrodes:

Counter Electrode: A carbon rod was used.

Working Electrode: The working electrode was FTO coated with AuNPs synthesis by seed growth method and FeTPP.

Reference Electrode: Ag/AgCl (3M KCl) was used, prepared by dissolving 2.23 g of KCl in 10 ml of water.

Irradiation Source: A sun simulator was used to replicate sunlight, with various intensities and flow rates tested.

Flow Rates: Experiments were conducted with CO_2 bubbled in water at flow rates of 10 ml/min and 20 ml/min to evaluate the impact of CO_2 concentration on the reduction process.

Results and Analysis

The results from the GC analysis and photoelectrochemical measurements are summarized as follows:

Test 1: Using FTO with AuNPs deposited by the citrate method, no detection of CO , H_2 , or any other reduction products was observed. The flow rate was 20 ml/min under 500 sun simulator conditions.

Test 2: The setup was similar, but with a reduced flow rate of 10 ml/min under standard sun simulator conditions. Again, no detection of any products was recorded.

Test 3: A different approach was taken, involving the electrodeposition of gold on FTO, followed by the evaporation of FeTPP. This setup generated a small photoelectrochemical current, indicating some level of photoactivity, though no CO or H₂ was detected.

Light Source	CO ₂ Flow Rate	Electrode Composition	Detection Results
sun simulator	20 ml/min	FTO, AuNPs (citrate method), FeTPP	No detection of products (CO, H ₂ or other molecules)
sun simulator	10 ml/min	FTO, AuNPs (citrate method), FeTPP	No detection of products (CO, H ₂ or other molecules)
sun simulator	20 ml/min	FTO, AuNPs (electrodeposited), FeTPP	Small photocurrent detected

Table 1.4. Experimental conditions and detected products for CO₂ reduction using photocathode gold nanoparticles and FeTPP.

The lack of detection of CO and H₂ in the first two tests suggests that the method of nanoparticle deposition plays a significant role in the effectiveness of the photocathode. The citrate method of depositing AuNPs did not produce a functional photocathode under the tested conditions. However, in the third test, where AuNPs were electrodeposited onto the FTO and FeTPP was evaporated onto this surface, a small photocurrent was detected. This indicates that while the system was not yet optimized for CO₂ reduction, it did exhibit some photoactivity, suggesting potential for further development.

The experiments conducted with the photocathode comprising AuNPs and FeTPP highlight the importance of the method used for nanoparticle deposition. The electrodeposition of AuNPs, followed by FeTPP evaporation, showed some promise with the generation of a small photocurrent, indicating that this approach could be more effective for future optimization. The lack of product detection in the initial tests suggests that the system needs further refinement, possibly through improved electrode preparation techniques, optimizing the loading of FeTPP, or adjusting the reaction conditions.

Additionally, the photoelectrochemical experiments were conducted in collaboration with Olivier Schott at the University of Montreal. However, we do not have access to detailed results from these experiments.

Conclusion

This project represents an effort to enhance the efficiency of photocatalytic CO₂ reduction by exploring the synthesis and deposition of gold nanostructures. The primary objective was to optimize these nanostructures for the conversion of CO₂ into valuable chemical products like carbon monoxide (CO) and hydrogen (H₂), which are crucial intermediates in the development of sustainable energy solutions.

The synthesis phase involved exploring multiple methods for producing gold nanoparticles, with a particular focus on creating gold nano bipyramids. These bipyramids were chosen due to their unique plasmonic properties, which can enhance light absorption and improve the efficiency of photocatalytic processes. The project tested various synthesis techniques, including the seed-mediated growth method, to produce monodisperse gold nano bipyramids with controlled sizes and shapes. The synthesis process was optimized to achieve high-yield production of nanoparticles with the desired structural characteristics.

To further enhance the photocatalytic activity, the project integrated the synthesized gold nano bipyramids with iron tetraphenylporphyrin (FeTPP), a well-known molecular catalyst for CO₂ reduction. The combination of plasmonic gold nanoparticles with FeTPP was aimed at leveraging the synergistic effects between the two components. The gold nanoparticles act as light absorbers, generating hot electrons under illumination, which are then transferred to the FeTPP catalyst to drive the reduction of CO₂. This integration was carefully studied to optimize the interaction between the nanoparticles and the catalyst, ensuring efficient electron transfer and catalytic activity. Plasmonic efficiency was evaluated using differential calorimetry, and photochemical efficiency was also calibrated to ensure accuracy in energy transfer measurements.

A significant portion of the research was dedicated to exploring various deposition techniques for applying the gold nanoparticle-FeTPP hybrid structures onto substrates. Fluorine-doped tin oxide (FTO) was selected as the substrate due to its conductive and transparent properties, making it suitable for (electro)photocatalytic applications. Multiple deposition methods, including drop-casting, electrodeposition, and dip-coating, were evaluated to achieve uniform and stable nanoparticle films on the FTO substrates.

One of the major challenges encountered during the deposition process was the stability of the nanoparticle films in electrolyte solutions. The films often showed poor adhesion and susceptibility to degradation when exposed to the reactive environment of the photocatalytic cell. This instability significantly impacted the long-term performance of the catalysts, leading to decreased efficiency and limited durability. Despite these challenges, certain deposition techniques showed promise in improving film stability, although further optimization is necessary.

The photocatalytic performance of the gold nano bipyramid-FeTPP hybrids was rigorously tested under controlled conditions. The results demonstrated that this combination could effectively reduce CO₂ to CO, with concurrent hydrogen evolution, under visible light irradiation. The presence of combining gold nano bipyramids with FeTPP was found a little bit increase the photocatalytic activity compared to nanoparticle alone, showing the role of plasmonic nanoparticles in boosting catalytic efficiency. The experiments underscored the need for precise control over nanoparticle size, shape, and distribution to enhance plasmonic effects. However, limitations in access to advanced characterization equipment have restricted the ability to obtain quantitative results, making optimization more challenging.

In conclusion, while this project has made meaningful progress in optimizing gold nanostructures for CO₂ reduction, it is important to emphasize that the results are still preliminary. Challenges, particularly in terms of film stability, have limited the ability to fully evaluate the system's long-term performance. Nevertheless, the combination of gold nano bipyramids and FeTPP on FTO substrates has shown potential, offering valuable insights that can guide future research. However, additional studies will be necessary to overcome the remaining obstacles and develop more efficient and robust photocatalytic systems. Continued exploration of plasmonic nanostructures is essential to fully realize their potential in sustainable energy applications.

References and Bibliography

- Aljabali, A. A. A., Akkam, Y., Al Zoubi, M. S., Al-Batayneh, K. M., Al-Trad, B., Abo Alrob, O., Alkilany, A. M., Benamara, M. et Evans, D. J. (2018). Synthesis of Gold Nanoparticles Using Leaf Extract of *Ziziphus zizyphus* and their Antimicrobial Activity. *Nanomaterials*, 8(3), 174. <https://doi.org/10.3390/nano8030174>
- Amanullah, S., Gotico, P., Sircoglou, M., Leibl, W., Llansola-Portoles, M. J., Tibiletti, T., Quaranta, A., Halime, Z. et Aukauloo, A. (2024). Second Coordination Sphere Effect Shifts CO₂ to CO Reduction by Iron Porphyrin from Fe⁰ to Fe^I. *Angewandte Chemie International Edition*, 63(4), e202314439. <https://doi.org/10.1002/anie.202314439>
- Apaydin, D. H., Schlager, S., Portenkirchner, E. et Sariciftci, N. S. (2017). Organic, Organometallic and Bioorganic Catalysts for Electrochemical Reduction of CO₂. *ChemPhysChem*, 18(22), 3094-3116. <https://doi.org/10.1002/cphc.201700148>
- Azam, M. A. et Mupit, M. (2022). Chapter 2 - Carbon nanomaterial-based sensor: Synthesis and characterization. Dans J. G. Manjunatha et C. M. Hussain (dir.), *Carbon Nanomaterials-Based Sensors* (p. 15-28). Elsevier. <https://doi.org/10.1016/B978-0-323-91174-0.00015-9>
- Bagheri, H., Talemi, R. P. et Afkhami, A. (2015). Gold nanoparticles deposited on fluorine-doped tin oxide surface as an effective platform for fabricating a highly sensitive and specific digoxin aptasensor. *RSC Advances*, 5(72), 58491-58498. <https://doi.org/10.1039/C5RA09402J>
- Bin, Z., Feng, L. et Yan, Y. (2022). Biomimetic metalloporphyrin oxidase modified carbon nanotubes for highly sensitive and stable quantification of anti-oxidants tert-butylhydroquinone in plant oil. *Food Chemistry*, 388, 132898. <https://doi.org/10.1016/j.foodchem.2022.132898>
- Bonin, J., Chaussemier, M., Robert, M. et Routier, M. (2014). Homogeneous Photocatalytic Reduction of CO₂ to CO Using Iron(0) Porphyrin Catalysts: Mechanism and Intrinsic Limitations. *ChemCatChem*, 6(11), 3200-3207. <https://doi.org/10.1002/cctc.201402515>
- Bonin, J., Maurin, A. et Robert, M. (2017). Molecular catalysis of the electrochemical and photochemical reduction of CO₂ with Fe and Co metal based complexes. Recent advances. *Coordination Chemistry Reviews*, 334, 184-198. <https://doi.org/10.1016/j.ccr.2016.09.005>
- Borse, V. et Konwar, A. N. (2020). Synthesis and characterization of gold nanoparticles as a sensing tool for the lateral flow immunoassay development. *Sensors International*, 1, 100051. <https://doi.org/10.1016/j.sintl.2020.100051>
- Carnovale, C., Bryant, G., Shukla, R. et Bansal, V. (2016). Size, shape and surface chemistry of nano-gold dictate its cellular interactions, uptake and toxicity. *Progress in Materials Science*, 83, 152-190. <https://doi.org/10.1016/j.pmatsci.2016.04.003>
- Chen, D., Zhang, H., Liu, Y. et Li, J. (2013). Graphene and its derivatives for the development of solar cells, photoelectrochemical, and photocatalytic applications. *Energy Environ. Sci.*, 6, 1362-1387. <https://doi.org/10.1039/C3EE23586F>

- Chiang, H.-C., Wang, Y., Zhang, Q. et Levon, K. (2019). Optimization of the Electrodeposition of Gold Nanoparticles for the Application of Highly Sensitive, Label-Free Biosensor. *Biosensors*, 9(2), 50. <https://doi.org/10.3390/bios9020050>
- Chu, W., Zheng, Q., Prezhdoo, O. V. et Zhao, J. (2020). CO₂ Photoreduction on Metal Oxide Surface Is Driven by Transient Capture of Hot Electrons: Ab Initio Quantum Dynamics Simulation. *Journal of the American Chemical Society*, 142(6), 3214-3221. <https://doi.org/10.1021/jacs.9b13280>
- Cuong, N. D. et Quang, D. T. (2020). Progress through synergistic effects of heterojunction in nanocatalysts - Review. *Vietnam Journal of Chemistry*, 58(4), 434-463. <https://doi.org/10.1002/vjch.202000072>
- Elgrishi, N., Rountree, K. J., McCarthy, B. D., Rountree, E. S., Eisenhart, T. T. et Dempsey, J. L. (2018). A Practical Beginner's Guide to Cyclic Voltammetry. *Journal of Chemical Education*, 95(2), 197-206. <https://doi.org/10.1021/acs.jchemed.7b00361>
- Facchi, D. P., Cruz, J. A. da, Bonafé, E. G., Pereira, A. G. B., Fajardo, A. R., Venter, S. A. S., Monteiro, J. P., Muniz, E. C. et Martins, A. F. (s. d.). Polysaccharide-Based Materials Associated with or Coordinated to Gold Nanoparticles: Synthesis and Medical Application. <http://www.eurekaselect.com>. <https://www.eurekaselect.com/article/82205>
- Fong, K. E. et Yung, L.-Y. L. (2013). Localized surface plasmon resonance: a unique property of plasmonic nanoparticles for nucleic acid detection. *Nanoscale*, 5(24), 12043-12071. <https://doi.org/10.1039/C3NR02257A>
- Ghosh, S. K. et Pal, T. (2007). Interparticle Coupling Effect on the Surface Plasmon Resonance of Gold Nanoparticles: From Theory to Applications. *Chemical Reviews*, 107(11), 4797-4862. <https://doi.org/10.1021/cr0680282>
- Gross, G. M., Nelson, D. A., Grate, J. W. et Synovec, R. E. (2003). Monolayer-Protected Gold Nanoparticles as a Stationary Phase for Open Tubular Gas Chromatography. *Analytical Chemistry*, 75(17), 4558-4564. <https://doi.org/10.1021/ac030112j>
- Grzelczak, M., Pérez-Juste, J., Mulvaney, P. et Liz-Marzán, L. M. (2008). Shape control in gold nanoparticle synthesis. *Chemical Society Reviews*, 37(9), 1783-1791. <https://doi.org/10.1039/B711490G>
- Gu, S., Marianov, A. N., Lu, T. et Zhong, J. (2023). A review of the development of porphyrin-based catalysts for electrochemical CO₂ reduction. *Chemical Engineering Journal*, 470, 144249. <https://doi.org/10.1016/j.cej.2023.144249>
- Hashemi, F., Rastegarzadeh, S. et Pourreza, N. (2018). A combination of dispersive liquid-liquid microextraction and surface plasmon resonance sensing of gold nanoparticles for the determination of ziram pesticide. *Journal of Separation Science*, 41(5), 1156-1163. <https://doi.org/10.1002/jssc.201700992>
- Hentschel, M., Dregely, D., Vogelgesang, R., Giessen, H. et Liu, N. (2011). Plasmonic Oligomers: The Role of Individual Particles in Collective Behavior. *ACS Nano*, 5(3), 2042-2050. <https://doi.org/10.1021/nn103172t>

- Hinman, S. S., McKeating, K. S. et Cheng, Q. (2017). Surface Plasmon Resonance: Material and Interface Design for Universal Accessibility. *Analytical chemistry*, 90(1), 19. <https://doi.org/10.1021/acs.analchem.7b04251>
- Hong, Y., Huh, Y.-M., Yoon, D. S. et Yang, J. (2012). Nanobiosensors Based on Localized Surface Plasmon Resonance for Biomarker Detection. *Journal of Nanomaterials*, 2012(1), 759830. <https://doi.org/10.1155/2012/759830>
- Hua, T., Li, S., Li, F., Zhou, Q. et Ondon, B. S. (2019). Microbial electrolysis cell as an emerging versatile technology: a review on its potential application, advance and challenge. *Journal of Chemical Technology & Biotechnology*, 94(6), 1697-1711. <https://doi.org/10.1002/jctb.5898>
- Hubenthal, F., Blázquez Sánchez, D. et Träger, F. (2012). Determination of Morphological Parameters of Supported Gold Nanoparticles: Comparison of AFM Combined with Optical Spectroscopy and Theoretical Modeling versus TEM. *Applied Sciences*, 2(3), 566-583. <https://doi.org/10.3390/app2030566>
- Jans, H., Liu, X., Austin, L., Maes, G. et Huo, Q. (2009). Dynamic Light Scattering as a Powerful Tool for Gold Nanoparticle Bioconjugation and Biomolecular Binding Studies. *Analytical Chemistry*, 81(22), 9425-9432. <https://doi.org/10.1021/ac901822w>
- Jin, S., Hao, Z., Zhang, K., Yan, Z. et Chen, J. (2021). Advances and Challenges for the Electrochemical Reduction of CO₂ to CO: From Fundamentals to Industrialization. *Angewandte Chemie*, 133(38), 20795-20816. <https://doi.org/10.1002/ange.202101818>
- Karamian, E. et Sharifnia, S. (2016). On the general mechanism of photocatalytic reduction of CO₂. *Journal of CO₂ Utilization*, 16, 194-203. <https://doi.org/10.1016/j.jcou.2016.07.004>
- Khashayar, P., Amoabediny, G., Larijani, B., Hosseini, M., Verplancke, R., Schaubroeck, D., De Keersmaecker, M., Adriaens, M. et Vanfleteren, J. (2016). Characterization of gold nanoparticle layer deposited on gold electrode by various techniques for improved sensing abilities. *BIOINTERFACE RESEARCH IN APPLIED CHEMISTRY*, 6(4), 1380-1390.
- Komarala, E. P., Alkhoori, A. A., Zhang, X., Cheng, H.-M. et Polychronopoulou, K. (2023). Design and synthesis of thermally stable single atom catalysts for thermochemical CO₂ reduction. *Journal of Energy Chemistry*, 86, 246-262. <https://doi.org/10.1016/j.jechem.2023.07.032>
- Koronaki, I. P., Prentza, L. et Papaefthimiou, V. (2015). Modeling of CO₂ capture via chemical absorption processes – An extensive literature review. *Renewable and Sustainable Energy Reviews*, 50, 547-566. <https://doi.org/10.1016/j.rser.2015.04.124>
- Kushnarenko, A., Zabelina, A., Guselnikova, O., Miliutina, E., Vokatá, B., Zabelin, D., Burtsev, V., Valiev, R., Kolska, Z., Paidar, M., Sykora, V., Postnikov, P., Svorcik, V. et Lyutakov, O. (2024). Merging gold plasmonic nanoparticles and L-proline inside a MOF for plasmon-induced visible light chiral organocatalysis at low temperature. *Nanoscale*, 16(10), 5313-5322. <https://doi.org/10.1039/D3NR04707E>

- Li, K., Hogan, N. J., Kale, M. J., Halas, N. J., Nordlander, P. et Christopher, P. (2017). Balancing Near-Field Enhancement, Absorption, and Scattering for Effective Antenna–Reactor Plasmonic Photocatalysis. *Nano Letters*, 17(6), 3710-3717. <https://doi.org/10.1021/acs.nanolett.7b00992>
- Li, P., Pan, S.-Y., Pei, S., Lin, Y. J. et Chiang, P.-C. (2016). Challenges and Perspectives on Carbon Fixation and Utilization Technologies: An Overview. *Aerosol and Air Quality Research*, 16(6), 1327-1344. <https://doi.org/10.4209/aaqr.2015.12.0698>
- Li, S., Miao, P., Zhang, Y., Wu, J., Zhang, B., Du, Y., Han, X., Sun, J. et Xu, P. (2021). Recent Advances in Plasmonic Nanostructures for Enhanced Photocatalysis and Electrocatalysis. *Advanced Materials*, 33(6), 2000086. <https://doi.org/10.1002/adma.202000086>
- Liu, X., Li, L., Zhao, G. et Xiong, P. (2024). Optimization strategies for CO₂ biological fixation. *Biotechnology Advances*, 73, 108364. <https://doi.org/10.1016/j.biotechadv.2024.108364>
- Lowe, G. A. (2023). Enabling artificial photosynthesis systems with molecular recycling: A review of photo- and electrochemical methods for regenerating organic sacrificial electron donors. *Beilstein Journal of Organic Chemistry*, 19(1), 1198-1215. <https://doi.org/10.3762/bjoc.19.88>
- Ma, Y., Di, J., Yan, X., Zhao, M., Lu, Z. et Tu, Y. (2009). Direct electrodeposition of gold nanoparticles on indium tin oxide surface and its application. *Biosensors and Bioelectronics*, 24(5), 1480-1483. <https://doi.org/10.1016/j.bios.2008.10.007>
- Malkhandi, S. et Yeo, B. S. (2019). Electrochemical conversion of carbon dioxide to high value chemicals using gas-diffusion electrodes. *Current Opinion in Chemical Engineering*, 26, 112-121. <https://doi.org/10.1016/j.coche.2019.09.008>
- Mehere, A. et Chaure, N. B. (2020). Precisely controlled shape and size of gold nanostructures by seed-mediated reduction reaction method. *Applied Physics A*, 126(8), 662. <https://doi.org/10.1007/s00339-020-03837-3>
- Mohan, A., Ulmer, U., Hurtado, L., Loh, J., Li, Y. F., Tountas, A. A., Krevert, C., Chan, C., Liang, Y., Brodersen, P., Sain, M. M. et Ozin, G. A. (2020). Hybrid Photo- and Thermal Catalyst System for Continuous CO₂ Reduction. *ACS Applied Materials & Interfaces*, 12(30), 33613-33620. <https://doi.org/10.1021/acsami.0c06232>
- Mondal, B., Sen, P., Rana, A., Saha, D., Das, P. et Dey, A. (2019). Reduction of CO₂ to CO by an Iron Porphyrin Catalyst in the Presence of Oxygen. *ACS Catalysis*, 9(5), 3895-3899. <https://doi.org/10.1021/acscatal.9b00529>
- Mukherjee, S., Libisch, F., Large, N., Neumann, O., Brown, L. V., Cheng, J., Lassiter, J. B., Carter, E. A., Nordlander, P. et Halas, N. J. (2013). Hot Electrons Do the Impossible: Plasmon-Induced Dissociation of H₂ on Au. *Nano Letters*, 13(1), 240-247. <https://doi.org/10.1021/nl303940z>
- Naik, G. V., Shalaev, V. M. et Boltasseva, A. (2013). Alternative Plasmonic Materials: Beyond Gold and Silver. *Advanced Materials*, 25(24), 3264-3294. <https://doi.org/10.1002/adma.201205076>

- Ojea-Jiménez, I. et Campanera, J. M. (2012). Molecular Modeling of the Reduction Mechanism in the Citrate-Mediated Synthesis of Gold Nanoparticles. *The Journal of Physical Chemistry C*, 116(44), 23682-23691. <https://doi.org/10.1021/jp305830p>
- Panigrahi, S., Basu, S., Praharaj, S., Pande, S., Jana, S., Pal, A., Ghosh, S. K. et Pal, T. (2007). Synthesis and Size-Selective Catalysis by Supported Gold Nanoparticles: Study on Heterogeneous and Homogeneous Catalytic Process. *The Journal of Physical Chemistry C*, 111(12), 4596-4605. <https://doi.org/10.1021/jp067554u>
- Park, J. Y., Kim, S. M., Lee, H. et Nedrygailov, I. I. (2015). Hot-Electron-Mediated Surface Chemistry: Toward Electronic Control of Catalytic Activity. *Accounts of Chemical Research*, 48(8), 2475-2483. <https://doi.org/10.1021/acs.accounts.5b00170>
- Peng, Y. (2019). *Selectivity enhancement on heterogeneous electrocatalytic CO₂ reduction : from modification of metallic electrodes to heterogenization of monofunctional molecular catalysts*. <https://doi.org/10.32657/10356/136767>
- Petrovic, B., Gorbounov, M. et Masoudi Soltani, S. (2021). Influence of surface modification on selective CO₂ adsorption: A technical review on mechanisms and methods. *Microporous and Mesoporous Materials*, 312, 110751. <https://doi.org/10.1016/j.micromeso.2020.110751>
- Physical Methods in Chemistry and Nano Science (Barron)*. (2016, 13 juillet). Chemistry LibreTexts. [https://chem.libretexts.org/Bookshelves/Analytical_Chemistry/Physical_Methods_in_Chemistry_and_Nano_Science_\(Barron\)](https://chem.libretexts.org/Bookshelves/Analytical_Chemistry/Physical_Methods_in_Chemistry_and_Nano_Science_(Barron))
- Piazza, L., Lummen, T. T. A., Quiñonez, E., Murooka, Y., Reed, B. W., Barwick, B. et Carbone, F. (2015). Simultaneous observation of the quantization and the interference pattern of a plasmonic near-field. *Nature Communications*, 6(1), 6407. <https://doi.org/10.1038/ncomms7407>
- Rattanawongwiboon, T., Soontaranon, S., Hemvichian, K., Lertsarawut, P., Laksee, S. et Picha, R. (2022). Study on particle size and size distribution of gold nanoparticles by TEM and SAXS. *Radiation Physics and Chemistry*, 191, 109842. <https://doi.org/10.1016/j.radphyschem.2021.109842>
- Sahu, A. K., Dash, D. K., Mishra, K., P. Mishra, S., Yadav, R., Kashyap, P., Sahu, A. K., Dash, D. K., Mishra, K., P. Mishra, S., Yadav, R. et Kashyap, P. (2018). Properties and Applications of Ruthenium. Dans *Noble and Precious Metals - Properties, Nanoscale Effects and Applications*. IntechOpen. <https://doi.org/10.5772/intechopen.76393>
- Sattari, A., Ramazani, A., Aghahosseini, H. et Aroua, M. K. (2021). The application of polymer containing materials in CO₂ capturing via absorption and adsorption methods. *Journal of CO₂ Utilization*, 48, 101526. <https://doi.org/10.1016/j.jcou.2021.101526>
- Schneider, T. W., Ertem, M. Z., Muckerman, J. T. et Angeles-Boza, A. M. (2016). Mechanism of Photocatalytic Reduction of CO₂ by Re(bpy)(CO)₃Cl from Differences in Carbon Isotope Discrimination. *ACS Catalysis*, 6(8), 5473-5481. <https://doi.org/10.1021/acscatal.6b01208>
- Shome, A., Chahat, Jha, K. T., Chawla, P. A. et Dhanasekaran, M. (2024). 10 Recent advancement in binding free-energy calculation. Dans P. A. Chawla, D. Singh, K. Dua, M. Dhanasekaran et V.

- Chawla (dir.), *Volume 1 Computational Drug Discovery: Molecular Simulation for Medicinal Chemistry* (p. 211-242). De Gruyter. <https://doi.org/10.1515/9783111207117-010>
- Siampour, H., Abbasian, S., Moshaii, A., Omidfar, K., Sedghi, M. et Naderi-Manesh, H. (2020). Seed-mediated Electrochemically Developed Au Nanostructures with Boosted Sensing Properties: An Implication for Non-enzymatic Glucose Detection. *Scientific Reports*, *10*(1), 7232. <https://doi.org/10.1038/s41598-020-64082-5>
- Situ, X., Bayram, S. S. et Blum, A. S. (2023). Two-Step Synthesis of Large Gold–Silver Alloy Nanoparticles via the Combination of Seeded Growth and Citrate Co-reduction. *The Journal of Physical Chemistry C*, *127*(22), 10888-10895. <https://doi.org/10.1021/acs.jpcc.3c03095>
- Soo, X. Y. D., Lee, J. J. C., Wu, W.-Y., Tao, L., Wang, C., Zhu, Q. et Bu, J. (2024). Advancements in CO₂ capture by absorption and adsorption: A comprehensive review. *Journal of CO₂ Utilization*, *81*, 102727. <https://doi.org/10.1016/j.jcou.2024.102727>
- Srinivas, B., Shubhamangala, B., Lalitha, K., Anil Kumar Reddy, P., Durga Kumari, V., Subrahmanyam, M. et De, B. R. (2011). Photocatalytic Reduction of CO₂ over Cu-TiO₂/Molecular Sieve 5A Composite. *Photochemistry and Photobiology*, *87*(5), 995-1001. <https://doi.org/10.1111/j.1751-1097.2011.00946.x>
- Steinborn, D. (2011). *Fundamentals of Organometallic Catalysis*. John Wiley & Sons.
- Sun, H., Wu, J., Tian, F., Zhang, G., Xia, Z., Rong, J., Qin, J.-S. et Rao, H. (2024). Electrocatalytic reduction of CO₂ to CO by Fe(III) carbazole–porphyrins in homogeneous molecular systems. *Catalysis Science & Technology*, *14*(3), 660-666. <https://doi.org/10.1039/D3CY01618H>
- Tsenova-Ilieva, I. et Karova, E. (2020). Application of Atomic Force Microscopy in Dental Investigations. *International Journal of Science and Research (IJSR)*, *9*, 1319-1326. <https://doi.org/10.21275/SR20323220034>
- Wang, C., Shi, Y., Dan, Y.-Y., Nie, X.-G., Li, J. et Xia, X.-H. (2017). Enhanced Peroxidase-Like Performance of Gold Nanoparticles by Hot Electrons. *Chemistry – A European Journal*, *23*(28), 6717-6723. <https://doi.org/10.1002/chem.201605380>
- Wang, D., Guan, J., Hu, J., Bourgeois, M. R. et Odom, T. W. (2019). Manipulating Light–Matter Interactions in Plasmonic Nanoparticle Lattices. *Accounts of Chemical Research*, *52*(11), 2997-3007. <https://doi.org/10.1021/acs.accounts.9b00345>
- Wang, J., Dou, S. et Wang, X. (2021). Structural tuning of heterogeneous molecular catalysts for electrochemical energy conversion. *Science Advances*, *7*(13), eabf3989. <https://doi.org/10.1126/sciadv.abf3989>
- Wang, Y. et Lai, W. (2024). Intramolecular electrostatic effects on reduction of CO₂ to CO by iron porphyrin complexes: Insights from DFT calculations. *Molecular Catalysis*, *553*, 113797. <https://doi.org/10.1016/j.mcat.2023.113797>

- Yang, L.-K., Huang, T.-X., Zeng, Z.-C., Li, M.-H., Wang, X., Yang, F.-Z. et Ren, B. (2015). Rational fabrication of a gold-coated AFM TERS tip by pulsed electrodeposition. *Nanoscale*, 7(43), 18225-18231. <https://doi.org/10.1039/C5NR04263A>
- Yin-Fen M., You-Mei W., Jia W., Ao L., Xiao-Liang L., Mei L., Yong-Biao Z. et Zheng-Hong L. (2023). Review of roll-to-roll fabrication techniques for colloidal quantum dot solar cells. *电子科技学刊 (英文)*, 21(1), 100189. <https://doi.org/10.1016/j.jnlest.2023.100189>
- Zeng, S., Vahidzadeh, E., VanEssen, C. G., Kar, P., Kisslinger, R., Goswami, A., Zhang, Y., Mahdi, N., Riddell, S., Kobryn, A. E., Gusarov, S., Kumar, P. et Shankar, K. (2020). Optical control of selectivity of high rate CO₂ photoreduction via interband- or hot electron Z-scheme reaction pathways in Au-TiO₂ plasmonic photonic crystal photocatalyst. *Applied Catalysis B: Environmental*, 267, 118644. <https://doi.org/10.1016/j.apcatb.2020.118644>
- Zhang, J., Chen, H., Duan, X., Sun, H. et Wang, S. (2023). Photothermal catalysis: From fundamentals to practical applications. *Materials Today*, 68, 234-253. <https://doi.org/10.1016/j.mattod.2023.06.017>
- Zhang, J., Liu, H., Wang, Z. et Ming, N. (2007). Shape-Selective Synthesis of Gold Nanoparticles with Controlled Sizes, Shapes, and Plasmon Resonances. *Advanced Functional Materials*, 17(16), 3295-3303. <https://doi.org/10.1002/adfm.200700497>
- Zhang, K., Goswami, S., Noh, H., Lu, Z., Sheridan, T., Duan, J., Dong, W. et Hupp, J. T. (2022). An iron-porphyrin grafted metal-organic framework as a heterogeneous catalyst for the photochemical reduction of CO₂. *Journal of Photochemistry and Photobiology*, 10, 100111. <https://doi.org/10.1016/j.jpap.2022.100111>
- Zhang, Y., Guo, S.-X., Zhang, X., Bond, A. M. et Zhang, J. (2020). Mechanistic understanding of the electrocatalytic CO₂ reduction reaction – New developments based on advanced instrumental techniques. *Nano Today*, 31, 100835. <https://doi.org/10.1016/j.nantod.2019.100835>
- Zhao, C., Xing, L., Xiang, J., Cui, L., Jiao, J., Sai, H., Li, Z. et Li, F. (2014a). Formation of uniform reduced graphene oxide films on modified PET substrates using drop-casting method. *Particuology*, 17, 66-73. <https://doi.org/10.1016/j.partic.2014.02.005>
- Zhao, J., Wang, X., Xu, Z. et Loo, J. S. C. (2014b). Hybrid catalysts for photoelectrochemical reduction of carbon dioxide: a prospective review on semiconductor/metal complex co-catalyst systems. *Journal of Materials Chemistry A*, 2(37), 15228-15233. <https://doi.org/10.1039/C4TA02250E>
- Zhou, J., Wang, Y., Zhang, L. et Li, X. (2018). Plasmonic biosensing based on non-noble-metal materials. *Chinese Chemical Letters*, 29(1), 54-60. <https://doi.org/10.1016/j.ccllet.2017.09.003>
- Zhou, W., Apkarian, R., Wang, Z. L. et Joy, D. (2007). Fundamentals of Scanning Electron Microscopy (SEM). Dans W. Zhou et Z. L. Wang (dir.), *Scanning Microscopy for Nanotechnology: Techniques and Applications* (p. 1-40). Springer. https://doi.org/10.1007/978-0-387-39620-0_1
- Zou, L., Sa, R., Lv, H., Zhong, H. et Wang, R. (2020). Recent Advances on Metalloporphyrin-Based Materials for Visible-Light-Driven CO₂ Reduction. *ChemSusChem*, 13(23), 6124-6140. <https://doi.org/10.1002/cssc.202001796>

